



CRCLEME

Cooperative Research Centre for
Landscape Evolution & Mineral Exploration



**OPEN FILE
REPORT
SERIES**



CSIRO
EXPLORATION
AND MINING

**GEOCHEMICAL DISPERSION IN THE
OLARY DISTRICT, SOUTH AUSTRALIA:
INVESTIGATIONS AT FAUGH-A-BALLAGH
PROSPECT, OLARY SILVER MINE,
WADNAMINGA GOLDFIELD AND
BLUE ROSE PROSPECT**

Volume I: Text

M.S. Skwarnecki, Li Shu and M.J. Lintern

CRC LEME OPEN FILE REPORT 113

September 2001

(CSIRO Exploration and Mining Report 794R /
CRC LEME Report 156R, 2001. Second impression 2001)

CRC LEME is an unincorporated joint venture between The Australian National University, University of Canberra, Australian Geological Survey Organisation and CSIRO Exploration and Mining, established and supported under the Australian Government's Cooperative Research Centres Program.





**GEOCHEMICAL DISPERSION IN THE
OLARY DISTRICT, SOUTH AUSTRALIA:
INVESTIGATIONS AT FAUGH-A-BALLAGH
PROSPECT, OLARY SILVER MINE,
WADNAMINGA GOLDFIELD AND
BLUE ROSE PROSPECT**

Volume 1: Text

M.S. Skwarnecki, Li Shu and M.J. Lintern

CRC LEME OPEN FILE REPORT 113

September 2001

(CSIRO Exploration and Mining Report 794R /
CRC LEME Report 156R, 2001. Second impression 2001)

© CRC LEME 2001

© CRC LEME

This report presents outcomes of a collaborative research project between Lynas Corporation Ltd., CRC LEME and the Department of Primary Industries and Resources, South Australia (PIRSA) that commenced in mid 2000 and continued until early 2001. Confidentiality on the data and report expired on 1st August 2001.

This report (CRC LEME Open File Report 113) is a second impression (second printing) of CRC LEME Restricted Report 156R, first issued in April 2001.

Copies of this publication can be obtained from:

The Publication Officer, c/- CRC LEME, CSIRO Exploration and Mining, P.O. Box 1130, Bentley, WA 6102, Australia. Information on other publications in this series may be obtained from the above or from <http://leme.anu.edu.au/>

Cataloguing-in-Publication:

Skwarnecki, M.S.

Geochemical dispersion in the Olary District, South Australia: Investigations at Faugh-a-Ballagh Prospect, Olary Silver Mine, Wadnaminga Goldfield and Blue Rose Prospect.

ISBN V1:0 643 06769 8 V2:0 643 06770 1 set:0 643 06771 X

1. Geochemistry - South Australia 2. Regolith - South Australia 3. Silver ores - South Australia

Li Shu. II. Lintern, M.J. III Title.

CRC LEME Open File Report 113.

ISSN 1329-4768

Addresses and affiliations of authors

M.S. Skwarnecki

Cooperative Research Centre for Landscape
Evolution and Mineral Exploration
c/- CSIRO Land and Water
Private Mail Bag 2,
Glen Osmond 5064
South Australia

Li Shu

Cooperative Research Centre for Landscape
Evolution and Mineral Exploration
c/- CSIRO Exploration and Mining
Private Bag 5,
Wembley 6913
Western Australia

M.J. Lintern

Cooperative Research Centre for Landscape
Evolution and Mineral Exploration
c/- CSIRO Exploration and Mining
Private Bag 5,
Wembley 6913
Western Australia

DISTRIBUTION LIST

	<u>Copy No</u>
LYNAS CORPORATION LTD	
Mr P.J. Davies	1, 2
PIRSA	
Mr R.S Robertson	3
CRC LEME	
Dr M.J. Skwarnecki	4
Dr L. Shu	5
Mr M.J. Lintern	6
Dr. C.R.M. Butt	7
Records CRC LEME	8

This is copy () of 8

PREFACE

The Olary Regolith Project was established in July 2000 as a jointly funded project between CRC LEME, Lynas Corporation Ltd and the Department of Primary Industries and Resources, South Australia (PIRSA). The duration of the project was six months. The principal objective by CRC LEME was to conduct a regolith mapping and orientation geochemical sampling program that would provide targets for further exploration and a basis to conduct effective further geochemical exploration in the Olary region. Specific objectives were to:

- i) characterise and map the regolith covered by the Olary and Anabama 1:100 000 map sheets;
- ii) determine the uses and limitations of calcrete, soil and other regolith materials as sampling media in different types of terrain, including outcrop, thin cover and areas with deeper transported overburden;
- iii) examine the role of topography and terrain-forming processes on the dispersion of elements in the regolith;
- iv) provide the results to sponsors and, after the confidentiality period (3 months), the exploration industry as a whole.

The project delivered in, and exceeded in some cases, all the above objectives as follows:

- i) two 1:100 000 scale regolith landform maps were produced (Olary and Anabama);
- ii) three 1:5000 scale regolith landform maps were produced of the Blue Rose, Wadnaminga and Faugh a Ballagh prospects;
- iii) geochemical data sets have been provided for Blue Rose, Wadnaminga, Faugh-a-Ballagh and the Olary Silver Mine.

Detailed investigation of the geochemistry from the three areas revealed several areas worthy of further exploration. Follow-up targets for investigating copper mineralisation were generated at Blue Rose and Faugh-a-Ballagh. Optimal geochemical sampling procedures were developed for each regolith unit sampled during the course of the project, including sampling of calcrete, lag and soil. These should form the basis for any future regional exploration in the Olary area.

M.J. Lintern
Project Leader

January 2001

CONTENTS

1	INTRODUCTION	11
1.1	Location	11
1.2	Regional geology	11
1.3	Objectives and work programme	16
2	STUDY METHODS	16
2.1	Regolith mapping	16
2.2	Sample collection	17
2.2.1	Soil and lag collection	17
2.2.2	Stream sediment collection	17
2.2.3	Calcrete sampling	17
2.2.4	Augered samples	17
2.3	Sample preparation	18
2.4	Partial analyses	18
2.5	Geochemical analysis	18
2.6	Standards and statistical treatment of data	18
3	REGOLITH MAPPING	19
3.1	Regolith classification	19
3.2	Regolith landform units	19
4	WADNAMINGA	20
4.1	Geological setting	20
4.2	Mineralisation	20
4.3	Regolith	21
4.4	Vegetation	25
4.5	Geochemistry	25
4.5.1	Sampling	25
4.5.2	Rock-chip sample geochemistry	25
4.5.3	Calcrete geochemistry	25
4.5.4	Geochemistry of augered samples	28
4.6	Summary	31
5	FAUGH-A-BALLAGH	31
5.1	Geological setting	31
5.2	Mineralisation	32
5.3	Regolith	33
5.4	Vegetation	33
5.5	Geochemistry	37
5.5.1	Sampling	37
5.5.2	Rock-chip sample geochemistry	37
5.5.3	Stream-sediment geochemistry	37
5.5.4	Compositions of selected stream-sediment size fractions	40
5.5.5	Orientation soil-lag traverse	40
5.5.6	Regional <6 mm soil sampling	42
5.5.7	Geochemistry of magnetic versus non-magnetic fractions	43
5.6	Summary	45
6	OLARY SILVER MINE	46
6.1	Geological setting	46
6.2	Regolith	46
6.3	Geochemistry	46
6.3.1	Sampling	46
6.3.2	Rock-chip sample geochemistry	46
6.3.3	Orientation soil-lag traverse	46
6.4	Summary	50

7	BLUE ROSE.....	50
7.1	Introduction	50
7.2	Geological setting.....	50
7.3	Mineralisation.....	51
7.4	Vegetation.....	51
7.5	Sampling.....	51
7.6	Regolith	52
7.7	Geological cross-sections	52
7.8	Geochemistry.....	64
7.8.1	Geochemistry of mineralised intervals.....	64
7.8.2	Rock-chip sample geochemistry.....	64
7.8.3	Geochemistry of pit samples	64
7.8.4	Geochemistry of augered samples.....	65
7.8.5	Soil geochemistry	68
7.8.6	Lag geochemistry.....	68
7.8.7	Partial leach analyses.....	68
7.9	A comparison of geochemical responses in augered, soil and lag samples along grid lines 427600E and 428820E	69
7.9.1	<6 mm versus >6 mm augered samples (428820E).....	70
7.9.2	<2 mm soils versus >6 mm augered samples (427600E)	70
7.9.3	<2 mm soils versus >6 mm augered samples (428820E)	70
7.9.4	<2 mm soils versus 2-6 mm lags (428820E)	71
7.10	Summary.....	72
8	MISCELLANEOUS REGIONAL ROCK-CHIP SAMPLES	72
9	CONCLUSIONS AND NEW TARGETS.....	73
9.1	Wadnaminga.....	73
9.1.1	Summary.....	73
9.1.2	Implications for exploration	73
9.1.3	Further work	73
9.2	Faugh-a-Ballagh	73
9.2.1	Summary.....	73
9.2.2	Implications for exploration	74
9.2.3	Further work	74
9.3	Blue Rose.....	74
9.3.1	Summary.....	74
9.3.2	Implications for exploration	74
9.3.3	Further work	74
10	ACKNOWLEDGEMENTS.....	76
11	REFERENCES	77

LIST OF FIGURES

Figure 1: Regolith landform maps of the four study areas and the exploration licences held by Lynas Corporation Ltd in the Olary area. The 2 regolith-landform maps (Anabama and Olary 1:100000) that comprise this figure show the depositional and erosional regolith units. Full unit descriptions and map plans covering this area can be found on the CD.....	12
Figure 2: Simplified map of the Curnamona Province showing areas of outcrop.....	13
Figure 3: Tectonic interpretation of the Nackara Arc, Fleurieu Arc and basement to the Murray Basin (after Preiss, 1995).....	15
Figure 4: Geological map of part of the Wadnaminga Goldfield in the vicinity of the Virginia, New Milo, Great Eastern and Thunder Queen mines (after Morris, 1975). See Figure 1 for location of the study area.....	22
Figure 5 Wadnaminga. a , a barren earlier quartz vein, with later mineralised vein with old workings; Great Eastern mine; b , siltstone outcrops and abundant lag at the Great Eastern mine; in the middle distance, the hills are Burra Group metasedimentary rocks, whereas the hills on the horizon are Anabama Granite; c , the soil profile at Great Eastern: an upper horizon of calcareous soil (10-20 cm thick), overlying a layer of nodular calcrete (about 20 cm thick), resting on weathered siltstone (6398794N, 429316E); d , massive calcrete in creek cementing siltstone and quartz fragments (6399009N, 429125E).....	23
Figure 6: Regolith-landform map of part of the Wadnaminga Goldfield in the vicinity of the Virginia, New Milo, Great Eastern and Thunder Queen mines. Full regolith landform unit descriptions are found in Appendix 6.....	24
Figure 7: Distribution of Au (ppb) in augered and calcrete samples, Wadnaminga. Gold concentrations for calcrete are labelled. Full regolith landform unit descriptions and are found in Appendix 6.....	27
Figure 8: Plot of Factor 1 versus Factor 3 from principal component analysis of augered samples. Note the general groupings of elements: Ca-S (associated with calcrete), As-Au-Bi-Cd-Cu-In-Pb-Zn (associated with the lode horizons), and two groups with lithological associations.....	29
Figure 9: Geological map of Faugh-a-Ballagh prospect (after Beckton, 1993). See Figure 1 for location of Faugh-a-Ballagh.....	34
Figure 10: Ironstones at Faugh-a-Ballagh.....	35
Figure 11: Regolith-landform map of Faugh-a-Ballagh prospect. Full regolith landform unit descriptions are found in Appendix 6.....	36
Figure 12: Distribution of Cu (ppm) in <2 mm stream sediments, Faugh-a-Ballagh.....	38
Figure 13: Distribution of Cu (ppm) in various size fractions along the orientation traverse.....	41
Figure 14: Distribution of Au (ppb) in <6 mm soils, Faugh-a-Ballagh. Full regolith landform unit descriptions are found in Appendix 6.....	44
Figure 15: Distribution of Cu (ppm) in <6 mm soils, Faugh-a-Ballagh. Full regolith landform unit descriptions are found in Appendix 6.....	44
Figure 16: Geological map (after Chapman, 1988) showing location of the Olary Silver Mine and orientation soil traverse. See Figure 1 for location of Olary Silver Mine.....	47
Figure 17: Distribution of Au (ppb) in various size fractions along the orientation traverse, Olary Silver Mine.....	48
Figure 18: Distribution of Cu (ppm) in various size fractions along the orientation traverse, Olary Silver Mine.....	49
Figure 19: Regolith-landform map of the Blue Rose prospect, showing location of RC drill holes. Full regolith landform unit descriptions are found in Appendix 6.....	53
Figure 20: Blue Rose prospect. a , general view of Blue Rose prospect, illustrating the flat topography (viewed to the north, from 6388650N, 428830E) Burra Group sedimentary rocks form the hills on the horizon; b , silicified outcrop containing disseminated pyrite and 950 ppm Cu at sample locality EBBR2 (6387914N, 429581E); the soil is calcareous.....	55
Figure 21: Interpreted geological cross-section on line 427250E, showing interpreted distribution of Cu (ppm). See Figure 19 for locations of drill holes.....	56

Figure 22: Interpreted geological cross-section on line 427620E, showing interpreted distribution of Cu (ppm). See Figure 19 for locations of drill holes.....	57
Figure 23: Interpreted geological cross-section on line 428220E, showing interpreted distribution of Cu (ppm). See Figure 19 for locations of drill holes.....	58
Figure 24: Interpreted geological cross-section on line 428820E, showing interpreted distribution of Cu (ppm). See Figure 19 for locations of drill holes.....	59
Figure 25: Interpreted geological cross-section on section 428925E, showing interpreted distribution of Cu (ppm). See Figure 19 for location of drill hole.....	60
Figure 26 (previous page): Selected photomicrographs of lithologies from Blue Rose. a , silcrete, comprising cemented lithic fragments (including quartz, ferruginised siltstone, and buckshot gravel) in a very fine-grained matrix of silica and iron oxides (BRR13, 6-7 m; x250); b , calcite rim on silcrete – the carbonate rind on the exterior of a calcite nodule (BRR13, 6-7 m; x250); c , carbonate-tremolite rock with disseminated sulphides (BRR9, 63-64m; x250); d , banded, clastic albite-quartz rock, with disseminated mica and sulphides (BRR9, 63-64m; x250); e , fractured and twinned carbonate porphyroblast in dolomite (BRR5, 61-62 m; x300); f , hydrothermal alteration of marble, destroying metamorphic fabric of the rock; some of the opaques are sulphides (BRR18, 64-65 m; x180); g , silicified rock with largely destroyed fabrics and partially preserved disseminated pyrite (EBRR2; plane polarised light; x200); h , same view in reflected light, showing pyrite grains partially to completely replaced by hematite.	62
Figure 27: Depths to base of transported cover (in metres) from RC and RAB drilling, Blue Rose prospect. Full regolith landform unit descriptions are found in Appendix 6.	63
Figure 28: Element concentrations down the soil profile at Blue Rose (6388074N 428818E. The y axis is the depth (cm), whereas the x axis is concentration.....	66
Figure 29: Distribution of Au (ppb) in >6 mm augered samples (soil and calcrete) and rock chip samples, Blue Rose. Full regolith landform unit descriptions are found in Appendix 6. A simplified regolith landform unit code is used here.	67
Figure 30: Distribution of Cu (ppm) in >6 mm augered samples (soil and calcrete) and rock chip samples, Blue Rose. Full regolith landform unit descriptions are found in Appendix 6. A simplified regolith landform unit code is used here.	67
Figure 31: The concentration of Cu (ppm) in soil (<2 mm, 0.1-0.2 m depth) along grid line 428820E showing the responses from various sample media and partial leaches. Note that the presence of mineralisation has not been identified in the partial leach analyses. The lag, soil and calcretes sample analyses were determined by ICP-OES after dissolution by mixed acid digest.	69
Figure 32: Comparison of Au and Cu geochemistry for different sample media on 427600E at Blue Rose:	70
Figure 33: Comparison of Au and Cu geochemistry for different sample media on 428820E at Blue Rose: a) Augered sample (>6 mm) vs soil sample. b) Fine augered sample (<6 mm) vs coarse augered sample (>6 mm). c) Soil sample vs lag sample (>2<6 mm).	71
Figure 34: Areas for further investigation, Faugh-a-Ballagh prospect. Full regolith landform unit descriptions are found in Appendix 6.....	75
Figure 35: Areas for further investigation, Blue Rose prospect. Full regolith landform unit descriptions are found in Appendix 6.....	75

LIST OF TABLES

Table 1: Vertical distribution of elements in the soil profile, Blue Rose prospect. Antimony, Se and Te are below detection.	65
---	----

EXECUTIVE SUMMARY

The Olary Regolith Project was established in July 2000 as a jointly funded project between CRC LEME, Lynas Corporation Ltd and the Department of Primary Industries and Resources, South Australia (PIRSA). The principal objective was to conduct a regolith mapping and orientation geochemical sampling program that would provide targets for further exploration and a basis to conduct effective further geochemical exploration in the Olary region. Three principal areas were selected for study: the Faugh-a-Ballagh prospect (Olary Domain); the Great Eastern-New Milo mines in the Wadnaminga Goldfield; and the Blue Rose prospect (Nackara Arc). An orientation soil traverse was investigated at the Olary Silver Mine (Olary Domain).

At Faugh-a-Ballagh (20 km northwest of Olary), Cu mineralisation occurs in magnetite veins (ironstones) and zones of magnetite dissemination in the upper part of the Quartzofeldspathic Suite of the Olary Domain. Most of the area belongs to an erosional regime, the dominant landforms being high hills formed by slightly weathered gneisses and schists. Soils are skeletal to colluvial, and little or no deeply-weathered regolith is present. Although mineralised ironstones (magnetite-rich veins) are anomalous in Ag, Au, Cu, In, Zn, Al, Ga, Cs, K, Rb, Mg, Sr, REE, Th, Ti, U and Y, stream-sediment sampling (<2 mm fraction) indicates that Cu is the only reliable indicator of mineralisation and that dispersion is very limited. Preliminary studies show that the <75 µm fraction is the optimum sample medium and that Cu dispersion is probably greatest in this fraction. Similarly, orientation soil sampling across a mineralised ironstone vein suggests that Cu is the only reliable indicator of mineralisation. The finer fractions (75-180 µm and <75 µm) are optimum fractions, although the bulk <6 mm fraction is an acceptable (average) compromise.

Orientation studies on magnetic versus non-magnetic fractions in <2 mm soils, <2 mm stream sediments and 2-6 mm lags suggest that there is no advantage in using the magnetic fraction, since Cu is irregularly distributed between the fractions. Regional <6 mm soil sampling was carried out on a 400 m triangular grid, with infill at 100 m spacings on Faugh-a-Ballagh Hill. Only Cu and Au consistently delineate the mineralised zones. The most prospective areas are on the southern side of Faugh-a-Ballagh Hill, in an area of relatively intense ironstone veining, to the north of an east-west shear, and the shear itself. Copper is dispersed irregularly over an area 750 m by 250 m. The Au dispersion is much narrower and extends for about 1500 m along the shear. Other, less well-defined zones with anomalous Cu occur to the west and southwest, in zones of disseminated magnetite in albitic rocks. The principal targets are the southern side of Faugh-a-Ballagh Hill and the east-west shear.

At the Olary Silver Mine (about 5 km north of Olary), sampling of the dumps suggests that geochemical indicators of the mineralisation are likely to be Ag, As, Au, Bi, Cu, Hg, Mo, Se and Te in fresh rock. The orientation soil survey indicates that Au and Cu are the best indicators of mineralisation and form an anomalous zone 40 m wide. The best response was in the <75 µm fraction but using the bulk <6 mm fraction would be acceptable.

At Wadnaminga (about 30 km south of Olary), Au mineralisation occurs in sulphidic quartz veins in metasedimentary rocks of the Burra Group, along the northern margin of the Wadnaminga Anticlinorium. High-grade mineralisation at New Milo contains significant concentrations of Ag, As, Au, Bi, Cd, Cu, Hg, Pb, S, Sb, Se and Zn. Most of the area investigated belongs to an erosional regime; dominant landform units are hills formed by weathered siltstones, dolomites and phyllites, with thin soils and abundant lag. Calcrete sampling along the lodes indicates that anomalous Au is associated with As, Cu, Pb and Zn; the narrow hydrothermal alteration halo gives rise to anomalous Ba, Mg, Sr, K, Na, Rb, Tl, U and W. Using calcrete as a sample medium, geochemical dispersion along the lode horizons is very limited. In augered samples, dispersion haloes are broader. The respective widths of dispersion are 25-50 m for ore-associated elements (As, Au, Cd, Cu, Pb and Zn), and of the order of 150 m for elements associated with hydrothermal alteration (Ba, K, Mg, Sr, Th, U

and W). Auger drilling and calcrete sampling are effective sampling techniques in this environment, although a sufficiently dense sampling grid (25 m) would be required for prospect-scale calcrete sampling. Other conventional sampling techniques, such as soil sampling, are likely to be valid.

The Blue Rose prospect is located about 40 km south of Olary and 10 km south of the New Milo and Great Eastern mines, and occurs on the southern limb of the Wadnaminga Anticlinorium in metasedimentary units of the Burra Group. Most of the prospect area is covered by alluvium, with transported cover locally 42 m thick. Disseminated Cu mineralisation occurs in dolomitic rocks. The geochemical signature of the Cu mineralisation is Bi, Cs, In, K, Mo, Rb, S, Se and Tl. Copper dispersion haloes in saprock and saprolite are broader than in bedrock and extend into the basal 2 m of transported overburden. There is a vertical zonation in the upper 50 cm of the soil-calcrete profile. Arsenic, Au, Ba, Ca, Mg, S, Se, Sr and Y are most abundant at 20-40 cm depth, whereas Ag, Al, Bi, Co, Cr, Cs, Cu, Ga, Fe, Hf, In, K, Mn, Mo, Na, Nb, Ni, Pb, REE, Rb, Sn, Th, Ti, Tl, U, V, W and Zn are most abundant at 0-10 cm depth. Soil sampling (<2 mm fraction) over the mineralised zone on grid line 428820E failed to detect the mineralisation. Similar disappointing results were achieved by >6mm and <6 mm augered samples, 2-6 mm magnetic lags and partial leach analyses (water, potassium cyanide, sodium pyrophosphate, MMI), even though transported overburden is only 8-9 m thick over part of the mineralised zone. Auger drilling was carried out on six traverses. In general terms, samples with the greatest element abundances in soils and calcrete occur where transported cover is relatively thin (<6 m). A zone anomalous in Au and Cu was outlined by <6 mm augered samples at the southern end of grid line 427250E (to the south-west of the presently known mineralised zone), and later confirmed by <2 mm soil sampling. Two other geochemically anomalous zones were also identified at Blue Rose.

At Wadnaminga, where cover is minimal, both auger drilling and calcrete sampling were effective sampling techniques. The geochemical suite for further exploration should include: As, Au, Ba, Ca, Cu, Fe, K, Mg, Mn, Pb, U, W and Zn. Although not used in this study, soil sampling would also be a valid sampling medium in this environment (erosional regime). At Faugh-a-Ballagh, soil sampling (<6 mm fraction) appears to be the most effective sampling medium in this environment (dominantly erosional regime). Stream-sediment and rock-chip sampling provide only limited Cu dispersion. There is no improvement using magnetic fractions of soil, lag or stream sediments. The geochemical suite for further exploration should include: As, Au, Bi, Ca, Cu, Fe, Mn, Na, U and W. At Blue Rose, which occurs in a dominantly depositional regime, soil sampling (<2 mm fraction) and auger drilling are effective techniques only where transported cover is thin (<6 m). Partial leach analyses failed to detect Cu mineralisation, even where transported cover was 8-9 m thick. This indicates that drilling is the only effective technique where cover is >6 m thick. However, broad Cu dispersion haloes in saprolite and basal parts of transported cover provide larger targets than the primary zones. The geochemical suite for further exploration should include: Au, Bi, Cu, Fe, K, Mg, Mn, Mo, Se and Tl.

GEOCHEMICAL DISPERSION IN THE OLARY DISTRICT, SOUTH AUSTRALIA: INVESTIGATIONS AT FAUGH-A-BALLAGH PROSPECT, OLARY SILVER MINE, WADNAMINGA GOLDFIELD AND BLUE ROSE PROSPECT

M.S. Skwarnecki, L. Shu and M.J. Lintern

1 INTRODUCTION

The Olary Regolith Project was jointly funded by the Cooperative Research Centre for Landscape Evolution and Mineral Exploration (CRC LEME), the Targetted Exploration Initiative South Australia (TEISA) through Primary Industries and Resources South Australia (PIRSA), and Lynas Corporation Ltd. The principal objective was to provide targets for further exploration at selected sites by conducting relevant regolith mapping and geochemical sampling programmes.

This report addresses geochemical dispersion at four selected sites (Faugh-a-Ballagh, Olary Silver Mine, Wadnaminga Goldfield and Blue Rose) in the Olary district of South Australia. Faugh-a-Ballagh and Olary Silver Mine occur within the Olary Domain, whereas Wadnaminga and Blue Rose occur in the Nackara Arc to the south. At Faugh-a-Ballagh, Cu-Au mineralisation is associated with magnetite-rich veins and breccias. At the Olary Silver Mine, mineralisation is associated with pyritic replacement of a magnetite-rich ironstone. At Wadnaminga, narrow sulphidic quartz veins are auriferous. The Blue Rose prospect is centred on disseminated Cu mineralisation in dolomitic rocks.

Previous mineral exploration in the Olary district has not been conducted within a regolith-landform framework. Existing evidence suggests that the geochemical effectiveness of surficial media (e.g., soils, lags and calcrete) is strongly dependent on the substrate (e.g., fresh rock, saprolite and transported overburden). Consequently, well-controlled geochemical sampling programmes are likely to provide targets and a framework for further studies of geochemical dispersion in the district.

1.1 Location

Olary is situated at 32°18' 140°25' on the Barrier Highway in South Australia, about 65 km west of the New South Wales border. It lies within the eastern pastoral province. The study area comprised two 1:100 000 map sheets (Olary and Anabama) with four areas of more detailed investigation (Figure 1). The latter include two areas 5 km north and 20 km northwest of Olary (Olary Silver Mine and Faugh-a-Ballagh respectively), and two to the south (Wadnaminga and Blue Rose, 30 and 40 km south respectively). The two main physiographic domains are the Olary Ranges and the Murray Basin, the latter located in the extreme south (Figure 1). The Olary Ranges have northeast trending ridges with intermediate gently sloping valleys, and form a spur and hills between Lake Frome and the Murray Basin (Forbes, 1991).

The climate is warm and dry, with a low annual rainfall of about 200 mm and a mean evaporation rate of about 2500 mm (Forbes, 1991). Average temperatures at Yunta (about 80 km west of Olary) range from a January maximum of 32.5° C to a July minimum of 3.1° C (Forbes, 1991).

1.2 Regional geology

The Proterozoic Curnamona Province extends across eastern South Australia and western New South Wales, and comprises a sequence of late Palaeoproterozoic metasedimentary and metavolcanic rocks (the Willyama Supergroup), locally with metamorphosed intrusive rocks, together with early Mesoproterozoic metavolcanic and metasedimentary rocks and granitoids (Robertson et al., 1998). The Willyama Inlier, the largest area of outcrop in the province, occurs as a series of blocks separated by corridors of the Neoproterozoic Adelaide Geosyncline sequences, and is partly concealed beneath Tertiary to Recent sediments (Figure 2). In South Australia, most of the Willyama rocks are referred

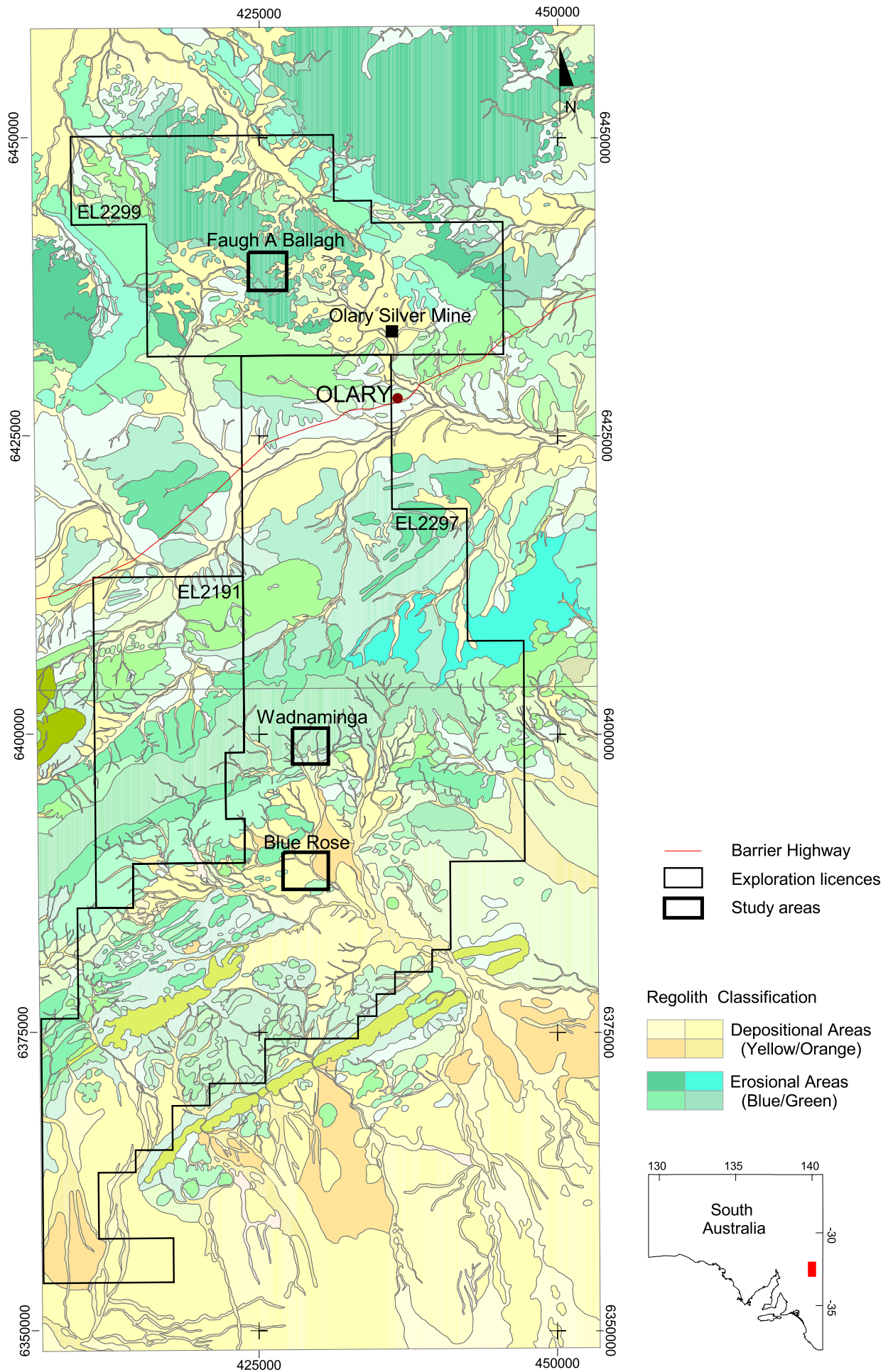


Figure 1: Regolith landform maps of the four study areas and the exploration licences held by Lynas Corporation Ltd in the Olary area. The 2 regolith-landform maps (Anabama and Olary 1:100000) that comprise this figure show the depositional and erosional regolith units. Full unit descriptions and map plans covering this area can be found on the CD.

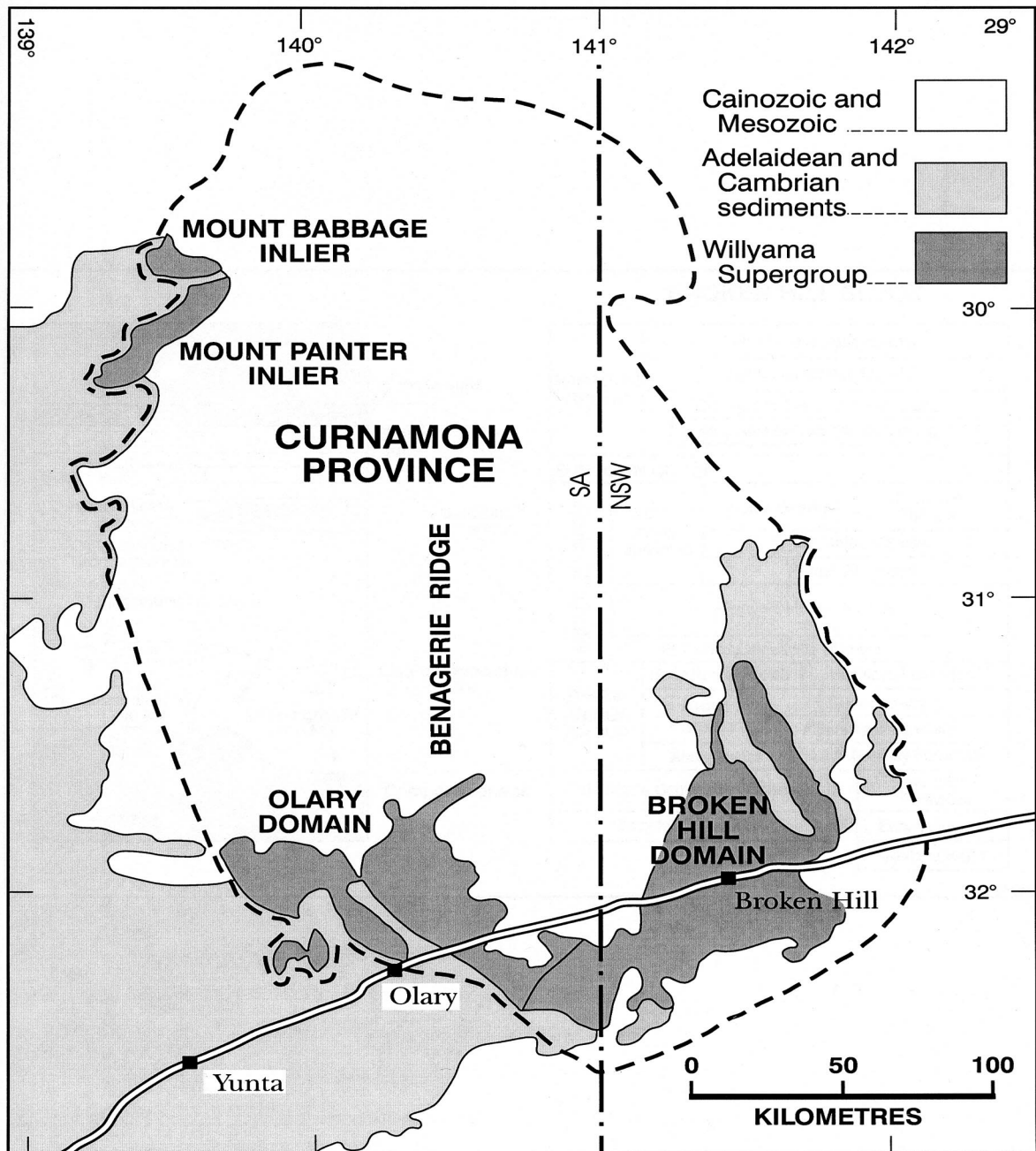


Figure 2: Simplified map of the Curnamona Province showing areas of outcrop.

to as the Olary Domain and are distinguished from the adjoining southwestern part of the Broken Hill Domain by different lithological, magnetic and gravity characteristics (Robertson et al., 1998).

The Olary Domain is composed of low- to high-grade regionally metamorphosed rocks and deformed late Palaeoproterozoic metasedimentary and minor volcanic/intrusive rocks. These sequences have been intruded by early Mesoproterozoic granitoids and Neoproterozoic mafic dykes. The stratigraphy of the domain has been summarised by Robertson et al. (1998) and comprises, from the base upwards:

Composite Gneiss Suite

Intermixed migmatitic gneisses and granitoids; the dominant lithology is coarse-grained and migmatitic quartz-feldspar-biotite+sillimanite+garnet gneiss; stratiform quartz-biotite-magnetite rocks.

Quartzofeldspathic Suite	Massive to well-layered quartz-albite-biotite±K feldspar gneiss, commonly with disseminated magnetite and pyrite; discontinuous quartz-magnetite±pyrite±barite horizons.
Calc-silicate Suite	Calc-silicate, calc-albite and feldspathic rocks interlayered with metasiltstone and potassic to sodic gneiss; magnetite (±hematite) throughout.
Bimba Formation	Thin (<50 m) laterally continuous, heterogeneous unit of albitic metasiltstone, marble, chert and calc-rock, commonly with disseminated, laminated and vein sulphides.
Pelite Suite	Graphitic quartz-mica-andalusite-sillimanite schist, and mica schist with interbedded quartzofeldspathic metasiltstone, garnet-quartz rock and thin quartzite.

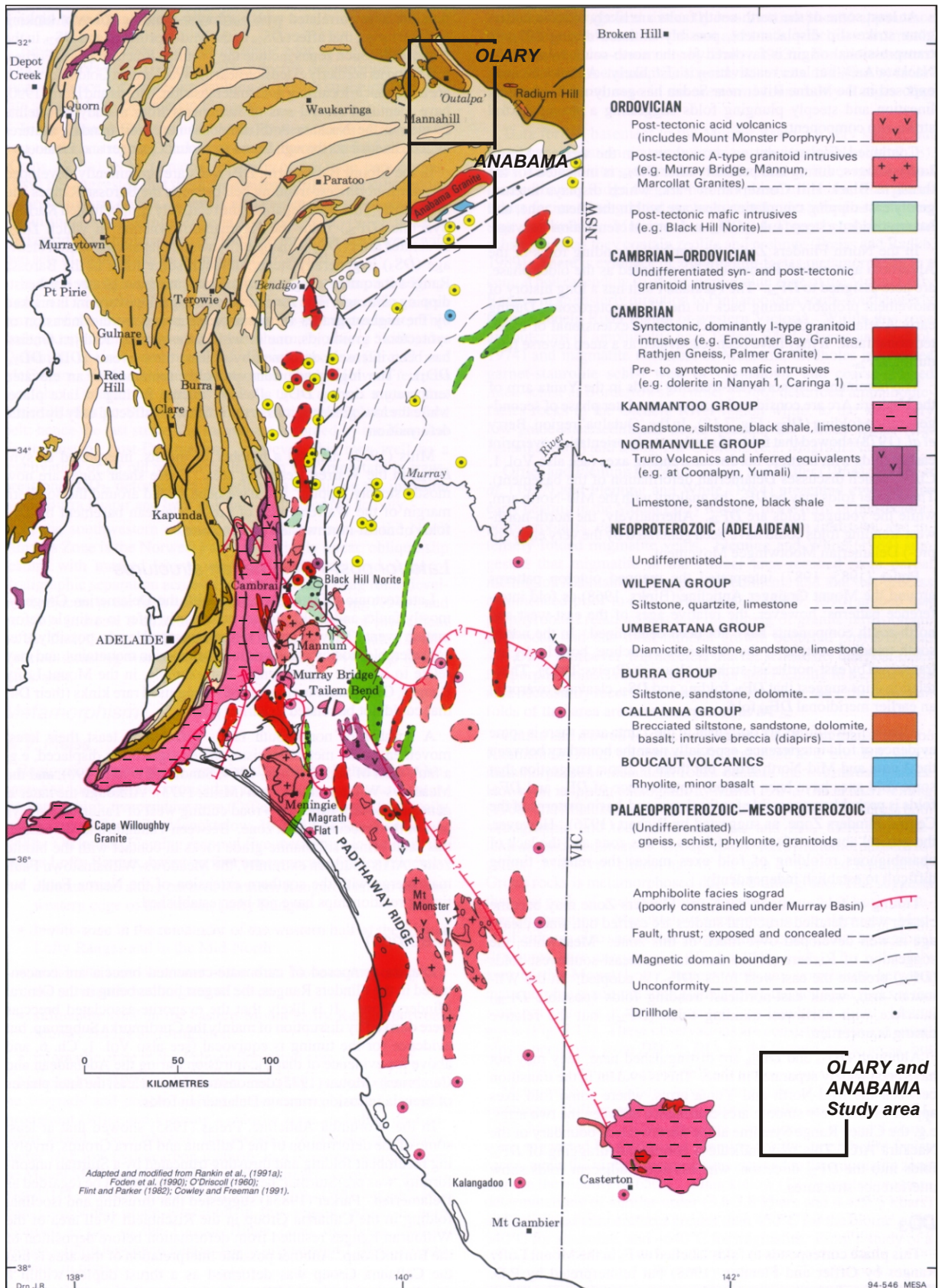
Most voluminous of the granitoids are the syn- to post-tectonic ‘regional granitoids’, and leucocratic, foliated to massive, biotite monzogranites. They are S-type and contain both muscovite and biotite. They appear to be broadly synchronous with high-grade metamorphism and deformation, and with the Hiltaba Suite-Gawler Range volcanic magmatic event at 1595-1585 Ma (Flint, 1993) and associated Olympic Dam-style mineralisation on the Gawler Craton (Cross et al., 1993). Pegmatites are common and widespread, and appear to be related to the regional granitoid magmatic event (Robertson et al., 1998).

Deformation was intense and complex, with three deformation phases in the Mesoproterozoic Olarian Orogeny and two in the Palaeozoic Delamerian Orogeny (Robertson et al., 1998). The strongest deformation (OD₁₋₂) coincided with peak prograde metamorphism (variable, up to upper amphibolite facies), dated at 1600±8 Ma at Broken Hill (Page and Laing, 1992). OD₃ deformation produced many folds and is associated with retrogressive greenschist and lower amphibolite facies metamorphism and development of retrograde shear zones (Robertson et al., 1998).

The Olary Domain has numerous occurrences of Cu, Zn, Pb, U and Au mineralisation associated with sulphidic, calc-silicate and albitic units. Copper and Au also occur in stratabound quartz-magnetite bodies lower in the stratigraphic sequence. Discordant, epigenetic, base-metal and auriferous veins are also common and are related to the retrogressive phase of the Olarian and Delamerian orogenies. In general, the Curnamona Province is prospective for stratiform and stratabound Pb-Zn, and Olympic Dam and Cloncurry Belt style Cu-Au(-U) mineralisation (Robertson et al., 1998).

To the south, the Nackara Arc is an arcuate belt of folded Adelaidean metasedimentary rocks on the eastern margin of the Adelaide Geosyncline, extending from Burra in the south to Olary in the north (Figure 3; Preiss, 1987; Morris and Horn, 1990). The lowest member of the stratigraphy is the Burra Group, comprising sandstone, siltstone, limestone and dolomite. It is overlain unconformably by the Umberatana Group, a series of glacial, fluvio-glacial and interglacial sediments, including tillites, siltstones, sandstones, shales, arkoses and quartzites. The youngest unit, the Wilpena Group, consists of sandstones and siltstones with limestones and dolomites.

Broad upright folds, with an axial planar slaty cleavage, formed during the Delamerian Orogeny. Burra Group rocks are usually located in the cores of regional anticlines, whereas Wilpena Group rocks occur in the cores of synclines (Morris and Horn, 1990).



Gold mineralisation is widespread and occurs mainly in the Umberatana Group, which accounts for 85% of the Au produced from the Nackara Arc (Morris and Horn, 1990). However, Au mineralisation also occurs in Burra Group rocks (e.g., at Wadnaminga). According to Morris and Horn (1990), Au deposits have a strong correlation with northwesterly-trending lineaments which tend to have a radial distribution indicating deep-seated tensional features related to the curvature of the arc. Significant Cu mineralisation in the Burra Group rocks occurs at Burra at the junction of two major lineaments, associated with subvolcanic intrusive rocks and hydrothermal alteration within the Skillogalee Dolomite (Olliver and Preiss, 1990). At Anabama Hill and Netley Hill, the Delamerian Anabama Granite contains porphyry-style Cu-Mo mineralisation.

1.3 Objectives and work programme

The principal geochemical objectives of this study are to provide drill targets at the Faugh-a-Ballagh and Blue Rose prospects and to provide a basis for further geochemical exploration in the Olary region. Specific objectives include:

- (i) determine the effectiveness of calcrete, soil and/or other regolith materials as sampling media in different types of terrain: in areas with abundant outcrop (Faugh-a-Ballagh, Olary Silver Mine, New Milo-Great Eastern) and in terrain with thin to deep cover (Blue Rose); and
- (ii) transfer information to sponsors and, after the confidentiality period has elapsed, to the exploration industry via an open file report.

There were two phases of fieldwork: mid-August to mid-September, and late October to early November, 2000. The first phase comprised auger drilling at Wadnaminga and Blue Rose, calcrete sampling at Wadnaminga, rock-chip and stream-sediment sampling at Faugh-a-Ballagh, orientation soil traverses at Faugh-a-Ballagh and Olary Silver Mine, and sampling of soil, lag and anomalous Cu-rich intervals in RC drill holes at Blue Rose. During this phase, fieldwork for the regolith-landform mapping at 1:100 000 Olary and Anabama sheets was carried out. During the second phase, the RC drill holes at Blue Rose were logged, chip reference samples of all drilling were collected, and selected intervals were sampled, and infill soil samples and samples for partial leaches at Blue Rose, and <6 mm soils at Faugh-a-Ballagh were collected. All samples collected have been archived at the PIRSA core library in Adelaide.

2 STUDY METHODS

2.1 Regolith mapping

The mapping of regolith-landform units in the Olary project area was primarily based on satellite TM7 imagery and radiometric data, with reference to aerial photography. Fieldwork was carried out to identify major regolith-landform units and their appearance on satellite images. The project region was visited via all accessible roads and tracks. Based on the interpretation of the satellite images and field observations, the regolith-landform maps of Olary (6933) and Anabama (6932) were produced to the scale of 1:100 000, covering about 5170 km² (Appendix 8). Three selected sites (Faugh-a-Ballagh, Blue Rose, and Wadnaminga), each about 3 x 3 km in size, were mapped at 1:5000.

Regolith classification is based on the erosional and depositional regimes modified from Anand et al. (1989, 1993, 1997; RED scheme). If a particular profile has lateritic materials or duricrust on mottled and/or bleached saprolite, the regolith unit was classified by the RED scheme as belonging to the relict regime, whereas if the upper part of the profile was absent, the unit was classified within the erosional regime. Similarly, if the surficial regolith comprised material of exotic derivation, the unit was classified within the depositional regime.

2.2 Sample collection

Five hundred and sixty-eight samples were collected at Wadnaminga, Faugh-a-Ballagh, Olary Silver Mine and Blue Rose, including:

- (i) 59 rock-chip samples: Wadnaminga (6), Faugh-a-Ballagh (32), Olary Silver Mine (4), Blue Rose (3) and regional (14);
- (ii) 43 calcrete samples: Wadnaminga (38) and Blue Rose (from a shallow pit: 5);
- (iii) 204 <2 mm soil samples (0-10 cm depth) from Wadnaminga (41), Faugh-a-Ballagh (117) and Blue Rose (46);
- (iv) 21 orientation soil-lag samples along two lines: Olary Silver Mine (9) and Faugh-a-Ballagh (12);
- (v) 16 stream sediment samples: Faugh-a-Ballagh;
- (vi) 155 >6 mm augered hole samples: Wadnaminga (51) and Blue Rose (124, including 20 of the <6 mm fraction);
- (vii) 20 2-6 mm lag samples: Blue Rose;
- (viii) 22 samples of relatively high-grade Cu intersections from RC drill holes: Blue Rose;
- (ix) 21 <2 mm soil samples (10-20 cm depth) for partial leaches: Blue Rose;
- (x) 7 samples (three stream sediments and four soils) for magnetic and non-magnetic fractions: Faugh-a-Ballagh.

2.2.1 Soil and lag collection

Lag was swept from the surface with a plastic brush and pan and about 0.5 kg of the 2-6 mm fraction was sieved (plastic and nylon sieves) and bagged on site. Soil was sampled from a shallow hole (to 10 cm depth) from which about 2 kg of <2 mm material was collected. In the vicinity of old drill holes, care was taken to avoid contamination from the spoil.

For the two orientation soil-lag lines, about 5 kg of material was collected at each site. At Faugh-a-Ballagh, three size fractions were collected: bulk <6 mm (about 1 kg), 2-6 mm lag (about 0.5 kg), and <2 mm soil (about 4-5 kg). At the Olary silver mine, only the <6 mm fraction was collected because samples were slightly damp and could not be properly sieved in the field. The samples were later sieved into 2-6 mm and <2 mm fractions in the laboratory after the samples had dried (40°C).

The soil samples for the partial leaches were collected at 10-20 cm depth and an aliquot (about 200 g) of the <2 mm fraction was analysed.

2.2.2 Stream sediment collection

Samples were collected at 50-200 m intervals in the creek at the foot of Faugh-a-Ballagh Hill. Only the active parts of the creek were sampled and heavy mineral trap sites, erosional gullies and other irregularities in the creek were avoided. Each sample was collected from 0-10 cm depth across the full width of the creek, taking care to avoid contamination from the banks or from alluvium. About 3 kg of the <2 mm fraction was collected (using plastic and nylon sieves).

2.2.3 Calcrete sampling

Calcrete samples were only specifically collected at Wadnaminga, either from along shallow pits along the old workings, or along the creeks. About 2 kg of material was collected at each site as a grab sample. Many of the augered samples at Blue Rose and Wadnaminga were calcareous.

2.2.4 Augered samples

The auger holes were drilled to depths between 0.2 m and 0.7 m, depending on the degree of penetration. The sample was sieved through a 6 mm plastic sieve, and both fractions were retained. Except where stated, only the >6 mm fraction was analysed.

2.3 Sample preparation

In the laboratory, a 200 g aliquot of sample was split and ground by AMDEL Laboratories Ltd in Adelaide. The samples were dried and about 200 g was milled in a Cr-free disc mill to a nominal 90% passing through 106 μm .

The <2 mm fractions (soils and stream sediments) were sieved in nylon sieves at CSIRO, Floreat Park, Western Australia, to 0.5-2 mm, 180-500 μm , 75-180 μm , and <75 μm . These were milled and analysed at AMDEL.

2.4 Partial analyses

Twenty-one samples were submitted for partial leaches and were collected along grid line 428820E at Blue Rose, over the mineralised zone intersected by RC drilling. The thickness of transported overburden varies between 8 and 19 m along the traverse, with 8-9 m over the mineralised zone. The following proprietary leaching solutions (from AMDEL's Deepleach series) were used: water (with 18 M Ω resistivity, i.e. 'ultra-pure' or 'millipore'), potassium cyanide, and sodium pyrophosphate (for Ag, As, Au, Bi, Cu, Fe, Mo, Mn, S, Se, Te and Tl), and solutions A (Cu), B (containing cyanide and potassium dichromate; Au) and F (As, Mo, Fe and Se), utilising the mobile metal ion (MMI) technique. The procedure for the water, potassium cyanide and sodium pyrophosphate leaches is that a 20 g sample is mechanically leached with 50 ml of solution by rolling for 8 hours. The solution is allowed to settle until clear (up to 2 hours) and a 15 ml aliquot is extracted for analysis. In certain circumstances (e.g., the potassium cyanide leach), colloids, which do not settle, may form and require centrifugation, prior to analysis. For MMI, a 50 g sample was statically leached in 50 ml of solution for 8 hours; a 15 ml aliquot of solution was taken and centrifuged to remove any suspended solids.

All elements were analysed by inductively coupled plasma mass spectrometry (ICP-MS) at AMDEL.

2.5 Geochemical analysis

The milled aliquots were analysed by atomic absorption spectrophotometry (AAS), inductively coupled plasma optical emission spectrometry (ICP-OES) and inductively coupled plasma mass spectrometry (ICP-MS) by AMDEL. The digestions, methods and respective element suites were:

- (i) Au – aqua regia digest (a mixture of nitric and hydrochloric acids) of sample (up to 50 g), extraction into di-isobutyl ketone (DIBK), and analysis on a graphite furnace AAS;
- (ii) ICP-OES suite (Al, Ba, Ca, Cr, Cu, Fe, K, Mg, Mn, Na, Nb, Ni, P, Pb, S, Ti, V, Zn); sample digestion with hydrochloric, nitric and hydrofluoric acids, with a final dissolution in hydrochloric acid (mixed acid digest);
- (iii) ICP-MS suite (Ag, As, Bi, Cd, Co, Cs, Ga, In, Mo, Rb, Sb, Se, Sn, Sr, Te, Th, Tl, U, W, Y, Hf, Ce, Dy, Er, Eu, Gd, Ho, La, Lu, Nd, Pr, Sm, Tb, Tm, Yb); mixed acid digest;
- (iv) Hg – aqua regia digest followed by generation of cold vapour and analysis by AAS.

Twenty-two samples were also analysed by X-ray fluorescence spectrometry (XRF) at CSIRO for SiO₂, Al₂O₃, Fe₂O₃, MnO, MgO, CaO, Na₂O, K₂O, TiO₂, P₂O₅, Ba, Ce, Cl, Cr, Co, Cu, Ga, La, Ni, Nb, Pb, Rb, S, Sr, V, Y, Zn and Zr on fused borate glass discs.

2.6 Standards and statistical treatment of data

A pulped in-house rock standard (CRC LEME Standard 7) was placed into the analytical stream (every 25 samples) to monitor precision. The results are given in Appendix 7. The recommended values were obtained from XRF and instrumental neutron activation analysis (INAA) data (reliable total analyses). They should not be compared too closely in absolute terms, since the mixed acid digests do not provide total element extractions and consequently element abundances are understated.

Statistical summaries are provided in the relevant appendices. Most data sets are relatively small (<50 samples) and there was generally little difference in the results of the statistical treatment of the data using either cumulative frequencies or probability plots. Consequently, the geochemical data was processed using the former method. For the purposes of this report, the ‘background’ value was taken as the 50th percentile, whereas ‘anomalous’ values were those above the 90th percentile. Spearman Rank correlation coefficients were computed using DataDesk (version 6).

3 REGOLITH MAPPING

3.1 Regolith classification

In the Olary region there are no lateritic materials or ferruginous duricrusts, although there are some bands of ironstone about 0.2 to 2 m wide. Accordingly, there is no relict regime. Due to the uncertainty of the former existence of the upper part of the “standard” profile, or perhaps because duricrusts or saprolite may have never formed on weathered bedrock, weathered bedrock subcrops or outcrops are considered to belong to an erosional regime.

Although the distinction between erosional and depositional units is straightforward in most cases, care should be taken when examining locally-derived sediments on saprock or saprolite. Strictly speaking, such sediments are derived from the weathered rocks directly underneath and thus, in situ materials seldom occur. However, if these sediments have moved only for a short distance from their origin and still reflect the composition of source bedrock, they are classified in the erosional regime. For example, a thin layer of colluvium mixed with locally-derived, weathered materials is regarded as belonging to the erosional regime.

3.2 Regolith landform units

3.2.1. Erosional regime

A number of erosional regolith-landform units have been recognised from the 1:100 000 regolith mapping. A complete list is given in Appendix 6.

Units of the erosional regime occur in a variety of landform settings (e.g., high hills, hills, low hills, ridges, low rises, undulating erosional plains, etc.), and are developed on rocks of all ages. For example, Burra Group rocks tend to form low hills and long ridges (unit Eobh), or the Anabama Granite forms prominent hills (Figure 5b), with little regolith derived from the mechanical and chemical breakdown of the granite (unit Eogh). However, not all erosional features form prominent features, e.g., unit Escp (colluvial and wash plains (comprising regolith materials of proximal source)). For many of these erosional units, outcrops are abundant and soils are typically skeletal. Thick regolith is relatively rare.

Carbonate (calcrete) is generally only rarely developed in regolith units on Olary Domain rocks, but is relatively abundant over Adelaidean rocks. The reasons for this are uncertain, but may involve greater rates of erosion in the Olary Domain, where there is generally more contrast in topography, such that calcrete horizons have not been preserved. Another possibility is that sources of Ca (e.g., carbonate rocks) are more abundant in Adelaidean terrains.

3.2.2. Depositional regime

Regolith-landform units of the depositional regime have been recognised from the 1:100 000 regolith mapping. These landforms include alluvial fans (unit Daf), floodplains (unit Dafp), and modern stream channels (unit Dss). These features are generally related to modern drainages and occur in areas of subdued topography. An exception is the valley silcrete and silicified sands and gravels (unit Dst), which may form low rises.

Carbonate is relatively abundant in brown soils and alluvium (units Daf, Dafp and Dap), including those in the Olary Domain.

4 WADNAMINGA

4.1 Geological setting

Gold mineralisation in the Wadnaminga Goldfield, about 30 km south of Olary, is hosted by metasedimentary rocks of the Belair Subgroup, a subdivision of the Adelaidean Burra Group (Olliver and Preiss, 1990). The lithologies comprise interbedded flaggy siltstones, quartzite, micaceous phyllite, medium-bedded dolomite, dolomitic siltstone and quartzite, and silty dolomite, and occur along the northern limb of the Wadnaminga Anticlinorium (Forbes, 1991). Morris (1975) divided the rocks in the Virginia-New Milo-Great Eastern-Thunder Queen area into several lithological groups (Figure 4); from the youngest unit to the earliest, the sequence is:

Belair Subgroup:

- (i) massive dolomite with mica flakes and grey calcareous siltstones; at the base interbedded phyllites and dolomites;
- (ii) interbedded phyllites and dark grey sandy siltstones;
- (iii) interbedded sandy dolomites, calcareous siltstones, dark grey siltstones with Fe oxide pseudomorphs after pyrite, calcareous phyllites and, at the base, a marker horizon of sandy dolomite (that weathers to a distinctive “honeycomb” texture);
- (iv) grey sandy siltstones and phyllites, becoming calcareous at the base.

Saddleworth Formation:

- (v) dark grey siltstone (with quartz veining and Fe oxide pseudomorphs after pyrite), siltstones and phyllites;
- (vi) interbedded dark calcareous siltstones, coarse-grained micaceous phyllites and sandy siltstones.

4.2 Mineralisation

Gold mineralisation extends along a strike length of 12 km along the northern margin of the anticlinorium. Records indicate that about 20 000 t of ore (at an average grade of 27 ppm Au) have been mined from 1888 to 1936, predominantly from the New Milo and Virginia deposits (Morris, 1975). In this more productive northeastern part of the field, quartz lodes occur in sandy siltstone, phyllite and dolomitic groups of the Belair Subgroup and were productive over strike lengths of 300 m (Morris, 1975). Auriferous quartz veins commonly occur in dark grey, non-calcareous siltstone, typically with disseminated pyrite. The veins are up to 2 m wide (average 30 cm) and commonly fill *en echelon* tension gashes. The rocks strike at about 075°-080° and dip at about 70° NNW, whereas the lodes trend WSW, dip at about 30°S and cross-cut lithological boundaries at low angles. Two generations of veins occur (Figure 5a): an earlier, barren set, and a later, mineralised generation, which may cross-cut earlier veining.

The main minerals found within the veins are quartz and pyrite, with minor galena, chalcopyrite, arsenopyrite, anglesite, cerussite, malachite, goethite, hematite, jarosite, scorodite, calcite, siderite and native gold (Morris, 1975). Petrographic evidence (Henley and Moeskops, 1976) indicates that Au occurs both as native gold and electrum, and is typically very fine-grained (<25 µm). It occurs mainly as inclusions or fracture infillings in pyrite, but some also occurs associated with quartz (Gartrell, 1934). There are two generations of electrum (Henley and Moeskops, 1976):

- (i) an earlier generation, containing 10-20% Ag, coeval with the initial deposition of pyrite and vein quartz; and
- (ii) a later generation, containing about 30% Ag, which mainly post-dated the fracturing of pyrite.

Most of the gold observed is of the later generation. Secondary native gold, found in the weathered portions of the veins, associated with Fe oxides, anglesite, scorodite, etc. contains no detectable Ag (<0.3%; Henley and Moeskops, 1976).

Two types of fluid inclusions occur (Henley and Moeskops, 1976):

- (i) primary inclusions (with no CO₂) from auriferous quartz veins; homogenisation temperatures 380°-510°C; salinities: 15-20 wt equiv. % NaCl in two-phase inclusions, and >26% in three-phase inclusions;
- (ii) secondary inclusions; homogenisation temperatures of 180-360°C, suggesting a metamorphic event post-dating crystallisation of the quartz.

The high fluid salinities and high homogenisation temperatures led Henley and Moeskops (1976) to tentatively suggest that the Anabama Granite to the south (Figure 5b) may have been the source of the fluids.

Primary dispersion haloes around the veins are narrow (<50 cm; Henley and Moeskops, 1976). Gold showed high significant positive correlations with Ag, As, Bi, Cu, Hg and Pb.

Soil sampling (size fraction not specified) along ten traverses (with some infill around Thunder Queen) was carried out by Morris (1975). Samples were collected at 50 m intervals and continuous rock-chip samples taken between soil sample sites. The soils were analysed for As, Au, Cu, Pb and Zn. Morris' (1975) conclusions were that, although most Au analyses were below detection limit (50 ppb), samples with concentrations above this value occurred close to known mineralisation and that As (>46 ppm) was an excellent pathfinder for Au mineralisation. Samples with anomalous Cu (>46 ppm), Pb (>211 ppm) and Zn (>82 ppm) concentrations were collected close to old workings; however, a few anomalies exist where there is no known mineralisation.

4.3 Regolith

Most of the area is in an erosional regime (Figure 6), with minor sediments along the creeks. The dominant landform units are hills formed by weathered siltstones, dolomites and phyllites of the Burra Group, with thin soils and abundant lag. On the lower slopes, particularly in the south, thin colluvial-alluvial soils overlie bedrock. The area is dissected by two major creeks with associated alluvium and fluvial gravels on the floodplains.

The soils are typically calcareous. A variety of calcrete types was collected. These are:

- (i) nodular (Figure 5c);
- (ii) powdery;
- (iii) massive, replacing bedrock;
- (iv) coating and/or replacing bedrock; locally associated with brecciation and re-cementation textures;
- (v) massive, cementing gravels (pebbles of quartz and siltstone; Figure 5d);
- (vi) platy or laminar, on bedrock;
- (vii) on joints in bedrock.

Powder calcrete commonly overlies more indurated forms. Nodular calcrete was the most common, particularly in augered samples. The other varieties appear to be more common on outcrops or in creek beds.

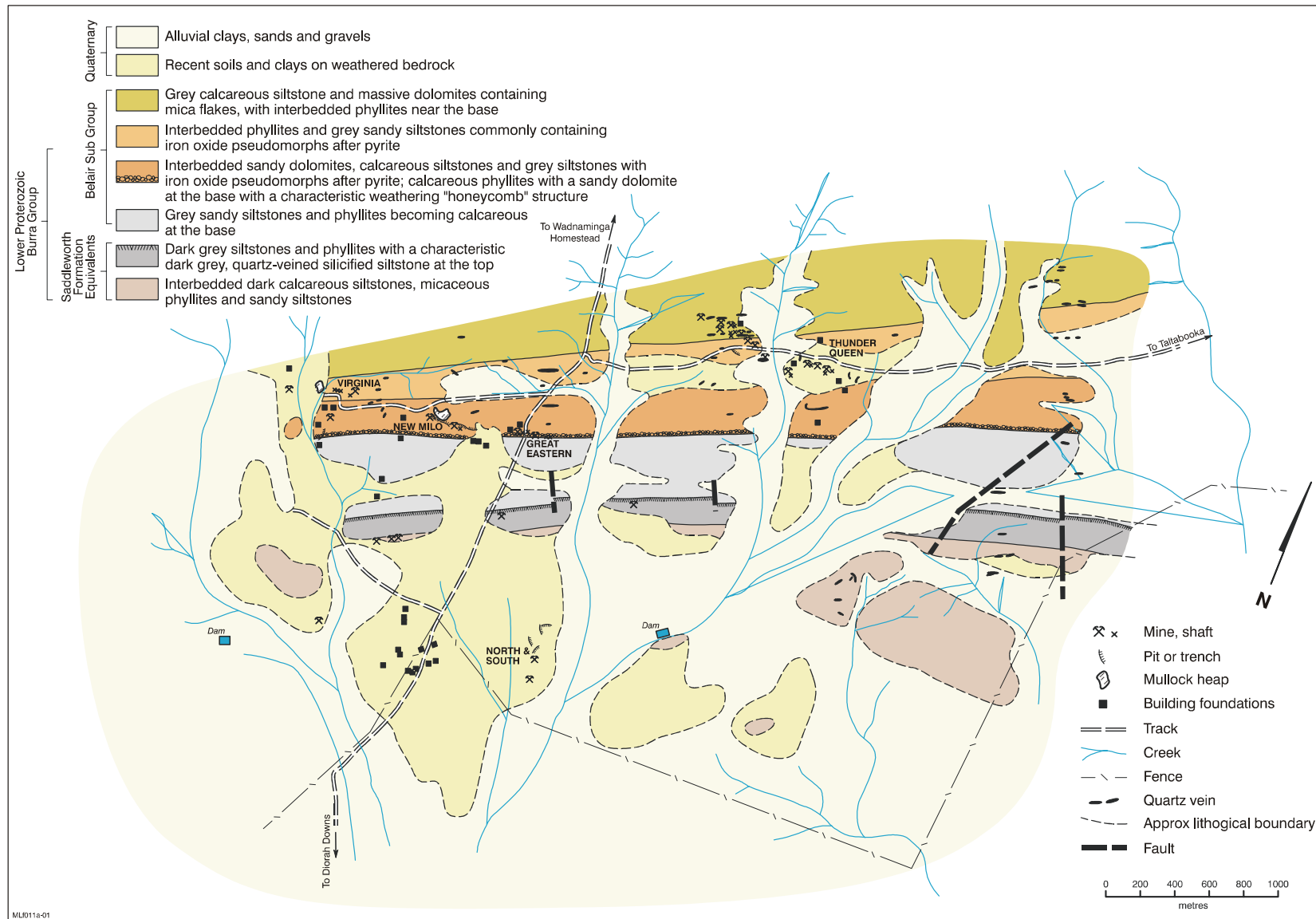


Figure 4: Geological map of part of the Wadnaminga Goldfield in the vicinity of the Virginia, New Milo, Great Eastern and Thunder Queen mines (after Morris, 1975). See Figure 1 for location of the study area.



Figure 5 Wadnaminga. **a**, a barren earlier quartz vein, with later mineralised vein with old workings; Great Eastern mine; **b**, siltstone outcrops and abundant lag at the Great Eastern mine; in the middle distance, the hills are Burra Group metasedimentary rocks, whereas the hills on the horizon are Anabama Granite; **c**, the soil profile at Great Eastern: an upper horizon of calcareous soil (10-20 cm thick), overlying a layer of nodular calcrete (about 20 cm thick), resting on weathered siltstone (6398794N, 429316E); **d**, massive calcrete in creek cementing siltstone and quartz fragments (6399009N, 429125E).

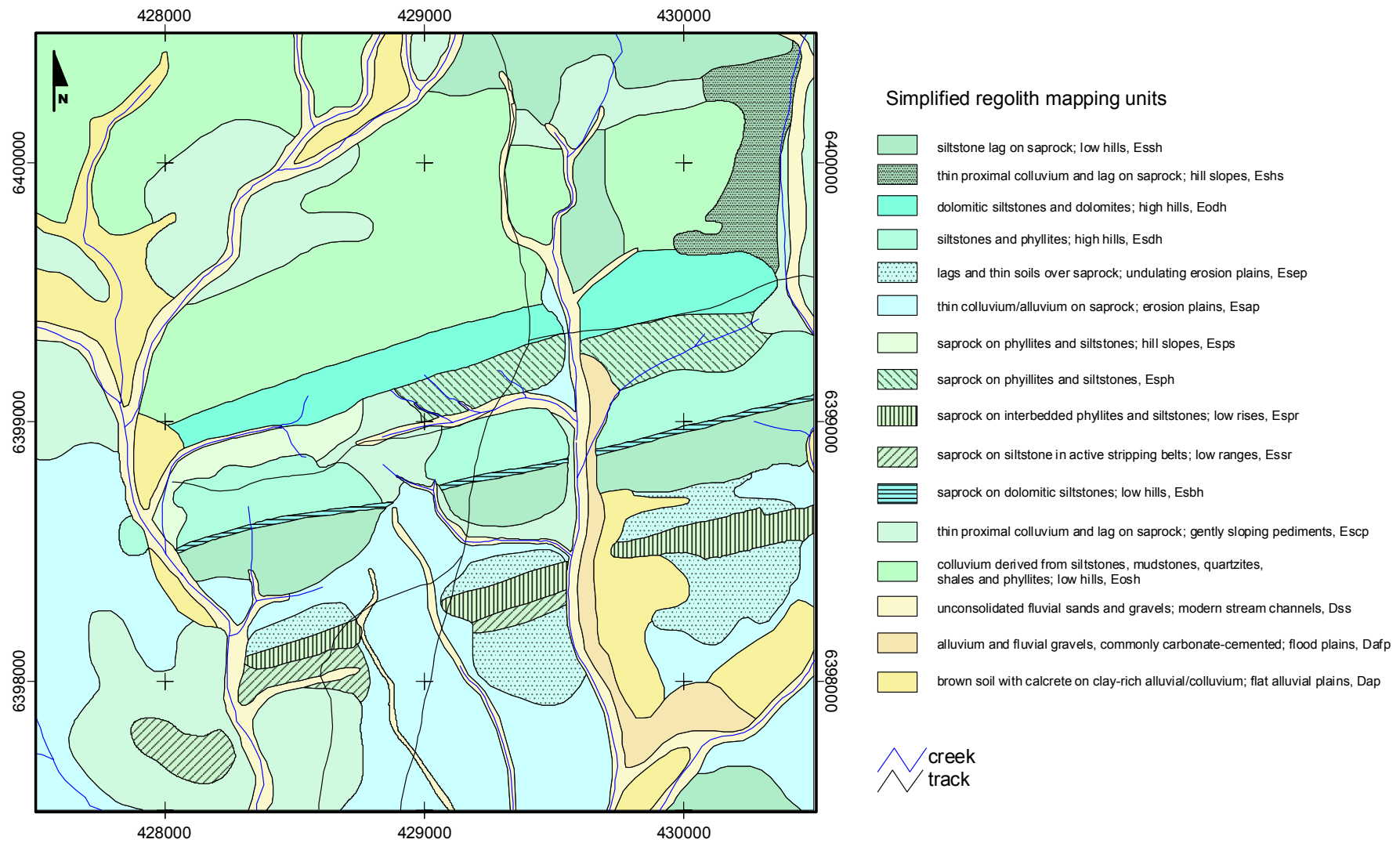


Figure 6: Regolith-landform map of part of the Wadnaminga Goldfield in the vicinity of the Virginia, New Milo, Great Eastern and Thunder Queen mines. Full regolith landform unit descriptions are found in Appendix 6.

4.4 Vegetation

The terminology for the vegetation structural classification system has been adapted from Keighery (1994). The mine area at Wadnaminga is a *Maireana sclerolaenoides* and *Sclerolaena patentiuspis* Low Shrubland over *Carrichtera annua* Open Herbland. Large trees of *Eucalyptus socialis* and *Myoporum platycarpum* occur around the mine, with examples of *Eucalyptus socialis* and *Eucalyptus gracilis* Open Tree Mallee on rises about a 1 km from the mine. Treeless hill tops are *Sida* sp. Open Herbland. The large creek west of the Virginia mine consists of *Eremophila sturtii* and *Acacia victoriaea* Open Tall Shrubland over *Maireana pyramidata* Low Open Shrubland over Very Open Grassland.

4.5 Geochemistry

4.5.1 Sampling

The following samples were collected:

- (i) 6 rock-chip samples; one sample of high-grade ore from New Milo, and four siltstones and carbonate-bearing rocks from the Great Eastern and New Milo dumps, and one sample of quartz-carbonate veining from the Great Eastern dump;
- (ii) 38 calcrete samples, from the walls of shallow pits along the lodes at Great Eastern and New Milo, and from creeks around the periphery of the mineralised area;
- (iii) 51 augered samples from holes along three traverses; samples were collected from depths between 0.2 and 0.65 m;
- (iv) 41 soil samples from 0-10 cm depth (along the auger lines); these samples were not analysed, since the auger samples were considered to have defined the Au anomalies.

4.5.2 Rock-chip sample geochemistry

The high-grade ore sample comprises very coarse-grained, massive pyrite with minor galena in quartz veining from the New Milo workings. The sample contains 49 ppm Au, 10 ppm Hg, 5150 ppm Pb, 14.5 ppm Ag, 2050 ppm As, 3 ppm Bi, 8 ppm Cd, 165 ppm Cu, 8 ppm Sb, 7 ppm Se, 9.74% S, and 440 ppm Zn; minor amounts of Te (0.4 ppm) and In (0.6 ppm) also occur. This element suite was considered to represent the geochemical signature of the mineralisation, since this corresponds to the data collected by Henley and Moeskops (1976).

The quartz-carbonate vein sample contains Au (34 ppb), Pb (125 ppm), As (23 ppm) and Cd (2.4 ppm). The siltstones contain minor Au (<5 ppb) and As (<5 ppm), but relatively large concentrations of Al (6.44-7.45%), K (2-2.4%), Mg (3.64-4.54%), Ti (3800-4250 ppm), Co (20-31 ppm), Rb (88-120 ppm) and Th (8.5-14 ppm) when compared to the veins. The “honeycomb”-textured rock (a dolomite, according to Morris (1975)) contains only 0.325% Mg and 0.565% Ca, but has relatively significant concentrations of U (8 ppm) and LREE.

4.5.3 Calcrete geochemistry

4.5.3.1 Element associations

The geochemical associations are essentially split into two groups: those elements associated with calcrete, and those that are not. However, because the calcrete has been superimposed as a cement on an existing geochemical pattern and acts as a diluent for most elements, the resulting associations are more a function of the variability of Ca concentrations than actual relationships; in addition, closure effects cannot be discounted. This results in the association of elements of apparently disparate geochemical behaviour, e.g., Zn exhibits a strong positive correlation with Au, Al, Cu, Fe, K, Mg, Mn, Ni, Pb, V, Ag, As, Ga, Rb, Tl and W, and a weak positive correlation with Cr, Na, Cd, Hf and some REE.

4.5.3.2 *Elements associated with mineralisation (Ag, As, Au, Bi, Cd, Cu, Hg, In, Pb, Sb, Se, Te, Zn)*

The best responses are generally found in samples from calcrete above the lodes at New Milo and Great Eastern. This is particularly the case for Au, As, Pb and, to a lesser extent, Cu and Zn. Of the remaining elements, Hg, Sb, Se and Te are below detection limits in calcrete, and In shows no clear association with the lode horizon (with many samples below detection limit), despite anomalous concentrations in high-grade ore. Cadmium and Bi concentrations are sporadically anomalous along the lode horizon, but S concentrations are generally minor.

All these elements (especially As, Cu and Zn) have negative correlations with Ca, suggesting that the calcrete has diluted an existing geochemical dispersion pattern. The concentrations of ore-associated elements in the calcrete are presumably related to unreplaced quartz veinlets and hydrothermally-altered wallrock fragments within the calcrete samples collected.

Silver: Silver concentrations are generally minor (<0.11 ppm). The greatest concentrations occur along the Great Eastern lode (Figure A1.4.3). There are no significant concentrations in samples from the creeks, the only sample above detection occurring in the creek to the north of Great Eastern.

Arsenic: Significant concentrations (>60 ppm) occur along the New Milo and Great Eastern lodes (Figure A1.4.5). In the creeks, concentrations above background (>7 ppm) occur only sporadically. Arsenic exhibits positive correlation with Ba, K, Mg, Pb, and Rb, and negative correlation with Ca.

Gold: Highly anomalous Au concentrations (>405 ppb) occur along the New Milo and, to a lesser extent, along the Great Eastern, lodes (Figure 7). Away from the main mineralisation lodes, Au concentrations rapidly decline although it is still detected in calcretes obtained from the base of creeks. Some of the higher concentrations in the creek to the south of the lode may in part be due to contamination from tailings. There are no Au concentrations above 18 ppb in samples from the creeks, including those downstream from old tailings. In general terms, Au appears to be associated with calcrete but may not be restricted to it since definitive profile samples were not taken. Gold exhibits positive correlation with Ba, K, Mg, Rb (alteration halo), but shows negative correlation with Ca.

Bismuth: Apart from one sample at Great Eastern, all samples along the lode horizon are below background (0.18 ppm; Figure A1.4.8). Only one relatively anomalous sample (>0.25 ppm) occurs in the creeks, near Virginia, and may relate to mineralisation.

Cadmium: Cadmium concentrations are relatively minor (<0.23 ppm), with relatively greater concentrations along the Great Eastern lode (Figure A1.4.10). In the creeks, most samples are below background (0.18 ppm).

Copper: Relatively anomalous concentrations (>37 ppm) occur along the New Milo and Great Eastern lodes (Figure A1.4.15). Apart from a sample close to the Virginia workings, Cu concentrations in the creeks are generally below background (19 ppm). Copper exhibits positive correlation with Al, Co, Cr, Fe, Ga, K, Mn, Ni, Rb, V and Zn.

Lead: Significant Pb concentrations (>66 ppm) occur along the New Milo and Great Eastern lodes (Figure A1.4.37). Most Pb concentrations in samples from the creeks are below background (6.5 ppm). Lead exhibits positive correlation with As and Sr.

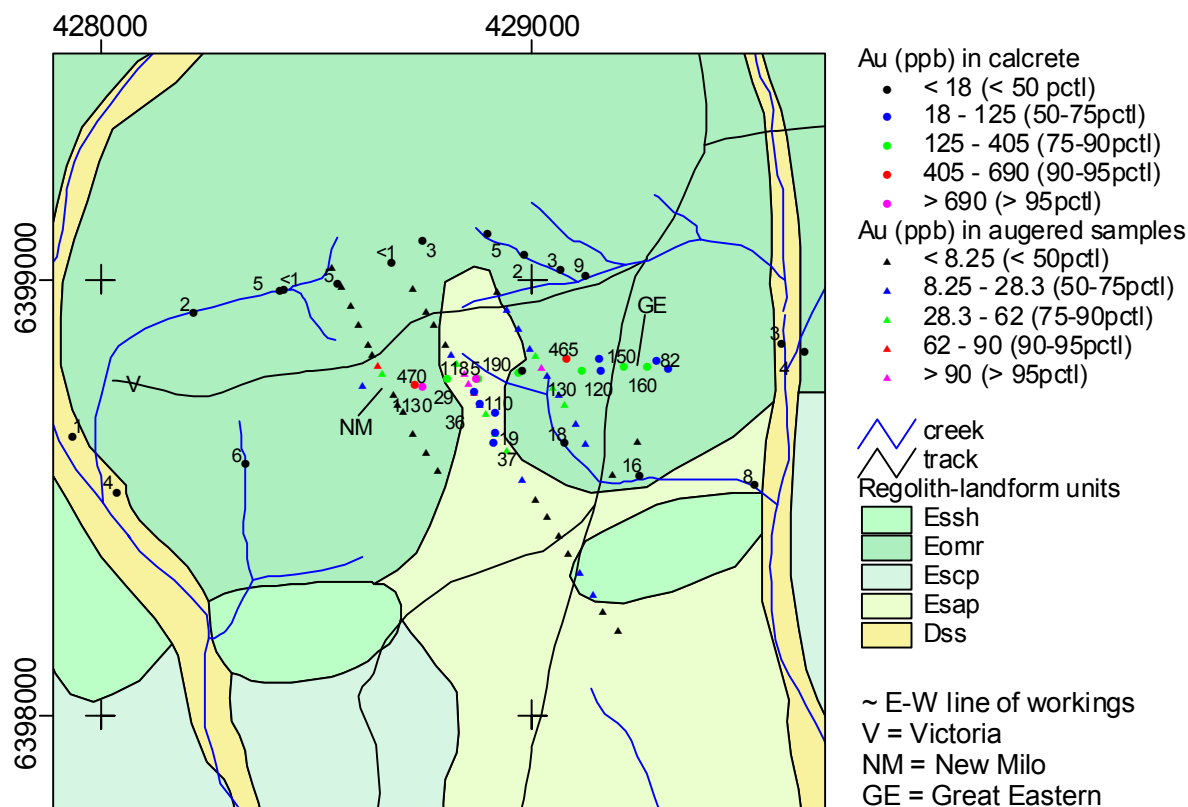


Figure 7: Distribution of Au (ppb) in augered and calcrete samples, Wadnaminga. Gold concentrations for calcrete are labelled. Full regolith landform unit descriptions and are found in Appendix 6.

Zinc: Significant Zn concentrations (>126 ppm) occur in samples along the New Milo and Great Eastern lodes (Figure A1.4.57). Only locally are Zn concentrations above background (32 ppm) in calcrete from the creeks. Zinc exhibits positive correlation with Al, Cu, Ga, K, Mn, Na, Ni, Pb, Rb and V, and negative correlation with Ca and S.

4.5.3.3 Elements associated with hydrothermal alteration (Ba, K, Mg, Na, Rb, Sr, Tl, U, W)

All the elements associated with hydrothermal alteration (especially K, Na, Rb and Tl) have negative correlations with Ca, suggesting that the calcrete may have diluted an existing pattern of geochemical dispersion. The concentrations of the elements associated with hydrothermal alteration in the calcrete are presumably related to unreplaced quartz veinlets and hydrothermally-altered wallrock fragments within the calcrete samples collected.

The greatest concentrations of these elements tend to occur along the Great Eastern and New Milo lodes (related to narrow alteration haloes around the the lodes) or in the creek draining the Great Eastern lode or, less commonly, in nodular calcrete to the south of the New Milo lode. Despite the association of Sr with Ca and S in Figure 8, Sr shows no significant correlation with Ca and S, and it is more closely associated with Ba.

4.5.3.4 Elements denoting lithology (Al, Co, Cr, Cs, Fe, Ga, Hf, Mn, Mo, Ni, P, REE, Sn, Th, Ti, V, Y)

Elements denoting lithology (especially Al, Cr, Cs, Fe, Ga, Mo, Ni, REE, Sn, Ti and V) show negative correlation with Ca. The lack of correlation with Ca suggests that the calcrete has diluted the

geochemical signature of bedrock. The concentrations of these elements are probably related to the presence of unreplaced rock fragments within the calcrete samples or clays in the powdery calcrete.

4.5.3.5 Elements associated with calcrete (Ca, S)

Calcium: Calcium concentrations are significant (generally >20%), with the greatest concentrations in calcrete from the creeks in the north and east (Figure A1.4.9). There is no general correlation between Ca concentration and calcrete type, except that there is less Ca in those samples with rock inclusions and in powdery calcrete from the creeks (where carbonate contents are <10%). Calcium concentrations along the lodes are relatively less, due to a significant lithological component. Calcium exhibits positive correlation with S, suggesting the presence of small amounts of gypsum. It shows negative correlation with most other lithology-related elements, particularly with Al, Co, Cr, Cs, Cu, Fe, Ga, K, Mg, Na, Ni, Rb, some REE, Th and V.

Sulphur: Sulphur concentrations are greatest (>520 ppm) in calcrete samples from the creeks (Figure A4.1.40) and in nodular calcrete south of the New Milo lode. Sulphur contents of samples along the lodes are unexpectedly relatively minor (<430 ppm). Sulphur is strongly positive correlated with Ca and so shows negative correlation with most other lithology-related elements, particularly with Al, Cr, Fe, Ga, K, Rb and V.

4.5.3.6 Element displaying no systematic distribution (Nb)

Niobium: Only one sample is above detection (5 ppm) and occurs in powdery calcrete in the drainage south of Great Eastern (Figure A1.4.33).

4.5.4 Geochemistry of augered samples

4.5.4.1 Elements associated with mineralisation (Ag, As, Au, Bi, Cd, Cu, Hg, In, Pb, Sb, Se, Te, Zn)

The geochemical association is shown in Figure 8. The best responses are generally found for As, Au, Bi, Pb and Zn. Despite anomalous Hg, Sb, Se and Te in high-grade ore, concentrations of these elements are below detection. Concentrations of In are close to detection (0.05 ppm) and the distribution of In shows no clear relationship to the positions of the lodes.

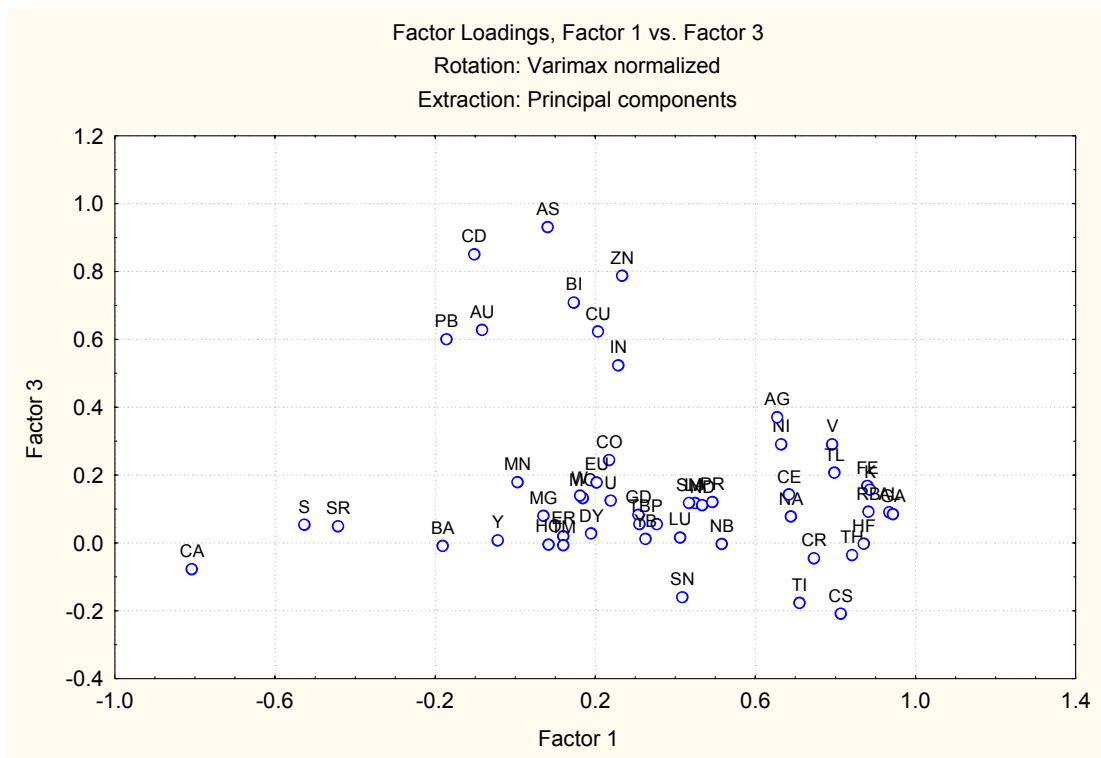


Figure 8: Plot of Factor 1 versus Factor 3 from principal component analysis of augered samples. Note the general groupings of elements: Ca-S (associated with calcrete), As-Au-Bi-Cd-Cu-In-Pb-Zn (associated with the lode horizons), and two groups with lithological associations.

Silver: The distribution of Ag is irregular and displays no clear pattern in relation to the position of the lodes (Figure A1.4.3).

Arsenic: The distribution of As highlights the positions of the New Milo and Great Eastern lodes (Figure A1.4.5). Arsenic defines a dispersion halo 50 m wide at >32 ppm, or up to 100 m width at >19 ppm. A sample with >32 ppm occurs towards the southern end of the middle line and is associated with small old workings. Arsenic exhibits positive correlation with Au, Ba, Cd and W.

Gold: The distribution of Au outlines the positions of the lodes (Figure A1.4.6) and defines a dispersion halo 50 m wide at >62 ppb, or up to 100 m wide at >28.3 ppb. Gold exhibits positive correlation with As and Ba, but none with Ca.

Bismuth: The distribution of Bi is irregular but defines a discontinuous dispersion halo about 25 m in width (at >0.43 ppm) along the lodes (Figure A1.4.8). A minor anomaly at the southern end of the middle traverse is associated with a small old working. Although Bi is a potentially useful pathfinder element, its lateral dispersion is limited.

Cadmium: Cadmium defines a relatively broad dispersion halo around the lodes (Figure A1.4.10) at up to 125 m at >0.31 ppm, or about 50 m at >0.67 ppm. A relatively anomalous sample also occurs at the northern end of the middle traverse. Cadmium exhibits positive correlation with As and Au.

Copper: Copper defines a dispersion halo about 50 m wide along the lodes at >43 ppm, but its distribution is irregular (Figure A1.4.15). A single anomalous sample is associated with old workings at the southern end of the middle traverse. There are also potential lithological responses along the drilling traverses at the northern end of the western traverse that could detract from its potential use as a pathfinder.

Lead: Lead defines a dispersion halo up to 75 m in width at >14 ppm along the lodes (Figure A4.1.37).

Zinc: Zinc forms a halo along the lodes (Figure A1.4.57). The halo width is about 75 m at >95 ppm, or up to 125 m at >70 ppm. Zinc exhibits positive correlation with Al, Cr, Fe, Ga, Ni and V, and negative correlation with Ca.

4.5.4.2 *Elements associated with hydrothermal alteration (Ba, K, Mg, Rb, Sr, Tl, U, W)*

Barium: Samples with anomalous Ba occur along the lode horizon (Figure A1.4.7) and define a lateral dispersion halo up to 150 m in width at >465 ppm. The irregular widths of the halo suggest a mechanical dispersion mechanism, in that fragments derived from the lodes and wallrocks have been incorporated into the soil horizon above calcrete. There are also two samples with >545 ppm Ba downslope from the Great Eastern workings. Barium exhibits a strong positive correlation with Au and U.

Potassium: The distribution of K around the lodes is irregular (Figure A1.4.26). The greatest concentrations occur down slope from the Great Eastern lode and may represent wallrock fragments mechanically dispersed and incorporated into soil. Potassium exhibits positive correlation with Al, Ce, Cr, Cs, Fe, Ga, Ni, Rb, Th, Tl, V and Zn, and negative correlation with Ca and S.

Magnesium: Samples with anomalous Mg occur along the lode horizons (Figure A1.4.29), defining a lateral dispersion halo up to 50 m in width (at >2.81%), and also occur downslope from the Great Eastern workings.

Rubidium: The greatest concentrations of Rb (>77 ppm) occur down slope from the Great Eastern lode and at the northern end of the western traverse (Figure A1.4.39). There is no clear spatial relationship between Rb concentration and position of the lode. Anomalous Rb concentrations in the north suggest a lithological component to the dispersion pattern. Rubidium exhibits positive correlation with Al, Ce, Co, Cr, Cs, Fe, Ga, K, Na, Ni, Th, Ti, Tl and V, and negative correlation with Ca.

Strontium: Samples with anomalous Sr occur along the lode horizon (Figure A1.4.45) and define a slightly irregular zone up to 50 m wide at >870 ppm or 100m at >525 ppm. Strontium exhibits positive correlation with Au and S, and negative correlation with Al, Cr, Fe, Ga, LREE, Th and Ti.

Thallium: Thallium forms an irregular halo up to 50 m wide (at >0.28 ppm) along the New Milo lode (Figure A1.4.50) on the central traverse. There also appear to be lithological responses (e.g., at the northern end of the western traverse) that would detract from its potential use as a pathfinder element. Thallium exhibits a strong positive correlation with Al, Cr, Fe, Ga, K, Ni, Rb, Th and V, and negative correlation with Ca.

Uranium: Samples with anomalous U occur along the lode horizons (Figure A1.4.52). The width of the dispersion halo is variable, with a maximum of about 75 m at >1.07 ppm. There appears to have been some down slope dispersion from the Great Eastern lode. Uranium exhibits positive correlation with Rb.

Tungsten: Samples with anomalous W occur along the lode horizons (Figure A1.4.54). The width of the dispersion halo is variable, with a maximum of about 75 m at >1.1 ppm. There also appears to have been downslope dispersion from the Great Eastern workings.

4.5.4.3 *Elements denoting lithology (Al, Co, Cr, Cs, Fe, Ga, Hf, Mn, Mo, Na, Ni, P, REE, Sn, Th, Ti, V, Y)*

The greatest abundances of these elements occur where there is a significant component of soil and/or bedrock (as opposed to dominant calcrete) in the augered sample, generally at the northern and

southern ends of the traverses. There is generally no spatial relationship between element concentrations and the positions of the lodes.

4.5.4.4 *Elements associated with calcrete (Ca, S)*

Calcium: Samples with the most significant Ca concentrations (>23%) occur to the south of the New Milo lode and occur in nodular calcrete (Figure A1.4.9). Samples with the least concentrations (<16.2%) tend to contain bedrock or relatively thick soil horizons. Calcium exhibits positive correlation with S, and negative correlation with Al, Ce, Cr, Cs, Fe, Ga, HREE, K, Mo, Ni, Rb, Sn, Th, Ti, V and Zn.

Sulphur: Samples with the most significant concentrations (>465 ppm) are either nodular calcrete or occur at the Great Eastern lode position on the easternmost traverse (Figure A1.4.40). The Ca-S association is presumably related to gypsum, which has not been recognised in hand specimen. Sulphur exhibits positive correlation with Ca and Sr, and negative correlation with Al, Cr, Cs, Fe, Ga, Th and Ti.

4.5.4.5 *Element showing no systematic distribution (Nb)*

Niobium: Only two samples have Nb concentrations above detection (5 ppm; Figure A1.4.33). Both samples contain siltstone.

4.6 Summary

- 1) High-grade mineralisation in fresh rock is characterised by Au, Hg, Pb, Ag, As, Bi, Cd, Cu, Sb, Se, S and Zn, with minor Te and In.
- 2) Calcrete sampling along the New Milo and Great Eastern lodes indicates that Au is associated with As, Pb, Cu, and Zn; Hg, Sb, Se and Te are below detection, whereas Cd, Bi and S are irregularly distributed. Gold appears to be associated with calcrete but may not be restricted to it since definitive studies such as profile sampling were not undertaken.
- 3) The signature of the very narrow hydrothermal alteration halo around the quartz veins in calcrete is: Ba, K, Mg, Rb, Sr, Tl, U and W.
- 4) In calcrete, geochemical dispersion for all elements along the lode horizons is very limited. The width of the halo is very dependent on sample spacing and availability of calcrete.
- 5) In augered samples, dispersion haloes are broader, owing to a more regular sampling pattern and to dispersion away from the lodes in the soil. The widths are 25-50 m for ore-associated elements (As, Au, Bi, Cd, Cu, Pb and Zn; Figure 7), and of the order of 150 m for elements associated with hydrothermal alteration (Ba, K, Mg, Sr, Tl, U and W).
- 6) Auger drilling and calcrete sampling are effective sampling techniques in this environment. In this erosional regime, any conventional sampling technique is likely to be valid.

5 FAUGH-A-BALLAGH

5.1 Geological setting

The Faugh-a-Ballagh prospect is located about 20 km northwest of Olary. Minor Cu mineralisation was discovered in the 1880s associated with magnetite-bearing veins and disseminations in rocks of the Outalpa Inlier of the Olary Domain. The stratigraphy of the prospect area belongs to the lower unit of the regional stratigraphic subdivisions of the Olary Domain. The units exposed are: the Composite Gneiss Suite (basal unit), the Quartzofeldspathic Suite, and the Calc-silicate Suite. The Bima and upper Pelite suites have not been recognised in this area.

The Composite Gneiss Suite consists of gneisses and migmatites derived from metasedimentary precursors (pelite, psammopelite, psammite, and a quartzofeldspathic rock), and is most abundant in northern and western parts of the prospect area (Figure 9). Petrographic studies (Beckton, 1993) show that the rocks are composed of quartz, plagioclase and biotite; pelitic rocks are formed of quartz and muscovite. In the north, syntectonic leucogranite bodies have intruded this unit.

Lithologies of the overlying Quartzofeldspathic Suite are generally composed of quartz (30-40%), albite (20-30%), muscovite-biotite (5-10%), magnetite (5-10%), potash feldspar (5-10%), and accessory calc-silicate minerals (Beckton, 1993), and resemble the granitoid of the Composite Gneiss Suite. The geochemistry of this suite is characterised by relatively high Na₂O contents, and relatively low contents of CaO, K₂O and P₂O₅ (Beckton, 1993). These rocks occur predominantly in the west and north of the prospect. This suite has been subdivided into three units:

- (i) The Lower Albite Unit; medium- to coarse-grained quartz-albite rock, with variable amounts of potash feldspar, biotite and magnetite;
- (ii) the Middle Schist Unit; micaceous schist marking the transition between the upper and lower units; and
- (iii) the Upper Albite Unit; fine- to medium-grained, well-laminated quartz-albite rock with variable amounts of biotite, muscovite, magnetite and hematite.

The Upper Albite Unit hosts all of the ironstones, apart from the ironstone at Sylvesters Bore (hosted by the Lower Albite Unit; Figure 9). Disseminated Cu mineralisation occurs at the top of the Upper Albite Unit (Beckton, 1993).

Ironstones, that strike E-W, occur within the Quartzofeldspathic Suite and are commonly associated with retrograde E-W shears. The rock is composed of bands of fine-grained quartz with minor muscovite and albite, and magnetite-hematite bands, locally with round clasts of quartz, although some varieties are composed of massive magnetite (Figure 10b) and hematite. The largest ironstone outcrop occurs on Faugh-a-Ballagh Hill and is part of an extensive quartz-magnetite/hematite breccia (clast-supported, with a crackle texture). The intensity of the brecciation is gradational from unveined quartz-albite rock, through magnetite-bearing quartz-albite rock (with magnetite veinlets and disseminations; Figure 10c), to a matrix-supported rock with rotated clasts (Beckton, 1993).

The Calc-silicate Suite occurs in the southwest of the prospect (Figure 9) and is intercalated with the Quartzofeldspathic Suite. It is differentiated from the latter by >5% (modal) clinopyroxene, amphibole, garnet and epidote (Beckton, 1993).

Granitoid intrusions associated with composite gneiss and migmatite occur mainly in the northern part of the prospect.

5.2 Mineralisation

Stratabound Cu mineralisation occurs in the Upper Albite unit of the Quartzofeldspathic Suite, at the contact with the overlying Calc-silicate Suite in magnetite-bearing quartzofeldspathic rocks (Beckton, 1993). The mineralised zone extends for about 2 km along strike. Malachite and azurite on fractures and as coatings are the most obvious expressions of mineralisation (Figure 10a). At the largest shaft (424551E 6438685N), brown, siliceous gossan with chrysocolla staining occurs on the dump, together with larger masses of azurite mantled by malachite, and magnetite veining. Wallrocks include biotite- and amphibole-bearing assemblages. Further to the east, several magnetite veins have been prospected by shallow trenching (Figure 10b) and a few veins contain disseminated chalcopyrite. The wallrocks of these veins commonly consist of coarse-grained quartz-albite±biotite with a pegmatitic texture. According to Beckton (1993), these magnetite veins have been remobilised, although the mechanism is not stated.

5.3 Regolith

Most of the area belongs to an erosional regime (Figure 11). The dominant landform units are high hills formed by slightly weathered gneisses and schists and, on Faugh-a-Ballagh Hill, ironstones (magnetite-rich, with variable amounts of hematite and quartz). Soils are skeletal to colluvial, and little or no deeply weathered regolith is present. Strongly incised and narrow creeks dissect the hills. Flat alluvial plains occur in the west and east (Figure 11). The soils developed on the alluvium are locally calcareous.

5.4 Vegetation

The terminology for the vegetation structural classification system has been adapted from Keighery (1994). The upper slopes of Faugh-a-Ballagh Hill are dominated by *Dodonaea lobulata* Low Shrubland. Of the larger shrubs and trees, *Acacia aneura* shrubs occur in thickets with many dead examples occurring on the mid-slope; a few examples of *Acacia tetragonophylla* occur here also. The lower slopes consist of *Dodonaea lobulata* Open Low Shrubland over *Ptilotus obovatus*, *Sclerolaena patenticuspis* and *Sclerolaena lanicuspis* Low Open Heath. In the low flat areas, *Sclerolaena patenticuspis* and *Sclerolaena lanicuspis* Low Open Heath occurs with patchy trees of *Alectryon oleifolium* subsp. *canescens*, *Eucalyptus* sp. and *Acacia aneura*. The larger creek bed has *Eucalyptus* sp. Open Woodland and Very Open Grassland, with *Dodonaea lobulata* Low Shrubland in the creek edges.

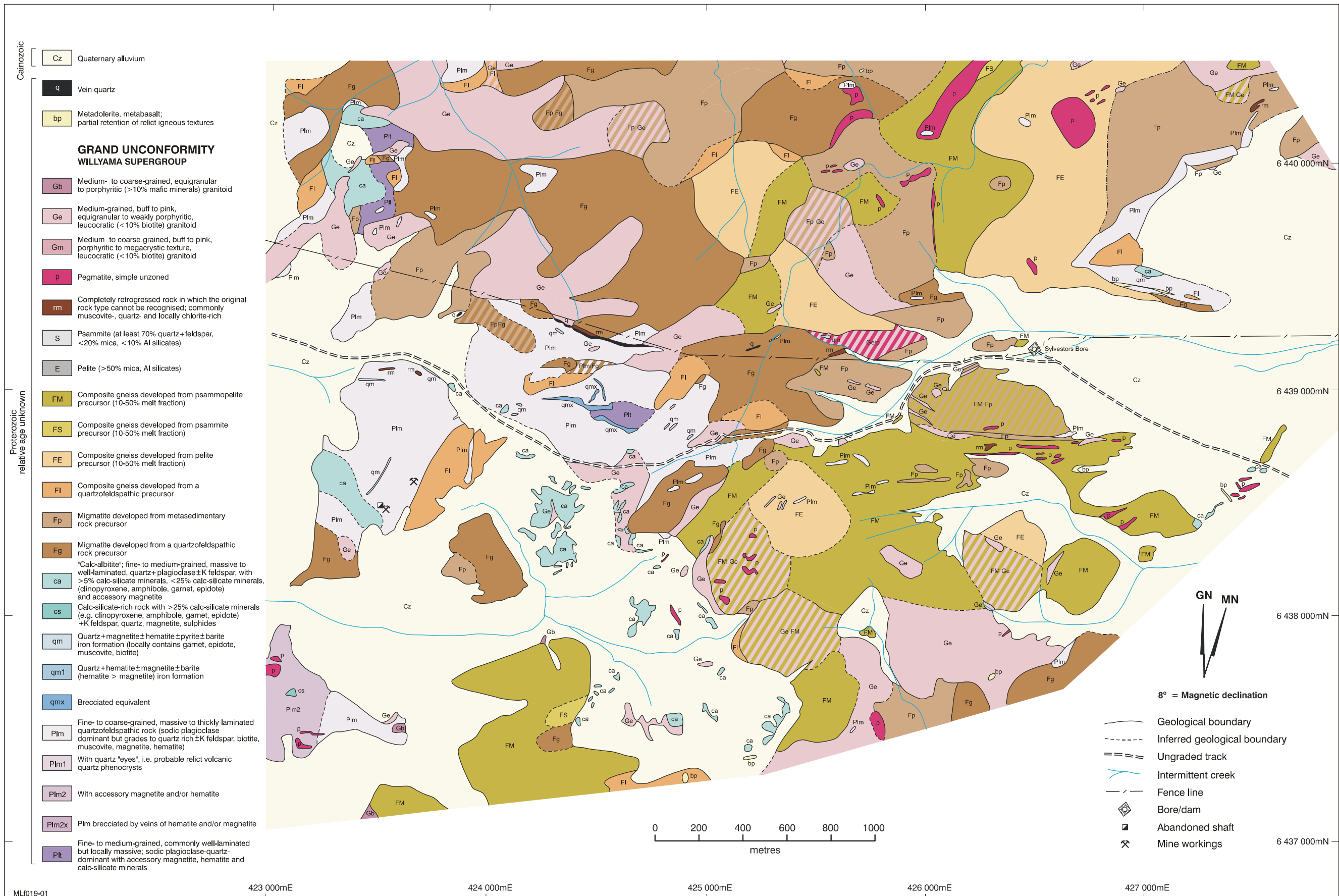


Figure 9: Geological map of Faugh-a-Ballagh prospect (after Beckton, 1993). See Figure 1 for location of Faugh-a-Ballagh.

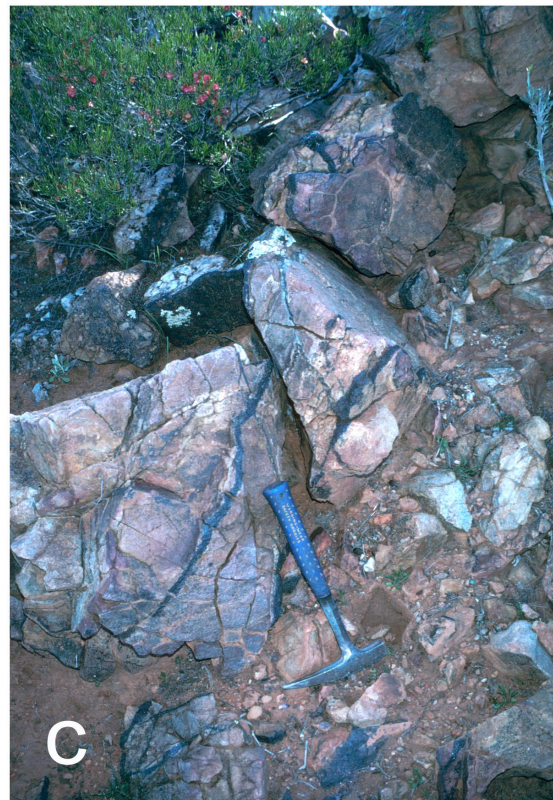


Figure 10: Ironstones at Faugh-a-Ballagh.

a, abundant malachite staining on chalcopyrite-bearing ironstone vein (6438748N, 424933E); **b**, old working on chalcopyrite-bearing magnetite vein with malachite staining; the vein occurs within a coarse-grained quartz-feldspar rock with a pegmatitic texture (6438815N, 424890E); **c**, brecciated felsic rock with magnetite veinlets (6438770N, 424889E).

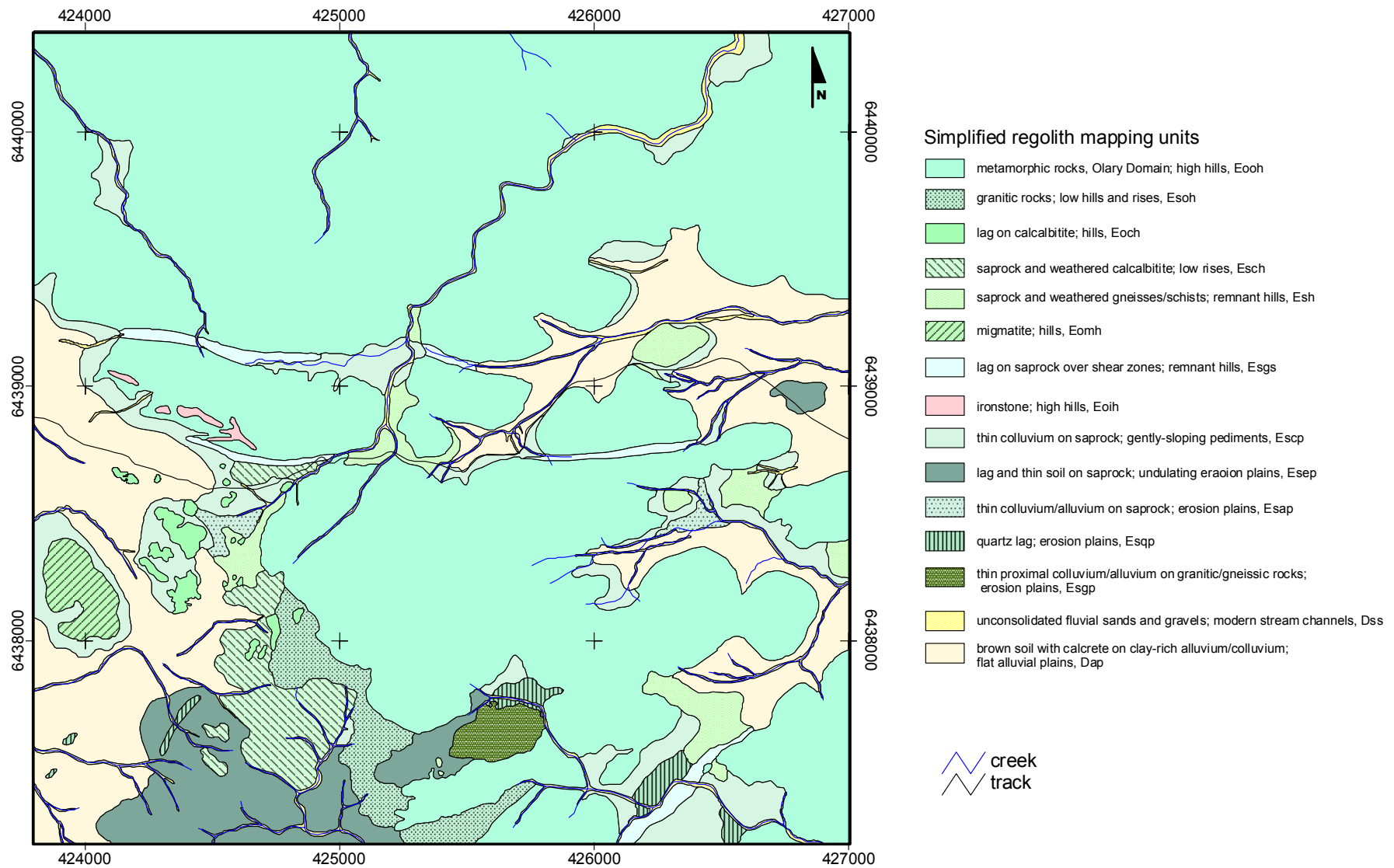


Figure 11: Regolith-landform map of Faugh-a-Ballagh prospect. Full regolith landform unit descriptions are found in Appendix 6.

5.5 Geochemistry

5.5.1 Sampling

The following samples were collected at the Faugh-a-Ballagh prospect:

- (i) 32 rock-chip samples from magnetite-bearing lithologies, including magnetite disseminations in quartzofeldspathic rocks; some samples (12) contain abundant malachite, azurite and/or sulphides (chalcopyrite, pyrite);
- (ii) 16 stream sediments (<2 mm fraction) collected in the creek up- and downstream of the mineralised ironstones on Faugh-a-Ballagh Hill; three samples were sieved into the following fractions: 0.5-2 mm, 180-500 µm, 75-180 µm and <75µm fractions, to determine element distributions between fractions; magnetic and non-magnetic fractions of three bulk <2 mm samples were prepared to compare the chemistry of the respective fractions;
- (iii) 12 soil-lag samples were collected along an orientation line across a zone of Cu-bearing ironstone veins and old workings; the following size fractions were analysed: bulk <6 mm, 2-6 mm, 0.5-2 mm, 180-500 µm, 75-180 µm, and <75µm; four samples of the 2-6 mm and <2 mm fractions were separated into magnetic and non-magnetic components, to compare the composition of the respective fractions;
- (iv) 117 <6 mm soil samples were collected over a triangular 400 m grid over the prospect, with 100 m infill over the main area of ironstones on Faugh-a-Ballagh Hill.

5.5.2 Rock-chip sample geochemistry

Most of the samples (27) were ironstones and fall into two groups:

- (i) ironstones with Cu mineralisation (11 samples, based on the occurrence of malachite, etc.);
- (ii) barren ironstones (16 samples, with no obvious Cu minerals and Cu <1000 ppm).

There are distinct chemical differences between the two groups. In the mineralised group, concentrations of Au, Al, Cu, K, Mg, Ti, Zn, Ag, REE, Y, Ga, In, Rb, Sr, Th and U are greater than in the barren group, in which Fe, V, Mo, Sn and Te concentrations are greater than in mineralised varieties. Concentrations of the remaining elements (As, Ba, Bi, Ca, Cd, Co, Cr, Cs, Hf, Mn, Na, Nb, Ni, P, Pb, S, Sb, Se, Tl, W and Zn) are similar in each group.

Sulphur concentrations are greater in mineralised samples only where sulphides occur. The lower Fe concentrations in mineralised ironstones may reflect introduction of silica.

The remaining four samples are quartzofeldspathic rocks with disseminated magnetite and sulphides (with malachite staining), one sample of epidote-amphibole-magnetite rock, and a cherty rock with disseminated pyrite. As a group, these samples have greater concentrations of Al, Ca, K, Mg, Mn, Na, P, S, As, Sb, REE, Y and Hg, but lower Fe, Nb, Ni and Mo, compared to the ironstones. Mineralised samples have similar Cu concentrations, but greater Zn, Ag, Sr, Th and U.

In the mineralised group, Fe is negatively correlated with many elements (including Cu), but significantly (at the 99.9% level) only with Al, Ca, Mg and Ti; it shows a significant positive correlation (at the 99.9% level) with Ni. Copper is significantly (at the 99.9% level) positively correlated with Ag, Au, Cs, Mg, and U. Element distributions are shown in Figures A2.6.2-A2.6.58.

5.5.3 Stream-sediment geochemistry

5.5.3.1 Elements associated with mineralisation in ironstones (Ag, Al, Au, REE, Cu, Ga, In, K, Mg, Rb, S, Sr, Th, Ti, Tl, U, Y, Zn)

Silver: There is no spatial relationship between Ag concentrations and the mineralised zone (Figure A2.5.2).

Aluminium: The most aluminous samples (>7.63% Al) occur upstream of the mineralised zone (Figure A2.5.3) and appear to be related to the occurrence of detritus derived from albitic rocks in the stream sediment. Aluminium is negatively correlated with most elements, but significantly only with Co, Cr, Cu, Fe, LREE, Ni, Rb, Sr, Th, U, V, Y and Zn (possibly due to closure); it exhibits positive correlation with Na (in albite).

Gold: There are only two samples with Au above detection (1 ppb) in the vicinity of the mineralised zone (Figure A2.5.5). There is no unequivocal spatial relationship to the mineralised zone.

Rare earth elements (REE) and yttrium: These elements exhibit similar distribution patterns (Figures A2.5.10 (Ce), A2.5.15-17 (Dy, Er Eu), A2.5.20 (Gd), A2.5.22 (Ho), A2.5.25-26 (La, Lu), A2.5.32 (Nd), A2.5.36 (Pr), A2.5.41 (Sm), A2.5.44 (Tb), A2.5.49 (Tm), and A2.5.53-54 (Y, Yb)). The greatest concentrations occur in samples close to the mineralised zone and for a distance of about 250 m downstream. Although ironstone detritus is present in the sediments, it is unclear whether this is the sole source of REE and Y. The rare earth elements (REE) correlate with each other and with Cr, Mn, Ti, V and Y, and may reflect the occurrence of detrital monazite, spinel and Ti-bearing minerals. The LREE correlate positively with Co, Fe, Ni, Zn, Th, U and Zn, but negatively with Al and Na, reflecting the occurrence of albite.

Copper: Copper concentrations above background (18 ppm) occur downslope from the mineralised zone and downstream for about 250 m (Figure 12). Except for one sample (165 ppm) from the small tributary, these concentrations are 40 ppm or less and are likely to be lost in background in regional stream sediment surveys. However, in absolute terms, in the main creek, samples upstream of the mineralised area contain <10 ppm Cu; those in the vicinity of the mineralised area generally contain 25-30 ppm, and about 20 ppm further downstream. In this sense, the <2 mm stream sediments have defined a zone anomalous in Cu. Copper exhibits positive correlation with Cr, Ni, V, Zn, Co, Th and U, and negative correlation with Na and Al.

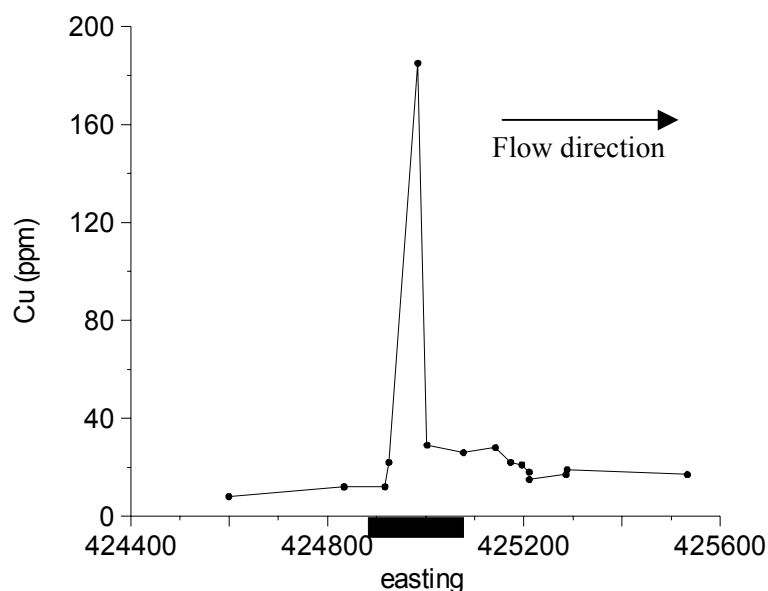


Figure 12: Distribution of Cu (ppm) in <2 mm stream sediments, Faugh-a-Ballagh.

Gallium: Relatively significant Ga concentrations (>22.1 ppm) occur up- and downstream of the mineralised zone (Figure A2.5.19). However, there is no clear spatial relationship between Ga concentrations and the mineralised zone. Gallium correlates negatively with Ba and K. Gallium shows no significant (at the 99.9% level) correlation with Al ($r=0.294$), probably due to the low variance in Ga concentrations (20-23 ppm) in the stream sediments, which have a relatively wide range of Al contents (6.28-8.53%).

Indium: Only one sample is above detection limit (0.05 ppm) and occurs in the small tributary (Figure A2.5.23). This suggests that, although In may be a potential pathfinder for mineralisation in the ironstones, its low concentrations and small distance of dispersion are of limited use.

Potassium: Although there are two samples with >1.25% downslope from the mineralised zone, the long dispersion trail downstream is probably related to lithology (Figure A2.5.24). Potassium exhibits positive correlation with Ba, Cs, Rb and Sr, and negative correlation with Ga.

Magnesium: Magnesium concentrations are greatest (>0.27%) upstream from the mineralised zone and in the tributary (Figure A2.5.27). However, they are probably related to lithology (e.g., detritus derived from calc-silicate rocks).

Rubidium: Although there are two samples with >43 ppm downslope from the mineralised zone, the long dispersion trail downstream is probably related to lithology (Figure A2.5.37). The distribution of Rb is very similar to that of K. Rubidium exhibits positive correlation with Co, Cs, K, Ni, Sr, Th and U, and negative correlation with Al and Na.

Sulphur: The distribution of S is erratic. There is no clear spatial relationship between S and mineralisation (Figure A2.5.38).

Strontium: The distribution of Sr is erratic. Although there are samples with above-background concentrations (>56.5 ppm) in the vicinity of the mineralised zone (Figure A2.5.43), the source of the Sr is more likely to be detritus derived from pegmatite, granitoid or epidote-bearing rocks. Strontium exhibits a positive correlation with Ba, Co, K, Ni, Rb and U, and negative correlation with Al and Na.

Thorium: The distribution of Th is erratic. Although there are samples with above-background concentrations (>13.5 ppm) in the vicinity of the mineralised zone (Figure A2.5.46), the source of the Th is more likely to be detritus derived from pegmatite or granitoid. Thorium exhibits positive correlation with Co, Cr, Cu, Fe, LREE, Mn, Ni, Rb, Sn, Sr, U, V, Zn and Y, and negative correlation with Al and Na.

Titanium: The distribution of Ti shows no spatial relationship to the mineralised zone (Figure A2.5.47), but is related to the incidence of Ti-bearing minerals in the sediments. Titanium exhibits positive correlation with Cr, Mn, REE, Sn, V and Y, and negative correlation with Na.

Thallium: There is only one sample above detection limit (0.2 ppm). This sample occurs in the tributary to the main creek (Figure A2.5.48) and may signify the presence of mineralised ironstone upstream. However, the low concentration and lack of dispersion do not make Tl a useful pathfinder.

Uranium: Samples with the greatest concentrations (>2.8 ppm) occur downslope and downstream from the mineralised zone (Figure A2.5.50). The sample with the greatest concentration occurs in the tributary to the main creek. However, it is unclear to what extent the other samples indicate dispersion from mineralised ironstones or from granitoid/pegmatite. Uranium correlates positively with Co, Cr, Cu, Fe, LREE, Ni, Rb, Sn, Sr, Th, V and Zn, and negatively with Al and Na.

Zinc: The greatest Zn concentrations occur downslope and downstream from the mineralised zone (Figure A2.5.55). However, absolute concentrations are relatively low (<25 ppm) and show relatively little variance, and would be lost among background values in a regional survey. Zinc correlates positively with Co, Cr, Cu, Fe, LREE, Ni, Th, U and V, and negatively with Al and Na.

5.5.3.2 *Elements not associated with mineralisation in ironstones (As, Ba, Bi, Ca, Co, Cr, Cs, Fe, Mn, Mo, Na, Ni, P, Sn, V, W)*

The abundances of these elements are generally related to lithology. For example, greater concentrations of Ba, Cs, Mo and Sn are related to detritus derived from granitic and pegmatitic rocks, or As, Bi and Na to detritus derived from albitic rocks. The distribution of Fe is related to the abundance of ironstone detritus.

5.5.3.3 *Elements commonly below detection limit or with low variance (Cd, Hf, Nb, Pb, Sb, Se, Te)*
Cadmium, Pb, Se and Te concentrations are below detection limit (0.5, 5, 0.5 and 0.2 ppm respectively); only two samples contain Sb above detection limit (0.5 ppm). Concentrations of Hf and Nb show little variance and no obvious trends are apparent.

5.5.4 *Compositions of selected stream-sediment size fractions*

Three stream-sediment samples were sieved into five size fractions (2-6 mm, 0.5-2 mm, 180-500 µm, 75-180 µm, and <75 µm).

The results (Appendix 2.9) indicate that the concentrations of most elements (Ag, As, Au, Al, Ba, Bi, Ca, Cs, Cu, In, K, Mg, Nb, Ni, P, REE, Rb, S, Sr, Th, Ti, Tl, U, W, Y and Zn) are greatest in the <75 µm fraction. The concentrations of some elements (Cr, Ga, Fe, Mn, Sn, Te and V) are greatest in the middle size fractions (180-500 µm and 75-180 µm). The distributions of the remaining elements (Co, Pb, Mo and Se) are either irregular, showing no affinity for any particular size fraction, or are below detection limit throughout (Cd and Sb). In the 2-6 mm fraction, Ba, Ca, Co, K, Mo and Rb concentrations are also significant.

The implications for exploration using stream-sediment sampling are that the <75 µm fraction appears to be a better medium than the bulk <2 mm fraction. For example, in sample FABSS15, the Cu concentration for the <75 µm fraction is 400 ppm, compared to 165 ppm for the <2 mm fraction. Other samples nearby, with 22-26 ppm Cu in the <2 mm fraction, contain 47 and 125 ppm Cu in the <75 µm fraction. There is potential to produce a larger dispersion halo using the <75 µm fraction, although it is also likely that background levels will also be correspondingly higher. This requires further investigation and may alter the conclusions based on the <2 mm fraction (section 5.5.3).

5.5.5 *Orientation soil-lag traverse*

5.5.5.1 *Sampling*

Twelve samples were collected on a N-S traverse about 135 m long (Figure A2.8.1) across E-W trending ironstone veins with disseminated chalcopyrite and pyrite and/or malachite and azurite staining. The following fractions have been sieved: 2-6 mm, 0.5-2 mm, 180-500 µm, 75-180 µm, and <75 µm. The soils on the traverse are generally red-brown and sandy, particularly in the vicinity of the ironstones. The following lag types were noted:

- (i) magnetite-rich ironstone lag, which is most abundant between samples FABS6 and FABS8 (Figure A2.8.1); malachite staining of some fragments in the vicinity of FABS1; rare magnetite-bearing lag is derived from veinlets in felsic schists;
- (ii) lag derived from felsic schists, across the whole traverse, typically associated with minor to rare quartz lag;
- (iii) coarse-grained felsic (?granitic) lag, adjacent to FABS6.

5.5.5.1 *Elements associated with mineralisation (Cu)*

Copper: Copper shows a relatively prominent peak about 25 m wide over the mineralised zone (Figure 13) in all fractions. Concentrations of Cu in the fine fractions (<180 µm) are greater than those in coarser fractions.

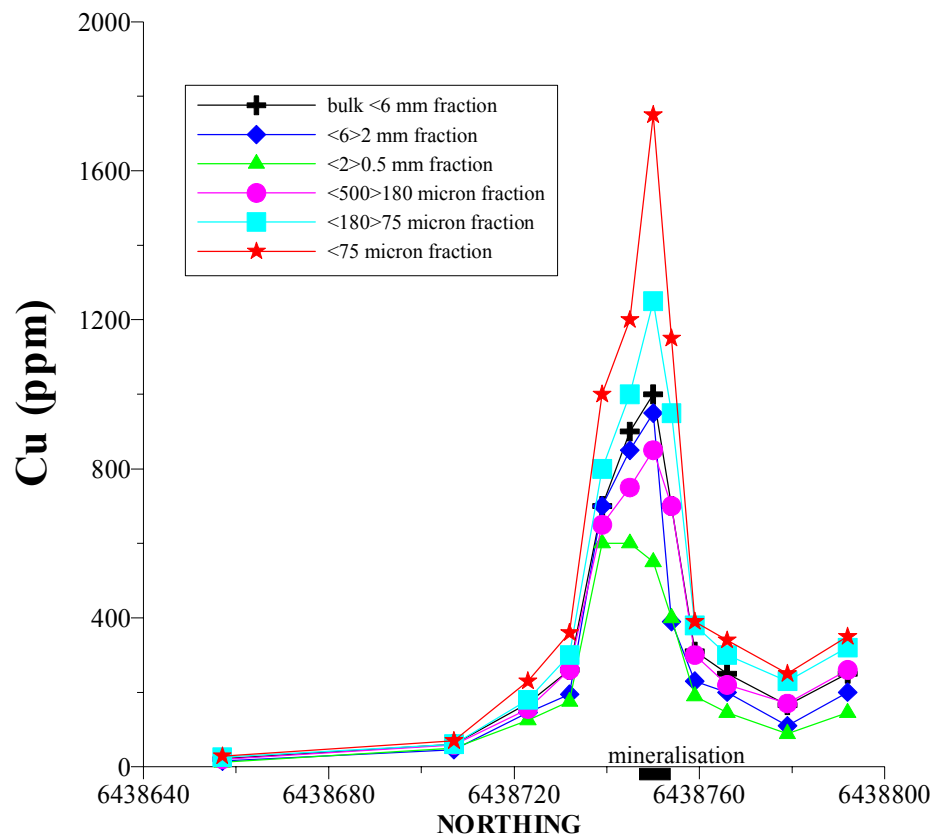


Figure 13: Distribution of Cu (ppm) in various size fractions along the orientation traverse.

5.5.5.2 Elements possibly associated with mineralisation (*As, Au, Bi, Pb, S, Se, W*)

Arsenic: Arsenic shows a peak (9 ppm) over mineralisation against a background of 5-6 ppm in the <75 μm fraction. In the other fractions, As behaves in the opposite fashion and shows a relative depletion over the mineralised zone (Figure A2.8.4). Concentrations are greatest in the <75 μm fraction.

Gold: Gold shows prominent peaks (>10 ppb) on the margins of the mineralised zone in the bulk <6 mm and 2-6 mm fractions (Figure A2.8.5). The distribution of Au in the other fractions is slightly erratic, but a small peak (<10 ppb) is discernible in all fractions on the southern margin of the mineralisation. Except for the two prominent peaks in the 2-6 mm fraction, Au concentrations in the <75 μm fraction are slightly greater than for other fractions.

Bismuth: Bismuth shows minor peaks in the 2-6 mm and <75 μm fractions over mineralisation (Figure A2.8.7), but absolute concentrations are less than 0.5 ppm.

Lead: Lead concentrations are erratic, with peaks in various coarser fractions on the margins of the mineralised zone (Figure A2.8.35).

Sulphur: Sulphur shows a prominent peak (>250 ppm) at the southern margin of the mineralised zone (Figure A2.8.38). The <75 μm fraction generally has the highest concentration levels.

Selenium: The distribution of Se is somewhat erratic in all fractions except the <75 μm (Figure A2.8.39). In the latter fraction, a peak occurs over the mineralised zone (1.5 ppm).

Tungsten: The distribution of W is somewhat erratic (Figure A2.8.50), but peaks (~4 ppm) occur over the mineralised zone in all fractions except the bulk <6 mm. The peak is most prominent in the 2-6 mm, 75-180 µm and <75 µm fractions.

5.5.5.3 Elements associated with felsic lithologies (Al, Ba, Ca, Cs, K, Mg, Mn, Na, Rb, Sr, Ti, Zn)

These elements generally exhibit decreased abundance over the mineralised zone and the associated ironstones. For most elements, concentrations are greatest in the finest fractions (75-180 µm and/or <75 µm), except Na (concentrations greatest in fractions >0.5 mm).

5.5.5.4 Elements associated with the ironstones (Co, Cr, Fe, Ga, Mo, Ni, P, REE, Sn, Th, Tl, U, V, Y)

These elements generally exhibit increased abundance in the zone of ironstones, but commonly also decreased abundance over the mineralised zone itself. The concentrations of many of these elements are greatest in the 180-75 µm and/or <75 µm fractions.

5.5.5.5 Elements commonly below detection limit or with low variance (Ag, Cd, Hf, In, Nb, Sb, Te)

All Sb and Te data are below detection (0.5 and 0.2 ppm respectively). The other elements exhibit low variance and no clear distribution patterns. Silver, Cd, Hf and In concentrations are generally greatest in the 75-180 µm and/or <75 µm fractions.

5.5.6 Regional <6 mm soil sampling

5.5.6.1 Elements associated with mineralisation (Au, Cu)

Gold: Samples with Au concentrations above background (2.9 ppb) occur in an arcuate zone along the southern margin of Faugh-a-Ballagh Hill (Figure 14) and appear to be related to a shear; the easternmost sample is related to an outcrop of pegmatite. In the west, anomalous Au is associated with zones of magnetite disseminated in albitic rocks. It appears that most of the area sampled is not prospective for Au mineralisation, although Au may be a useful pathfinder element for Cu mineralisation. Gold is positively correlated with Cu.

Copper: Anomalous Cu concentrations (>243 ppm) occur in the vicinity of known primary and secondary Cu minerals (Figure 15). The most anomalous area is on the south side of Faugh-a-Ballagh Hill, in part related to the mineralised ironstones and partly related to the E-W shear. Mildly anomalous concentrations (>43.5 ppm) in the southeast are associated with mafic amphibolites. Copper is positively correlated with Au.

5.5.6.2 Elements locally associated with mineralisation (As, Bi, S, U, W)

Arsenic: Arsenic concentrations are generally low (<6 ppm). Relatively anomalous concentrations occur in the southwest and southeast (Figure A2.4.4). There is no clear association between As and lithology. However, many anomalous samples contain quartz, others some magnetite. Samples collected around the old workings and the shear zone in the west are anomalous in As.

Bismuth: Bismuth concentrations are generally low (generally <0.5 ppm). The most anomalous samples occur along the ironstone ridge on Faugh-a-Ballagh Hill (Figure A2.4.7), and along a shear to the west. Weakly anomalous Bi (>0.24 ppm) is associated with the easternmost working.

Sulphur: The most anomalous (>330 ppm) areas are Faugh-a-Ballagh Hill and the shear to the west (Figure A2.4.38). This may relate to sulphides in the ironstone veins, but is more likely related to gypsum, since the S anomaly is coincident with above-background Ca concentrations. The anomaly (>330 ppm) in the northeast is coincident with weakly anomalous Ca, and may also be related to gypsum.

Uranium: The most anomalous zones (>4.3 ppm) are on the south of Faugh-a-Ballagh Hill associated with ironstone veins (and, locally, with Cu mineralisation; Figure A2.4.50). To the north of the hill, the anomalous sample is associated with granitoid. Uranium is positively correlated with Th and W.

Tungsten: Samples with relatively anomalous concentrations (>2.21 ppm) occur along the northern and southern slopes of Faugh-a-Ballagh Hill and appear to relate to migmatites (Figure A2.4.52). Anomalous samples also occur along the orientation line and may relate to mineralisation. Tungsten is positively correlated with U.

5.5.6.3 Elements with lithological associations (Al, Ba, Ca, Co, Cr, Cs, Fe, Ga, Hf, K, Mg, Mn, Mo, Na, Nb, Ni, P, Pb, Rb, REE, Sn, Sr, Th, Ti, Tl, V, W, Y, Zn)

The distributions of these elements are related to particular lithologies:

- i. felsic (igneous) rocks: greater concentrations of Al, Ba, Cs, Ga, K, Na, Pb, Rb, REE, Tl, Y;
- ii. albitic rocks: greater concentrations of Al, Na, Sr;
- iii. mafic (igneous) rocks: greater concentrations of Ca, Co, Cr, Mg, Nb, Ni, P, Sr, Ti, V, Zn;
- iv. metasedimentary (quartz-feldspar-mica) rocks: greater concentrations of Al, K, Mn, Rb, Sn, Th, Ti, Tl, W, Zn;
- v. ironstones: greater concentrations of Co, Fe, Hf, Mg, Mo, Nb, P, Th, V.

5.5.6.4 Elements showing no variance and below detection limit (Ag, Cd, In, Sb, Se)

All Sb concentrations are below detection (0.5 ppm). Most Cd, In and Se concentrations are below detection (0.5, 0.05 and 0.5 ppm respectively) and the remainder show no regular distribution patterns. Ag concentrations are low (<0.3 ppm); samples with the more anomalous values appear to be related to the abundance of quartz.

5.5.7 Geochemistry of magnetic versus non-magnetic fractions

5.5.7.1 Stream sediments

The magnetic fractions of three samples were separated, and both the magnetic and non-magnetic fractions were analysed (Appendix 2.10). The non-magnetic fraction dominantly consists of quartz, with some feldspar and minor hematite; the magnetic fraction is dominantly magnetite, with minor amounts of quartz and feldspar (in composite grains).

On the basis of limited data, concentrations of Bi, Co, Cr, Fe, Ga, Mn, Mo, Nb, Ni, Te, Th, V and Zn are greater in the magnetic fraction, reflecting a possible association of these elements with Fe and/or Mn oxides. The concentrations of Al, Ba, Ca, Cs, Cu, K, LREE, Mg, Na, Rb, Sn, Sr and Ti are greater in the non-magnetic fraction, reflecting their occurrence in silicates, carbonates, etc. The concentrations of the remaining elements (Ag, As, Au, Cd, Hf, HREE, In, P, Pb, S, Sb, Se, Th, U, W and Y) are similar for each fraction.

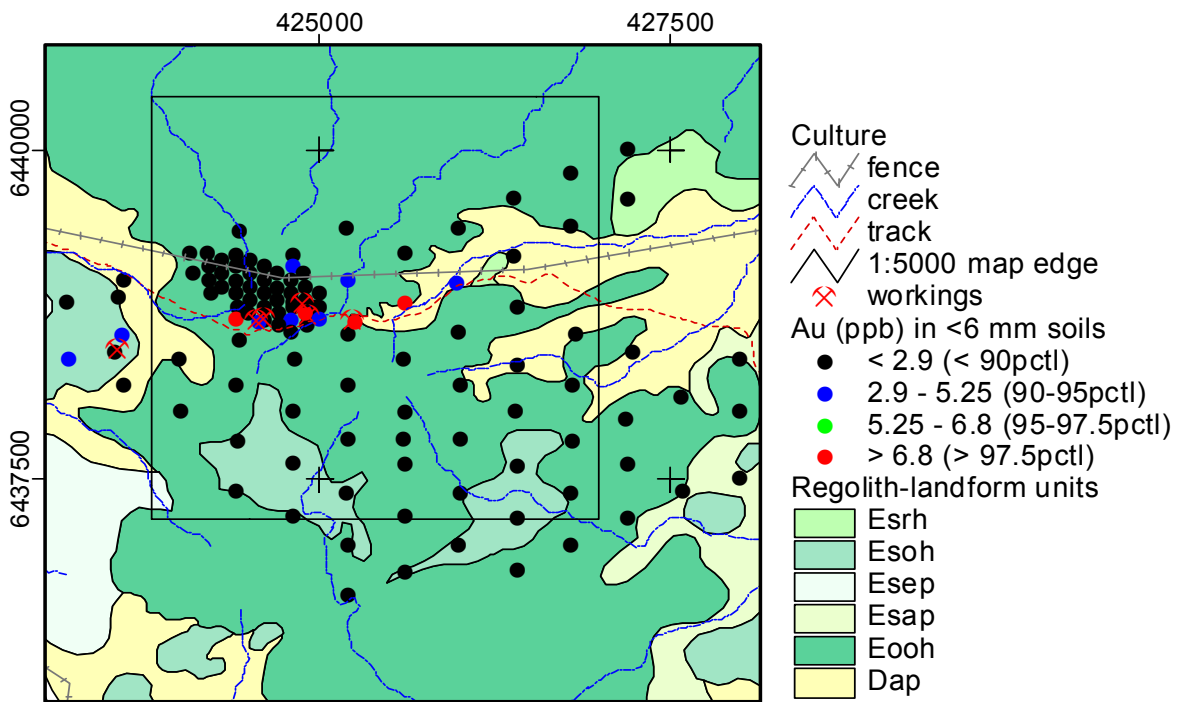


Figure 14: Distribution of Au (ppb) in <6 mm soils, Faugh-a-Ballagh. Full regolith landform unit descriptions are found in Appendix 6.

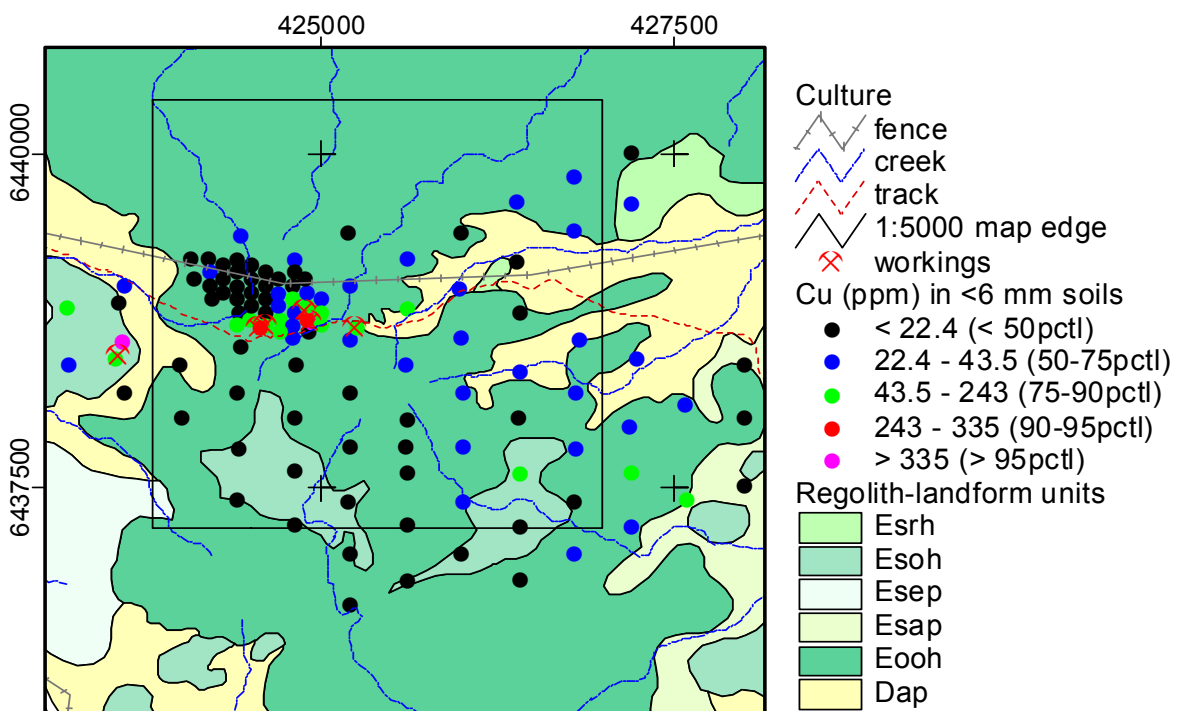


Figure 15: Distribution of Cu (ppm) in <6 mm soils, Faugh-a-Ballagh. Full regolith landform unit descriptions are found in Appendix 6.

5.5.7.2 Soils

Four <2 mm soil samples were separated into magnetic and non-magnetic fractions and analysed (Appendix 2.11). Most elements (including Cu) lack a consistent distribution pattern between the magnetic and non-magnetic fractions. Bismuth, Co, Fe, Mn, Mo, Ni, S, Te, V and Zn are consistently concentrated in the magnetic fraction, whereas the converse is true for Ag, Al, Ba, K, Na, Rb and W.

The maximum concentrations obtained for Au and Cu for the magnetic fraction respectively are 3 ppb and 950 ppm (compared to 3 ppb and 800 ppm respectively for the non-magnetic fraction). However, these values do not pertain to the same sample sites, adding further complexity. Compared to bulk fractions, the Au and Cu concentrations are randomly greater or lesser for any given sample. There is no advantage in analysing the magnetic fraction of these soils.

5.5.7.3 Lag

Four 2-6 mm lag samples were separated into magnetic and non-magnetic fractions, and analysed (Appendix 2.11). Most elements (including Cu) lack consistency in their distributions between the magnetic and non-magnetic fractions, or between magnetic, non-magnetic and bulk samples. Only Au, Bi, Ca, Co, Cr, Fe, Mn, Nb, Ni and Se concentrations are consistently greater in the magnetic fraction, whereas the reverse is true only for P.

5.6 Summary

- 1) The rock-chip samples indicate that mineralised ironstones are anomalous in Ag, Al, Au, Cs, Cu, Ga, In, K, Mg, REE, Rb, Sr, Th, Ti, U, Y and Zn. However, Cu correlates positively with Ag, Au, Cs, Mg and U.
- 2) The stream-sediment sampling indicate that dispersion of Cu and other elements is very limited in the <2 mm fraction. Only Cu, In and Tl appear to be directly associated with mineralisation. The abundances of In and Tl and their dispersion distances are low, so these elements are unlikely to be practical pathfinders.
- 3) The finer fractions (especially the <75 µm fraction) of stream sediments are potentially superior to the <2 mm fraction. Copper concentrations (>100 ppm) and dispersion distances appear to be greater (>100 m) than for the <2 mm fraction. However, further investigation of the <75 µm fraction is required to better define element dispersion characteristics.
- 4) The results of the soil orientation survey show that Cu is the only reliable indicator of mineralisation. The fine fractions (<180 µm) are probably the best fractions, although a bulk <6 mm fraction would be a practical compromise.
- 5) Regional <6 mm soil sampling indicates that Cu and Au are the most consistent elements in delineating mineralised zones. Arsenic, Bi, U and W are locally anomalous, but their usefulness as pathfinders may be limited. The most prospective areas appear to be the southern slopes of Faugh-a-Ballagh Hill and the east-west shear. There is also potential in albitic rocks to the southwest.
- 6) The investigation of magnetic and non-magnetic fractions of <2 mm soils, <2 mm stream sediments, and 2-6 mm lag are largely inconclusive, particularly regarding the distribution of Cu. There is no advantage in using the magnetic fraction of <2 mm soil or 2-6 mm lag, as Cu is irregularly distributed between magnetic and non-magnetic fractions. Larger sample populations are required to provide a definitive outcome.

6 OLARY SILVER MINE

6.1 Geological setting

The Olary Silver Mine is located on the western side of the Olary-Bimbowrie road, about 5 km north of Olary. The main shaft extends to 33.5 m depth; a surface sample in its vicinity assayed 105 ppm Ag (Brown, 1908). It occurs on the western contact of a laterally discontinuous, massive to poorly banded, siliceous hematite-magnetite ironstone that is pyritic at depth (Flint, 1977). Country rocks are predominantly quartzofeldspathic gneisses with porphyroblastic muscovite and have been intruded by pegmatites (Figure 16).

The ironstone strikes parallel to lithological layering, is lenticular, and grades along strike to quartz-chlorite-muscovite granofels (Flint, 1977). The lithological layering is parallel to the foliation and has been folded (D₃ phase; Flint, 1977). The mineralogy of the ironstone changes with depth, with up to 25% pyrite recorded locally (Westhoff, 1970). Drilling has indicated that the ironstone is discontinuous to the water table (Westhoff, 1970). Only narrow mineralised intervals were encountered, the best being 3.66 m @ 0.15% Cu, 3.05 m @ 0.17% Cu, and 0.61 m @ 0.1 % Cu and 4 ppm Ag. A significant IP response on an unexposed horizon about 175 m northwest of the ironstone was drilled. Sulphides (pyrite, pyrrhotite, chalcopyrite, sphalerite, arsenopyrite and galena) were intersected in fine-grained gneisses (Flint, 1977).

6.2 Regolith

The topography around the Olary silver mine is subdued, apart from the low ironstone ridge. Along the traverse, the soils are skeletal, sandy and small outcrops are common. There appears to be little or no deeply-weathered regolith evident and the terrain belongs to an erosional regime. The area away from the traverse was not investigated, but thin transported overburden may exist beyond the limits of the lithologies shown in Figure 16. No carbonate was recognised in the soils.

6.3 Geochemistry

6.3.1 Sampling

The following samples were collected:

- (i) 4 rock-chip samples from the dump and the ironstone ridge;
- (ii) 9 <6 mm soil-lag samples along a traverse across the strike of the mineralised horizon (Figure 16)

6.3.2 Rock-chip sample geochemistry

The maximum concentrations obtained from sulphidic samples for ore-associated elements from the dump were: Cu (750 ppm), Ag (1.4 ppm), As (26.5 ppm), Bi (15 ppm), Mo (13 ppm), Se (5 ppm), Te (2 ppm), Au (580 ppb) and Hg (0.25 ppm).

6.3.3 Orientation soil-lag traverse

Nine samples were collected along a traverse across strike of the mineralised horizon, through the main shaft (Figure 16). The soils are red-brown and quartz-rich (sandy), with locally abundant lag. The following lag types were recognised:

- (i) coarse- to fine-grained hematite-magnetite ironstone, mainly in the vicinity of the ironstone ridge;
- (ii) medium- to fine-grained quartz, along the whole traverse;
- (iii) medium- to fine-grained pegmatite, at the southern and northern ends of the traverse.

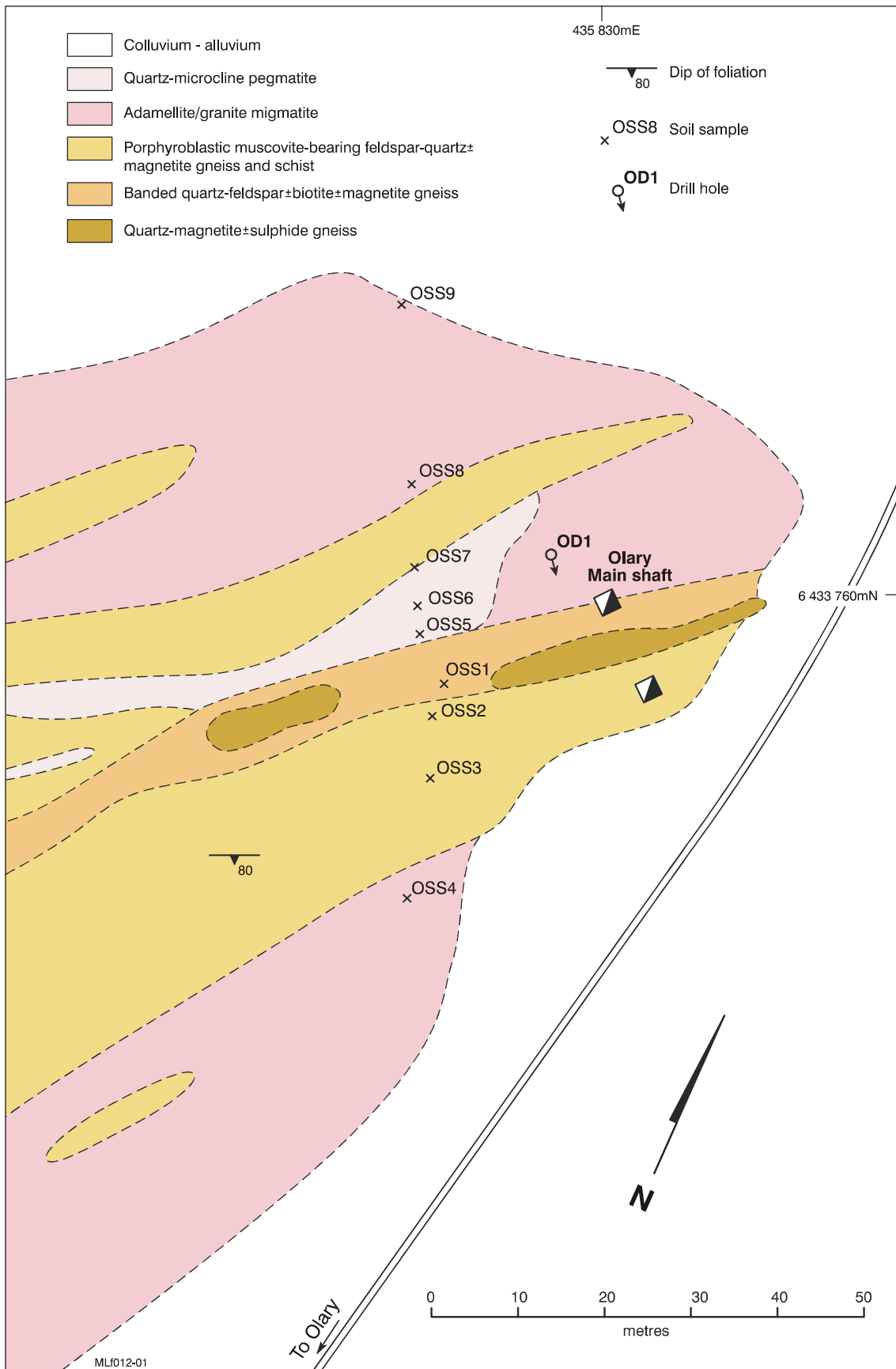


Figure 16: Geological map (after Chapman, 1988) showing location of the Olary Silver Mine and orientation soil traverse. See Figure 1 for location of Olary Silver Mine.

6.3.3.1 Elements associated with mineralisation (Au, Cu, S, W)

Gold: Gold shows a peak about 40 m wide over the mineralised zone in all fractions (Figure 17). Concentrations of Au are generally greatest in the <75 µm fraction (25 ppb, over a background of <10 ppb). The bulk <6 mm fraction has samples with prominent spikes (>20 ppb) at the ends of the traverse; the southernmost sample appears to be spurious, but the northernmost sample also has slightly anomalous Au contents in other fractions. It is also possible that these spikes are due analytical and/or sampling error or contamination, or to a nugget effect or to another source.

Copper: Copper shows a prominent peak about 40 m wide over the mineralised zone in all fractions (Figure 18), with the best response in the <75 µm fraction (peak value 160 ppm, over a background of <80 ppm). The peak to background value of about 2 also holds for all the other fractions.

Sulphur: Although S has relatively low variance, all fractions show a peak (200-300 ppm) over the mineralised zone (Figure A4.3.38).

Tungsten: All fractions (except 2-6 mm) show a peak over the mineralised zone (Figure A4.3.51). The most prominent peak is in the <75 µm fraction, at 5.5 ppm over a background of <2 ppm.

6.3.3.2 Elements possibly associated with mineralisation (Ag, Bi, Mo, P, Pb, Se, U)

Silver: The distribution patterns for Ag are somewhat erratic (Figure A4.3.2), but there is a peak over the mineralised zone (0.5 ppm peak over a background <0.3 ppm) and the area to the east in the <75 µm fraction.

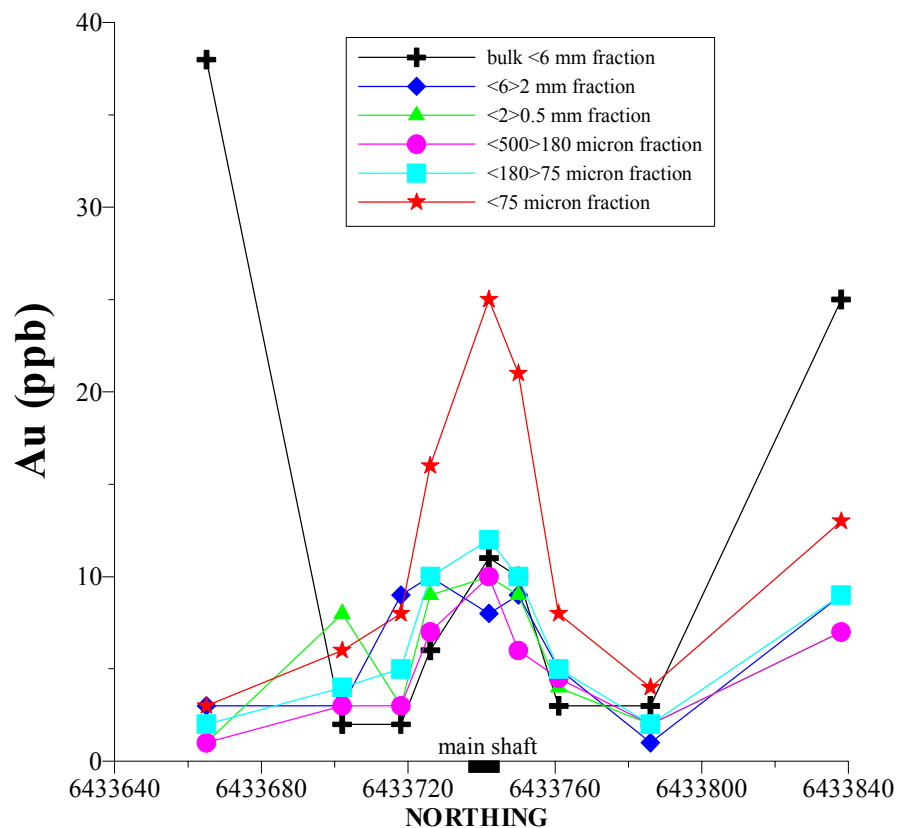


Figure 17: Distribution of Au (ppb) in various size fractions along the orientation traverse, Olary Silver Mine.

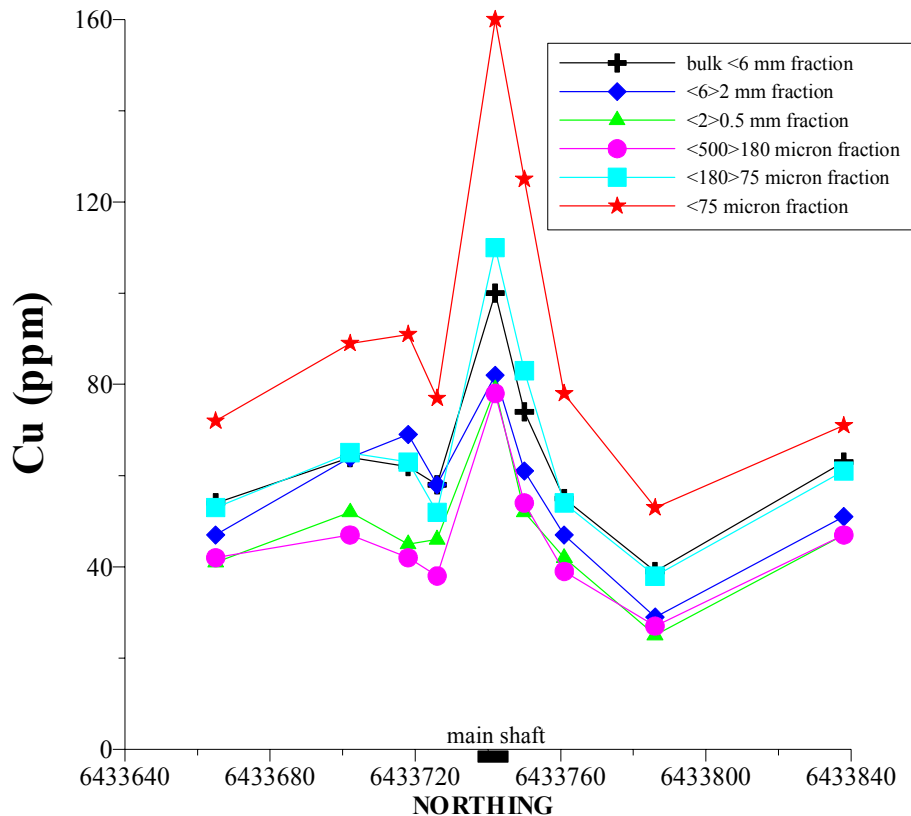


Figure 18: Distribution of Cu (ppm) in various size fractions along the orientation traverse, Olary Silver Mine.

Bismuth: There is a very subtle peak (1 ppm) over the mineralised zone in the 2-6 mm fraction (Figure A4.3.7). The reasons for the spikes (2.7 and 7.4 ppm) in the 0.5-2 mm fraction are unclear.

Molybdenum: The distribution patterns of Mo are irregular (Figure A4.3.29), but there are peaks (up to 1.6 ppm, over backgrounds <1.3 ppm) in all fractions except 180-500 µm over the mineralised zone.

Phosphorus: Phosphorus has maxima (>300 ppm) over the mineralised horizon in all fractions except 2-6 mm (Figure A4.3.34). Concentrations are greatest in the <75 µm fraction. It is possible that the P peak relates to the ironstone rather than mineralisation.

Lead: There are ill-defined Pb peaks (15 and 25 ppm respectively) over the mineralised zone for the bulk <6 mm and <75 µm fractions (Figure A4.3.35).

Selenium: Many Se analyses are below detection (0.5 ppm). Ill-defined peaks occur over the mineralised zone for the 180-500 µm and <75 µm fractions (Figure A4.3.40).

Uranium: There is a peaks in the <75 µm fraction (>2 ppm) over the mineralised zone (Figure A4.3.49). Peaks in the other fractions are erratic.

6.3.3.3 Elements associated with lithology (Al, As, Ba, Ca, Co, Cr, Cs, Fe, Ga, K, Mg, Mn, Na, Ni, P, REE, Rb, Sn, Sr, Th, Ti, U, V, Y, Zn)

Concentrations are greatest for the 75-180 µm and/or <75 µm fractions for most elements, except for Ba and Na, for which concentrations are greatest in the >0.5 mm fractions (Appendices 4.2 and 4.3). Most elements either show relatively little variation (As, Co, Cs, REE, Sr, Ti, Y, Zn), or a trough over

the mineralised zone and ironstone (Al, Ba, Ca, Cr, Ga, K, Mg, Mn, Na, Ni, Rb, Sn, Th and V). In contrast, Fe exhibits a peak over the ironstone.

6.3.3.4 Elements below detection or with low variance (Cd, Hf, In, Nb, Sb, Te, Tl)

Most or all Cd, Sb and Te analyses are below detection limit (0.5, 0.5 and 0.2 ppm respectively). The other elements (Hf, In, Nb and Tl) exhibit very little variance and no regular distribution patterns.

6.4 Summary

- 1) Sampling of the dumps at the Olary Silver Mine suggests that the geochemical signature of the mineralisation in fresh rock is Ag, As, Au, Bi, Cu, Hg, Mo, Se and Te.
- 2) Gold and Cu are the best indicators of mineralisation in soil, possibly reinforced by S and W.
- 3) The best soil responses were in the <75 µm fraction, although the <6 mm fraction would be acceptable.

7 BLUE ROSE

7.1 Introduction

The Blue Rose prospect is located about 10 km south of the New Milo-Great Eastern mines at the Wadnaminga Goldfield, 40 km south of Olary. The prospect was selected for exploration because of a coincidence of a prominent aeromagnetic anomaly (thought to be an intrusive rock at depth) with the junction of several faults. Dominion Metals Pty Ltd, investigating magnetic features in the district, drilled several widely-spaced RAB holes and intersected “skarn assemblages and high-level potassic intrusive rocks within Adelaidean metasedimentary rocks” (Shelton, 1999), with anomalous Cu intervals. Lynas Gold Corporation drilled RAB and aircore holes, intersecting anomalous Cu in the general area of the magnetic anomaly. Subsequent RC drilling targeted several geochemical and IP anomalies. Eighteen holes were drilled, the best intersections being (Shelton, 1999):

BRRC16	40-80 m	40 m @ 0.26% Cu including 12m @ 0.58% Cu (68-80 m)
BRRC18	10-98 m	88 m @ 0.39% Cu

The host for the mineralisation was a dolomitic sedimentary rock with extensive retrograde skarn alteration (magnetite, pyrite and chalcopyrite; Shelton, 1999), with the best intersections in the southeast, away from the apex of the main inferred intrusion. The exploration model adopted was a porphyry-skarn, with Cu-Au(-Mo) mineralisation derived from hydrothermal fluids from high-level felsic magmatism (Shelton, 1999).

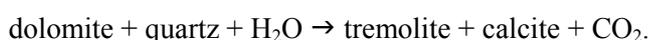
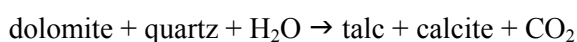
7.2 Geological setting

The Blue Rose prospect occurs on the southern limb of the Wadnaminga Anticlinorium in metasedimentary rocks of the Adelaidean Burra Group (Forbes, 1991) in similar lithological units to the Wadnaminga Goldfield. To the south, Burra Group rocks have been intruded by the early Ordovician Anabama Granite (Forbes, 1991). Some associated felsic dykes (e.g., at Anabama and Netley Hills) have undergone high-level hydrothermal alteration to pyritic quartz-muscovite greisen with minor amounts of chalcopyrite and molybdenite. Greisen also occurs at Giles Nob (about 13 km ENE of Blue Rose) and as narrow veins at Blue Rose. Weathered granitic rocks crop out on the south side of the prominent creek in the southeastern corner of the prospect (Figure 19). It is uncertain whether this outcrop is part of the main Anabama Granite, or a dyke related to it.

7.3 Mineralisation

Mineralisation occurs in dolomite- and calcite-rich metasedimentary rocks (impure dolomites) containing disseminated sulphides, biotite, serpentine, tremolite, talc and chlorite. Vermiculite is present in some samples – it is uncertain whether it is a low-temperature hydrothermal alteration or weathering product of biotite, or its occurrence is the result of contamination (from saprolite). The higher-grade zones contain disseminated chalcopyrite, but not all sulphidic zones are mineralised. The presence of serpentine (probably a hydrothermal alteration product) also appears to be generally indicative of mineralisation. Another feature of mineralised zones is recrystallisation, which proceeds along grain boundaries. From limited data, classification of the mineralisation type is not possible.

The mineralisation is superimposed upon carbonate rocks regionally metamorphosed at low grade, producing talc and tremolite:



No forsterite, or pseudomorphs after forsterite, have been recognised, and it is most likely that serpentine has formed by hydrothermal alteration of talc and/or tremolite.

The relatively anomalous Mo concentrations (up to 390 ppm) in drill hole BRRC18 suggest the presence of molybdenite (although none has been recognised in hand specimen), and may indicate some affinity with the mineralisation with the Anabama Granite, where low-grade Cu-Mo mineralisation occurs at the Netley Hill prospect (Morris, 1981).

7.4 Vegetation

The terminology for the vegetation structural classification system has been adapted from Keighery (1994). In the flat areas at Blue Rose, *Sclerolaena patenticuspis* and *Maireana sclerolaenoides* Open Low Heath is the dominant vegetation type with rare examples of *Myoporum platycarpum*, *Eremophila longifolia* and *Alectryon oleifolium* subsp. *canescens*, and a few patches of *Maireana sedifolia* and *Maireana pyramidata*. Creek lines consist of *Senna artemisioides* subsp. *petiolaris*, *Senna* sp. and *Eremophila sturtii* Open Tall Shrubland over mixed Chenopodaceae Low Shrubland over an Asteraceae and *Salvia verbenaca* Very Open Herbland. Creek edges are lined with *Acacia victoraea* Open Tall Shrubland over *Maireana sedifolia* and *Maireana pyramidata* Low Open Shrubland.

7.5 Sampling

The following samples were collected:

- (i) all RC drill holes were logged and cross-sections were drawn; 22 samples of relatively high-grade Cu intersections (in fresh rock and regolith) were analysed; the mineralogy of these samples was investigated with XRD and lithologies confirmed with 18 thin-sections; samples on either side of the interpreted transported-residual boundary were investigated to adjust the position of the contact, if necessary;
- (ii) 104 auger holes were drilled on six traverses across the interpreted position of the aeromagnetic anomaly; the lines were spaced 600 m apart, with holes generally 100 m apart, except over the mineralised zones, where spacings were 50 m; the >6 mm fraction (mainly calcrete and silcrete) was analysed for each hole; 20 samples of <6 mm fraction were separated and analysed for comparison (on grid line 428820E);
- (iii) the following samples were collected along grid line 428820E to determine whether there was any surficial response to underlying mineralisation:
 - (a) 20 <2 mm soils (from 0-10 cm depth) and 10 infill samples over the mineralised zone;

- (b) 20 2-6 mm lags; the magnetic fraction was separated and analysed;
- (c) 20 samples of <2 mm soil from 10-20 cm for partial leach analysis (water, cyanide, pyrophosphate and MMI); one sample was also collected close to BRRC18 (with the thickest intersection of mineralisation);
- (iv) 16 <2 mm soils along grid line 427250E, to confirm the Cu anomalies in the augered samples, where transported overburden is considered to be thin (<6 m);
- (v) 3 rock-chip samples from silicified outcrops in the south;
- (vi) 5 samples at 10 cm intervals, from a shallow pit in calcrete, adjacent to auger hole BRA24, above mineralisation, on grid line 428820E.

7.6 Regolith

Most of the area is in a depositional regime (Figure 19) though, in some parts of the prospect, transported overburden may be only 2 m thick. The nature of this transported overburden is described in section 7.6.1 below. The area is bisected diagonally by a major creek system. There is very little outcrop at Blue Rose, where the topography is very flat (Figure 20a). Gentle rises, with bluebush, signify areas where calcrete occurs at relatively shallow depth. Apart from minor outcrops in the creeks in the north and east, highly weathered exposures occur on the southern side of the major creek in the southeastern part of the prospect. These exposures have been silicified, although relatively unsilicified domains have been preserved. Locally, fresh pyrite and hematite after pyrite have been preserved in the silicified domains. The serpentine-bearing exposure in the creek to the east represents silicified carbonate rock.

7.7 Geological cross-sections

Geological cross-sections were drawn, after logging of RC drill holes, XRD and limited petrography, for sections 427250E, 427620E, 428220E, 428820E and 428925E, as shown in Figure 21 to Figure 25. Full descriptions, photographs and locations of the RC drill cuttings are found in Appendix 3.13.

Section 427250E

In the northwest of the prospect, RC drilling has intersected sulphidic shales below 2-10 m of transported cover (Figure 21). Transported cover in BRRC1 is significantly thicker (10 m) than in BRRC2, where colluvial gravels 2 m thick overlie saprock. In BRRC1, transported cover comprises colluvial gravels cemented by calcrete/silcrete (2 m thick) underlain by greyish brown to yellow clays and lithic gravels (siltstone, quartz, ferruginous lithic fragments) with chalcedony veining. Calcite is most abundant in the uppermost 2 m of the transported profile, but persists down to the base of transported cover at 10 m depth (in BRRC1).

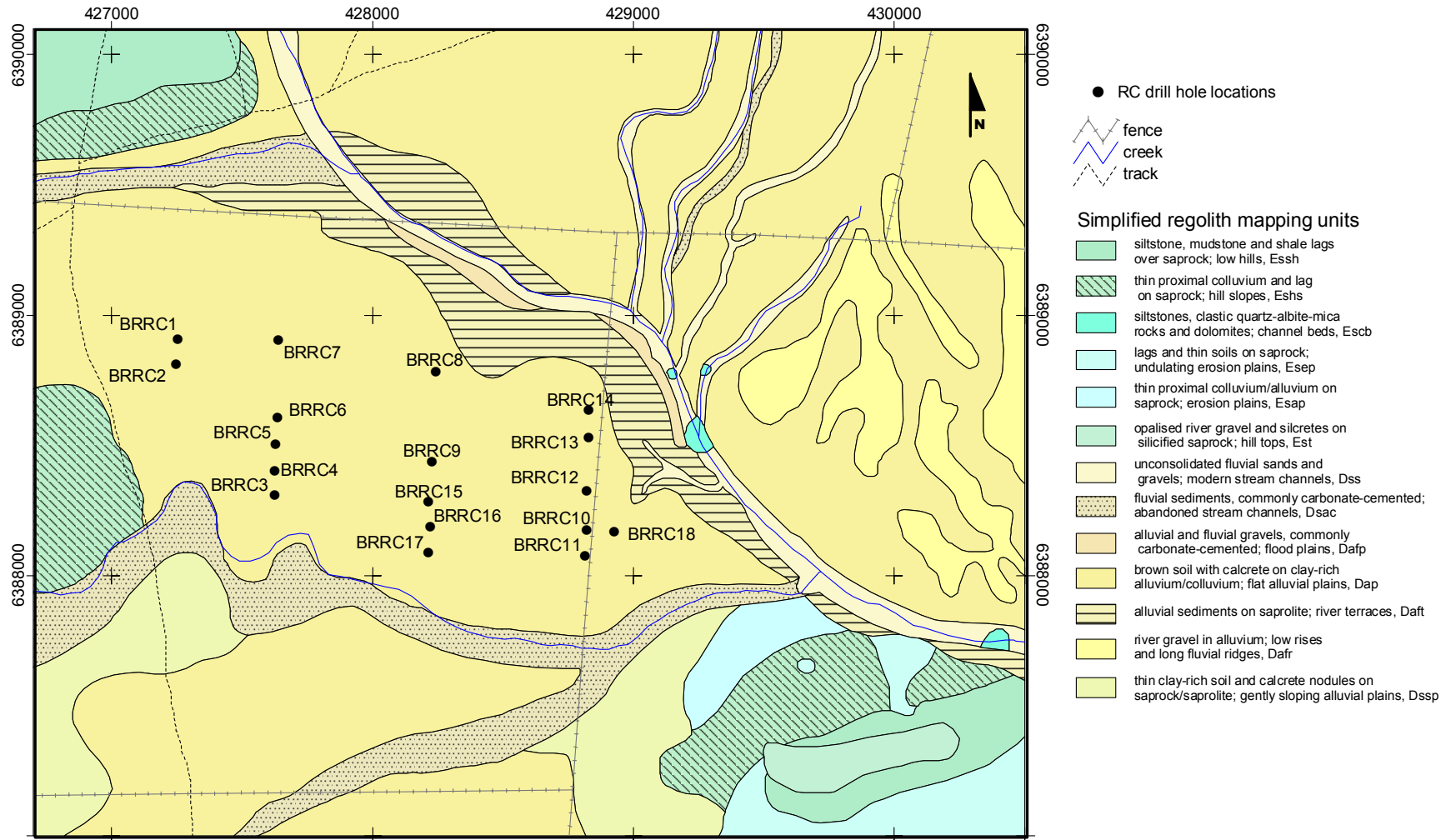


Figure 19: Regolith-landform map of the Blue Rose prospect, showing location of RC drill holes. Full regolith landform unit descriptions are found in Appendix 6.

In BRRC1, the saprolite contains vermiculite-rich clays and strongly bleached shale with Fe oxides after pyrite. Saprock (31-58 m thick) comprises foliated, white to grey, micaceous to siliceous rocks, with casts and Fe oxides after pyrite, coarse-grained mica (?vermiculite) on foliation planes, and jarosite and Fe oxide coatings on fractures. Weathering along joint planes (Fe oxide coatings) locally persists into the bedrock below.

The fresh shale is typically grey to black, argillaceous to siliceous, pyritic, and with coarse-grained mica on bedding planes.

Minor, anomalous Cu occurs in saprolite (in BRRC1), and in narrow zones in the saprock and bedrock below. The Cu is probably related either to minor chalcopryrite in the pyritic domains, or to very narrow sulphidic quartz veins.

Section 427620E

This section intersects thicker transported cover (up to 31 m in BRRC5; Figure 22) than on the previous section. In the transported unit, a basal lens of orange-brown, apple-green, white, grey, yellow-brown and red-brown mottled plastic clays (up to 22 m thick) is overlain by white, yellow-brown and orange-brown clays and colluvial gravels (composed of chert, siltstone, 'buckshot' gravel, quartz, saprolite, and albite-quartz-mica rock fragments), veined with chalcedony. Above this, the calcrete horizon varies from 2-3 m in thickness. Calcite is common in the upper 10 m of the transported profile. Thin calcareous soil occurs at the surface.

The saprolite is thin or absent in the southernmost drill holes (BRRC3-5) – it has been eroded prior to deposition of the mottled plastic clays. In BRRC3, the saprolite is vermiculite-bearing and lies above weathered albite-quartz-mica rock. To the north, in BRRC5-6, the saprolite consists of white to pale yellow-brown and grey-green quartz-rich clays which grade downwards into a weathered albite-quartz-mica rock. In BRRC7, relatively thick saprolite comprises vermiculite-rich clays over weathered shales and siltstones. Bedrock in the north is siltstone with argillaceous layers and shale, whereas, in the south, the principal rock type is a clastic, fine-grained albite-quartz-muscovite rock, intercalated with thin carbonate horizons.

The zones with anomalous Cu in bedrock and saprock appear to be related to thin zones with disseminated sulphides. However, the blanket of anomalous Cu at the top of the residual profile, extending into basal portions of transported cover, appears disproportionate in size to the thin zones of disseminated sulphides below, and may represent lateral dispersion of Cu from mineralisation to the east.

Section 428220E

Transported cover attains its greatest thickness (up to 42 m) on this section (Figure 23 and Figure 27). The uppermost unit is calcrete and silcrete of variable thickness (1-4 m) developed in clays and gravels. In the north (in BRRC8) this is underlain by silcrete with chalcedony veining, but calcite persists throughout. Below the calcrete-silcrete layer, a unit up to 14 m thick, locally with distinct gravel beds, contains weakly mottled, orange-brown, red-brown, white, yellow-brown and brown-orange clays, veined with chalcedony. These clays and gravels overlie a prominent unit (up to 14 m thick) of brick-red, grey, yellow-brown, orange-brown, pale green, red-brown, purple-brown and yellow-green plastic mottled clays. In deeper parts of the transported profile, in the south, this unit is underlain by monotonous white to grey plastic clay up to 15 m thick. Thin (1-2 m thick) basal lithic gravels (in BRRC8) and white clays with quartz gravels (in BRRC15) occur at the base of the transported profile.



Figure 20: Blue Rose prospect. **a**, general view of Blue Rose prospect, illustrating the flat topography (viewed to the north, from 6388650N, 428830E) Burra Group sedimentary rocks form the hills on the horizon; **b**, silicified outcrop containing disseminated pyrite and 950 ppm Cu at sample locality EBBR2 (6387914N, 429581E); the soil is calcareous.

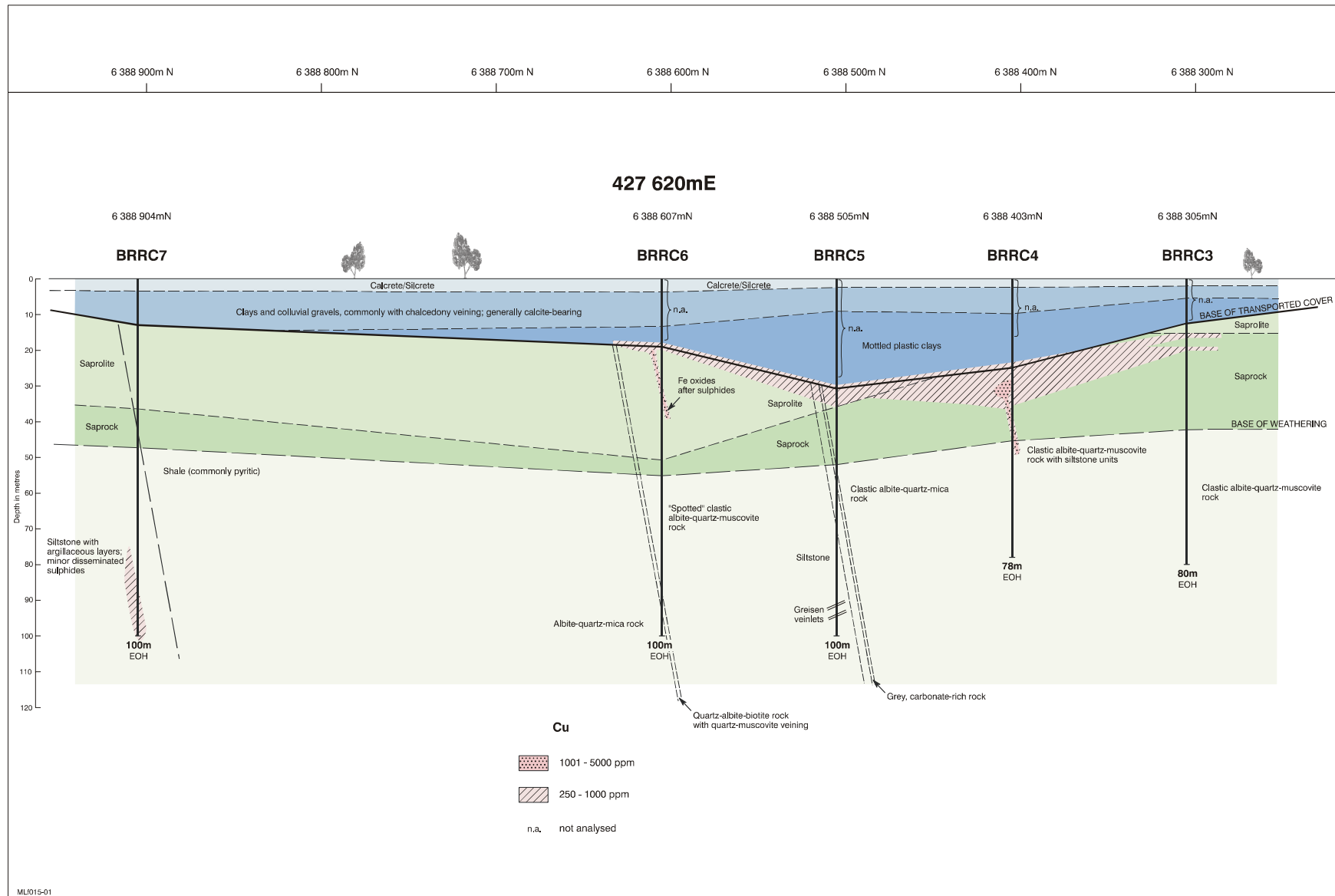


Figure 22: Interpreted geological cross-section on line 427620E, showing interpreted distribution of Cu (ppm). See Figure 19 for locations of drill holes.

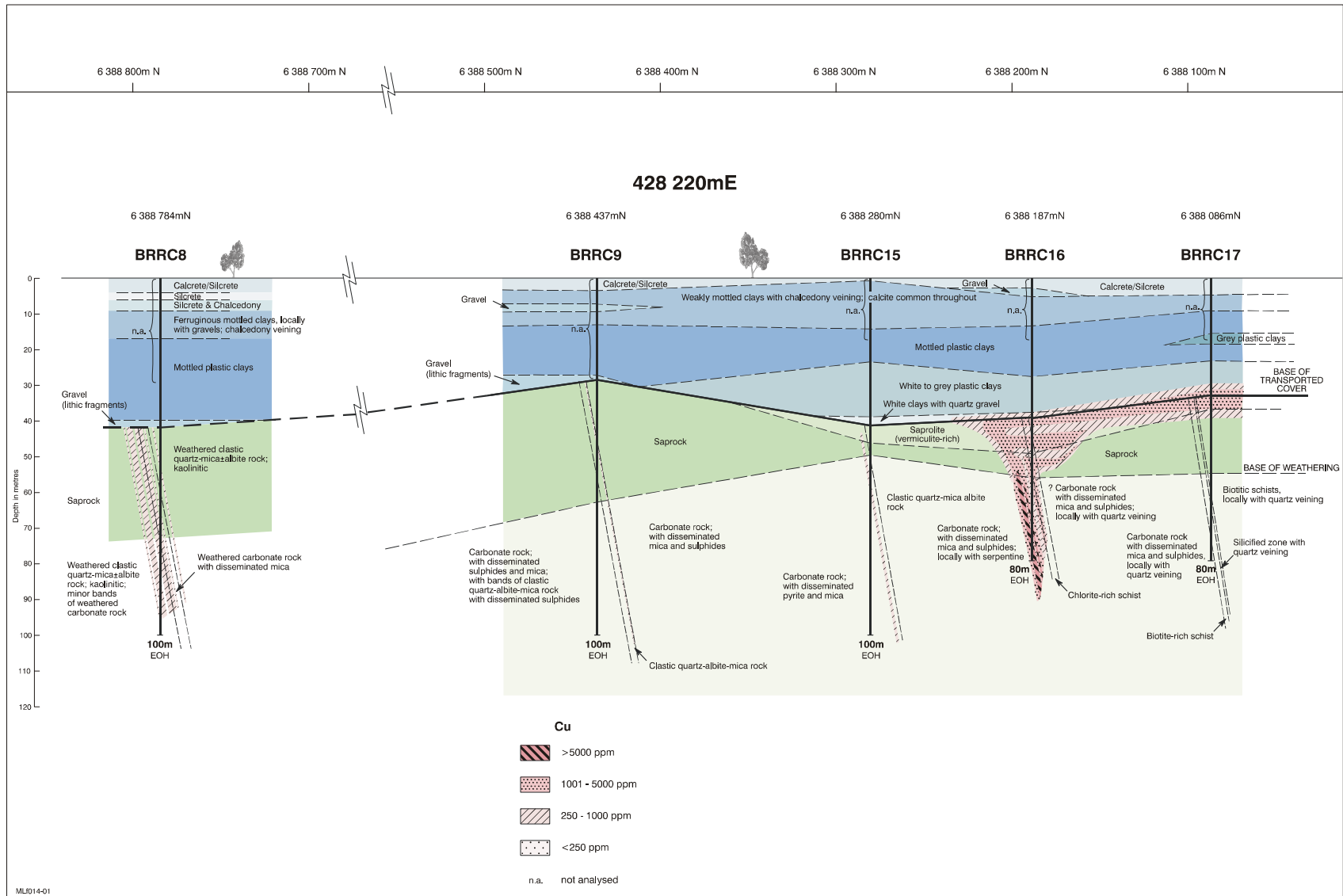


Figure 23: Interpreted geological cross-section on line 428220E, showing interpreted distribution of Cu (ppm). See Figure 19 for locations of drill holes.

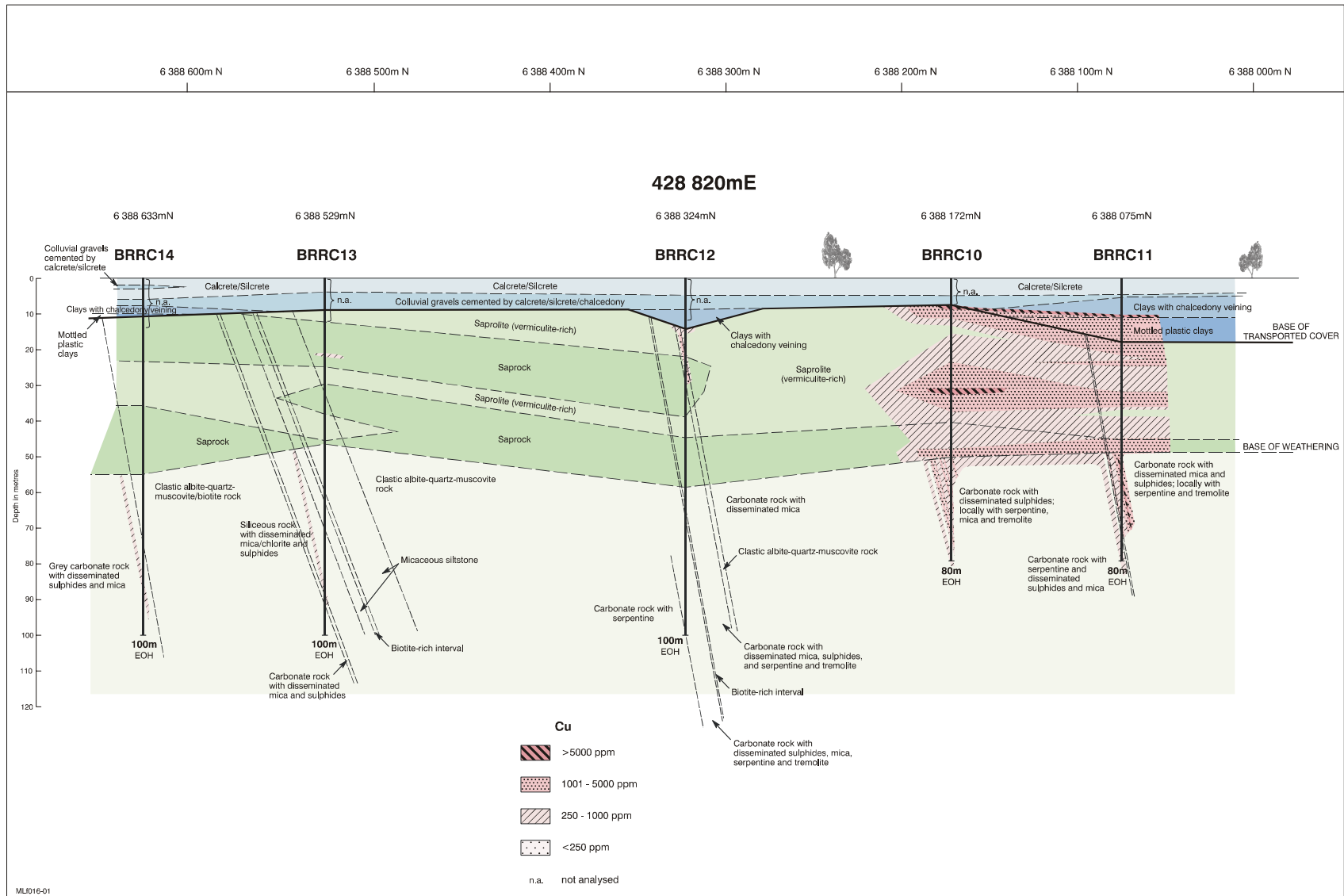


Figure 24: Interpreted geological cross-section on line 428820E, showing interpreted distribution of Cu (ppm). See Figure 19 for locations of drill holes.

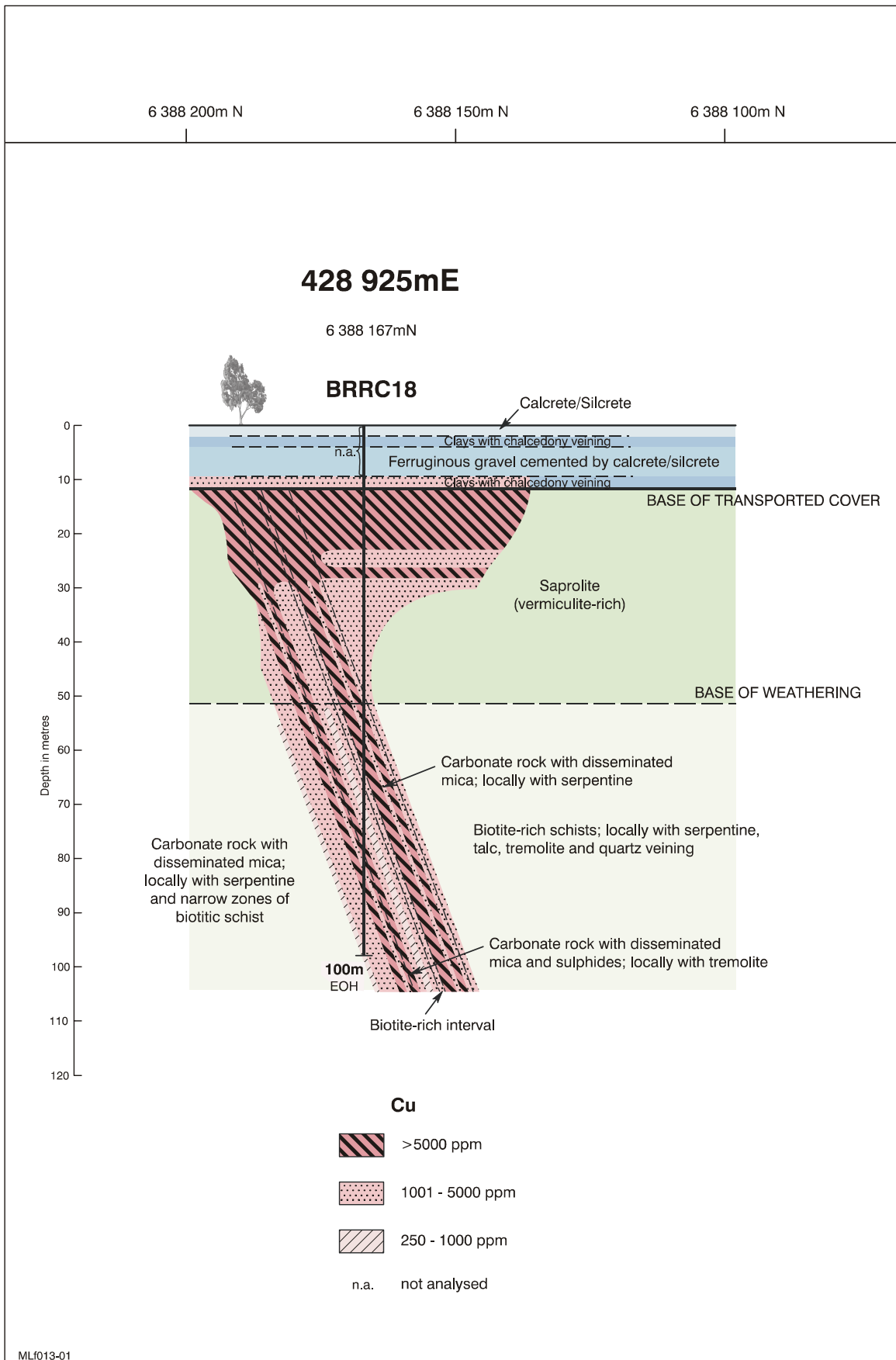


Figure 25: Interpreted geological cross-section on section 428925E, showing interpreted distribution of Cu (ppm). See Figure 19 for location of drill hole.

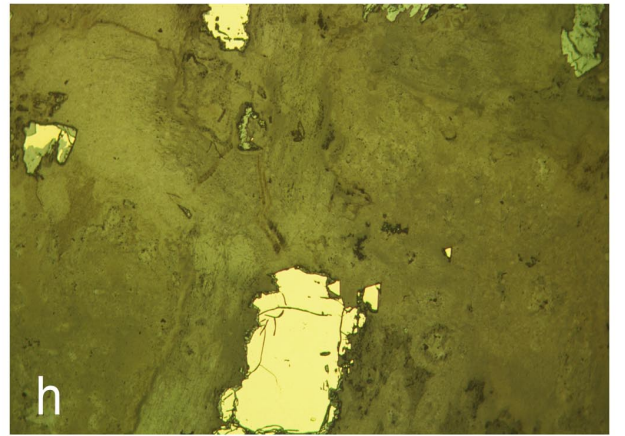
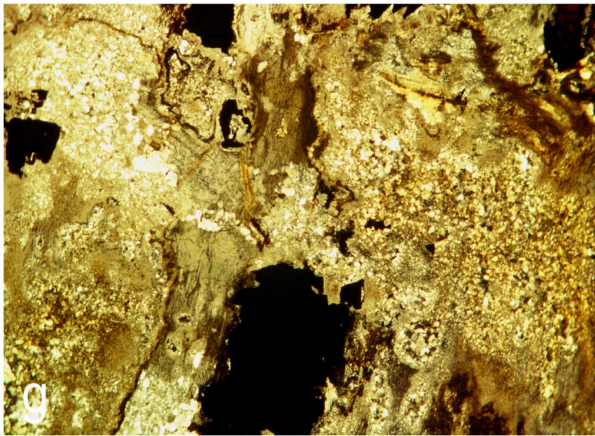
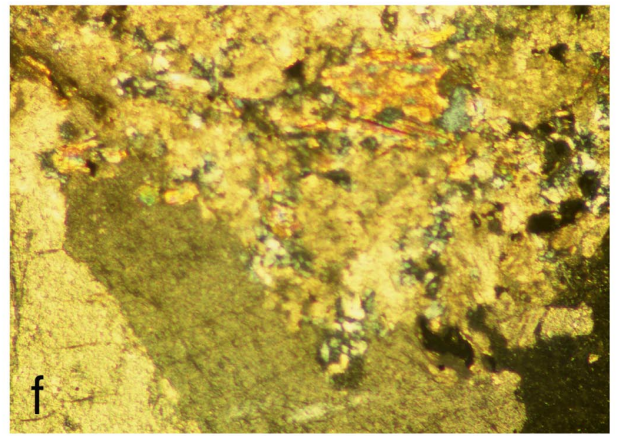
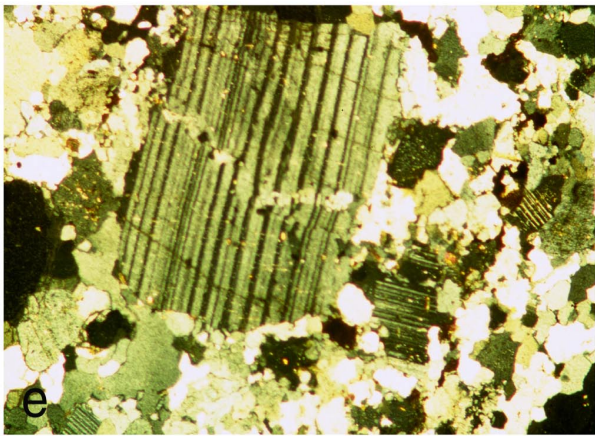
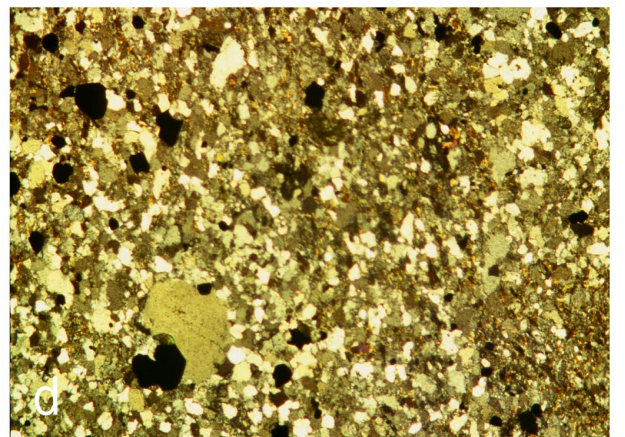
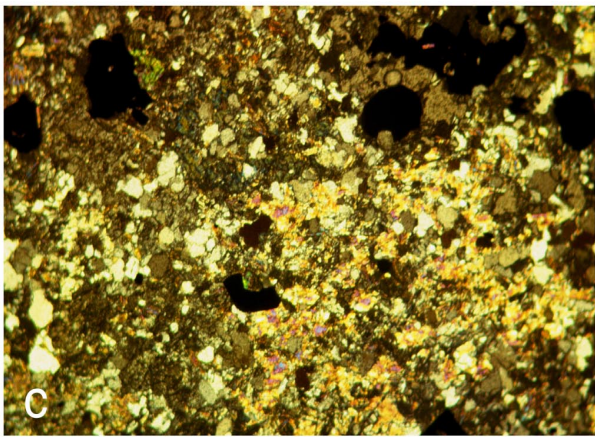
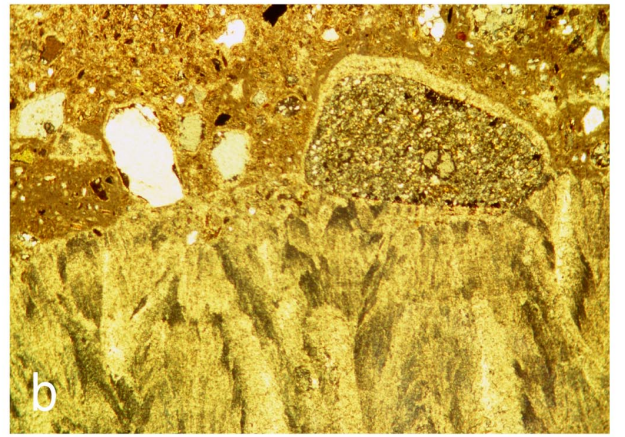
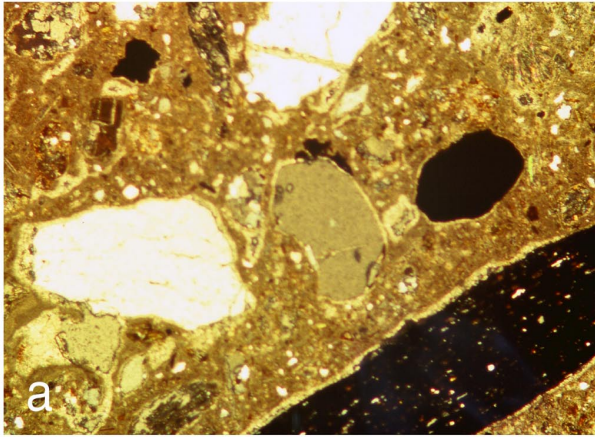


Figure 26 (previous page): Selected photomicrographs of lithologies from Blue Rose. **a**, silcrete, comprising cemented lithic fragments (including quartz, ferruginised siltstone, and buckshot gravel) in a very fine-grained matrix of silica and iron oxides (BRRC13, 6-7 m; x250); **b**, calcite rim on silcrete – the carbonate rind on the exterior of a calcrete nodule (BRRC13, 6-7 m; x250); **c**, carbonate-tremolite rock with disseminated sulphides (BRRC9, 63-64m; x250); **d**, banded, clastic albite-quartz rock, with disseminated mica and sulphides (BRRC9, 63-64m; x250); **e**, fractured and twinned carbonate porphyroblast in dolomite (BRRC5, 61-62 m; x300); **f**, hydrothermal alteration of marble, destroying metamorphic fabric of the rock; some of the opaques are sulphides (BRRC18, 64-65 m; x180); **g**, silicified rock with largely destroyed fabrics and partially preserved disseminated pyrite (EBRR2; plane polarised light; x200); **h**, same view in reflected light, showing pyrite grains partially to completely replaced by hematite.

In the south, the saprolite is composed of vermiculite-rich clays and is relatively thin (<10 m thick), whereas in the north, in drill hole BRRC8, where fresh bedrock was not intersected, the saprolite is at least 58 m thick and consists of kaolinitic clays derived from albite-quartz-mica rock with thin carbonate horizons.

Narrow, relatively high-grade zones (>5000 ppm Cu) occur in a carbonate unit with disseminated sulphides and serpentine (BRRC16). There is a slight thickening of the weathered residual profile above this zone. The Cu dispersion halo extends into saprolite and the basal 2 m of transported cover, forming an asymmetric blanket at least 160 m wide (at >250 ppm Cu), derived from a zone that is at least 12 m wide in bedrock. The main mineralised zone appears to be confined between drill holes BRRC15 and BRRC17. Only thin, weakly anomalous zones occur to the north.

In drill hole BRRC8, broad, low-grade (250-1000 ppm Cu) zones occur in the deep weathering profile. The significance of this deep weathering is unclear, but may indicate proximity to a fault.

Section 428820E

Transported cover is significantly thinner (<20 m) on this section (Figure 24). The transported sequence below a thin soil horizon is:

- (i) calcrete and silcrete, up to 5 m thick, cementing colluvial clays and gravel;
- (ii) colluvial gravel, up to 6 m thick, cemented by calcrete, silcrete and chalcedony veining;
- (iii) clays with chalcedony veining, up to 6 m thick; and
- (iv) orange-brown, red-brown, yellow-brown, emerald-green and green, mottled, plastic clay, up to 8 m thick, best developed where the transported profile is thickest (in BRRC11) in the south.

The residual regolith consists of a complex interdigitation between saprock and saprolite in the north, whereas, in the south, the profile is simpler, with saprolite overlying saprock. Saprolite along the section consists of vermiculite-rich clay.

In the south, the dominant rocks are carbonate-rich, with thin horizons of clastic albite-quartz-mica rock. The carbonate rocks contain disseminated mica and sulphides and, locally, tremolite and serpentine. Mineralisation is restricted to the southernmost drill holes (BRRC10-11). In the north, the clastic units appear to be more abundant.

Medium-grade (1000-5000 ppm Cu) mineralised zones in bedrock have produced a significant dispersion halo, at least 170 m wide in saprolite and saprock, extending into the basal part of transported cover. This anomalous zone is open to the south.

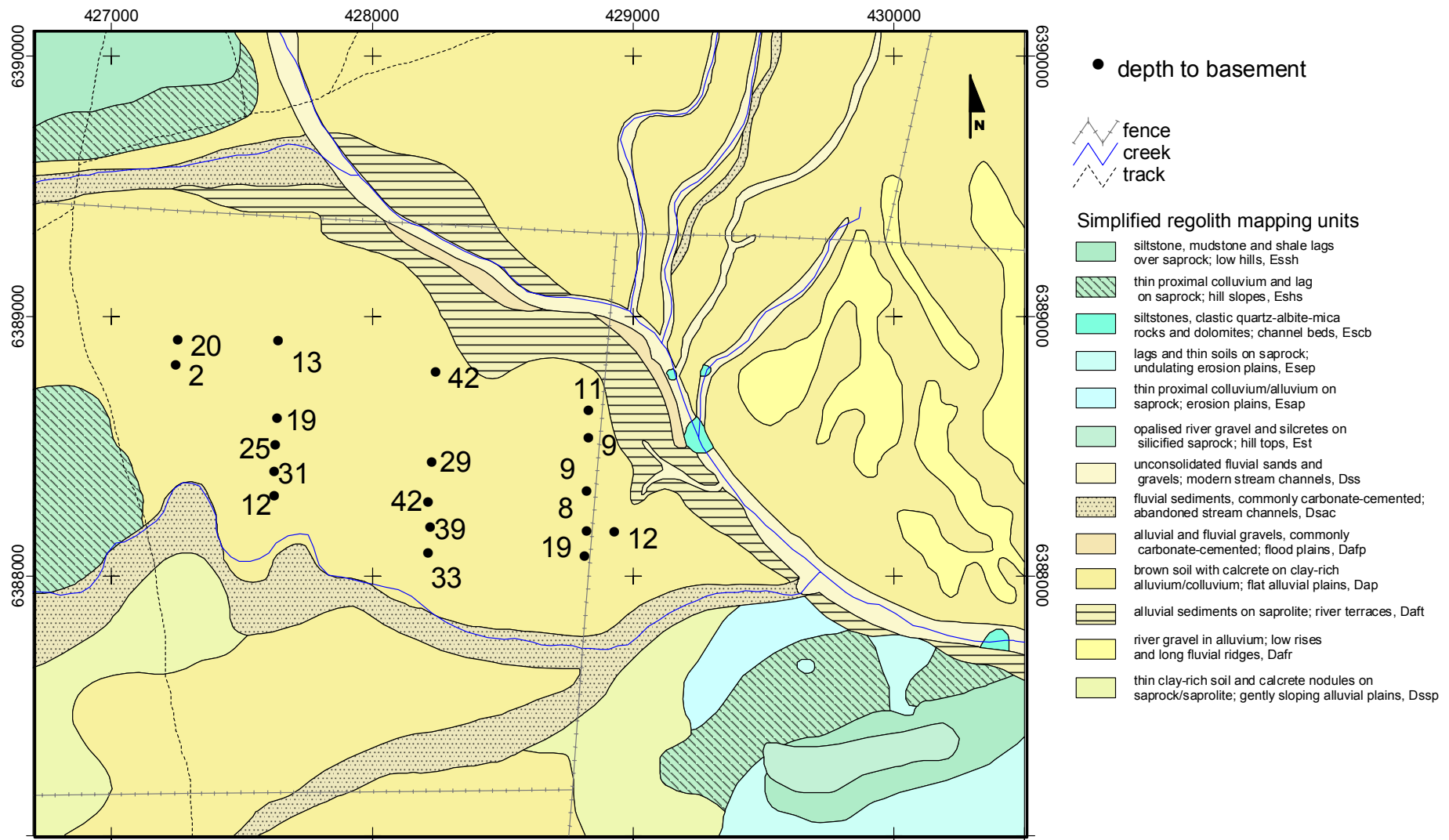


Figure 27: Depths to base of transported cover (in metres) from RC and RAB drilling, Blue Rose prospect. Full regolith landform unit descriptions are found in Appendix 6.

Section 428925E

Only one hole (BRRC18) has been drilled on this section (Figure 25), but has returned the thickest anomalous Cu intersection (88m @ 0.39% Cu). Transported cover consists of calcrete-silcrete (2 m thick), clay with chalcedony veining (2 m thick), and ferruginous gravel cemented by calcrete-silcrete (6 m thick), and clay with chalcedony veining (2 m thick) at the base.

Saprolite comprises vermiculite-rich clays. Bedrock consists of carbonate rocks (with disseminated sulphides, mica, serpentine, talc and tremolite) in contact with biotite-rich schist.

The relatively high-grade zones (>5000 ppm Cu) appear to be restricted to the carbonate rocks. Significant dispersion extends through saprock and saprolite into the basal layer of transported cover, and is open in every direction.

7.8 Geochemistry

7.8.1 *Geochemistry of mineralised intervals*

Twenty-two samples of relatively high-grade Cu intersections (including nine from regolith) were selected for detailed analysis, to determine the geochemical associations of the mineralised zone. Samples were chosen from drill holes BRRC10, BRRC11, BRRC16 and BRRC18.

In fresh bedrock, the more significant Cu intersections are associated with relatively anomalous Bi, Cs, In, K, Mo, Rb, S, Se and Tl concentrations, but Sr contents are relatively low. There is little correlation between Au and Cu. Regolith samples contain greater Al, As, Cr, Fe, Ga, LOD (loss on drying, i.e. moisture), Na, Ni, REE, Ti, V, and Y, but lesser Cs, K, Mg, Mn, Rb and S concentrations than fresh rock. Copper correlates positively with Co, In, Se and Sn (probably concentrated in chalcopyrite), but not with Au (which correlates positively with Bi and Te; possibly associated with Bi telluride(s)) or Mo (which correlates positively with Se, indicating Se in molybdenite). The association of Se with Cu-Mo mineralisation is a common feature worldwide.

The abundances of most of the other elements are dependent upon lithology. Those elements most abundant in the dolomitic rocks are K, Mn, S, Cs, Rb, Tl and, to a lesser extent, Ba and Ca, those most abundant in silicate rocks are Al, Cr, Na, Si, Ti, V, REE, Y, Ga, Sr, Th and Zr.

7.8.2 *Rock-chip sample geochemistry*

Three samples were collected from strongly weathered outcrops on the south side of the creek in the southeastern corner of the prospect. The results are shown in Figure 29, Figure 30 and Figures A3.4.2-56. Sample EBRR2 contains significant Cu (950 ppm) and also contains anomalous As, Bi, Cd, Co, In, Mo, S, Se, Tl and U. The S (1.33%) and Se (32 ppm) concentrations are due to sulphides.

7.8.3 *Geochemistry of pit samples*

A shallow pit was excavated to 0.5 m to expose powdery and nodular calcrete below a thin soil. Samples were taken over 10 cm intervals down the profile, to determine the distribution of elements.

The 0-10 cm soil is slightly calcareous (3.72% Ca), becoming more so with depth (11.9 % at 10-20 cm, and >20% below 20 cm). In contrast, concentrations of most other elements (either associated with Fe oxides or diluted by the carbonate) are greatest in the uppermost horizon (Table 1; Figure 28). Copper concentrations decrease slightly down the profile. However, there is little difference between the 0-10 and 10-20 cm samples, indicating that the depth of soil sampling is not critical for conventional techniques. Gold shows little variation with depth (analytical and/or sampling noise).

Table 1: Vertical distribution of elements in the soil profile, Blue Rose prospect. Antimony, Se and Te are below detection.

Depth	Maximum concentration
0-10 cm	Ag, Al, Bi, Co, Cr, Cs, Cu, Ga, Fe, Hf, In, K, Mn, Mo, Na, Nb, Ni, Pb, REE, Rb, Sn, Th, Ti, Tl, U, V, W, Zn
10-20 cm	REE
20-30 cm	As, Au, P, Y
30-40 cm	Ba, Ca, Cd, Mg, S, Sr, Y
40-50 cm	No element

7.8.4 Geochemistry of augered samples

The samples were collected from depths varying between 0.2 m and 0.7 m, depending on the degree of penetration by the auger. The regolith profiles intersected by the drilling comprised a soil horizon (of variable thickness) overlying calcrete (typically nodular). The >6 mm fraction of the calcrete was analysed.

Element abundances are generally greatest where transported cover is known to be relatively thin (<6 m), west of the fence line, and in the south. To the east of the fence line, interpretation of the geochemical data is hampered by uncertainty of the thickness of transported overburden.

Gold: Overall, Au concentrations are less than 6 ppb. Samples with relatively anomalous Au (>3.8 ppb) are irregular in distribution (Figure 29). However, the anomalous sample in the southwest can be ascribed to a domain where the thickness of transported cover is interpreted to be relatively thin (<6 m). The reasons for the anomalous results adjacent to a creek on grid line 429100E are unclear, but the samples lie approximately along strike from the mineralised zone intersected on grid lines 428820E and 428925E. Gold shows no significant correlation (at the 99.9% level) with any other element. There is no clear evidence for an association between Au and calcrete.

Calcium: The pattern of Ca distribution is similar to that of Ba and S. Calcium concentrations are greatest in the west and southwest (Figure A3.4.8). There is no correspondence between Ca concentration, calcrete type, thickness of transported cover or depth of auger hole. Calcium contents are generally >15%, except for a few samples where the calcrete content is minor, possibly due to a relatively thick soil. Calcium is positively correlated with Sr. Negative correlations with Al, Bi, Ce, Cr, Cs, Fe, Ga, K, La, Mn, Mo, Na, Ni, P, Sn, Th, Ti, Tl, V and Zn indicate dilution by carbonate.

Copper: Samples with relatively anomalous Cu (>30 ppm) are irregular in their distribution (Figure 30). However, anomalous samples in the southwest can be ascribed to a domain where the thickness of transported cover is thin (<6 m). This is a strong and coherent anomaly.

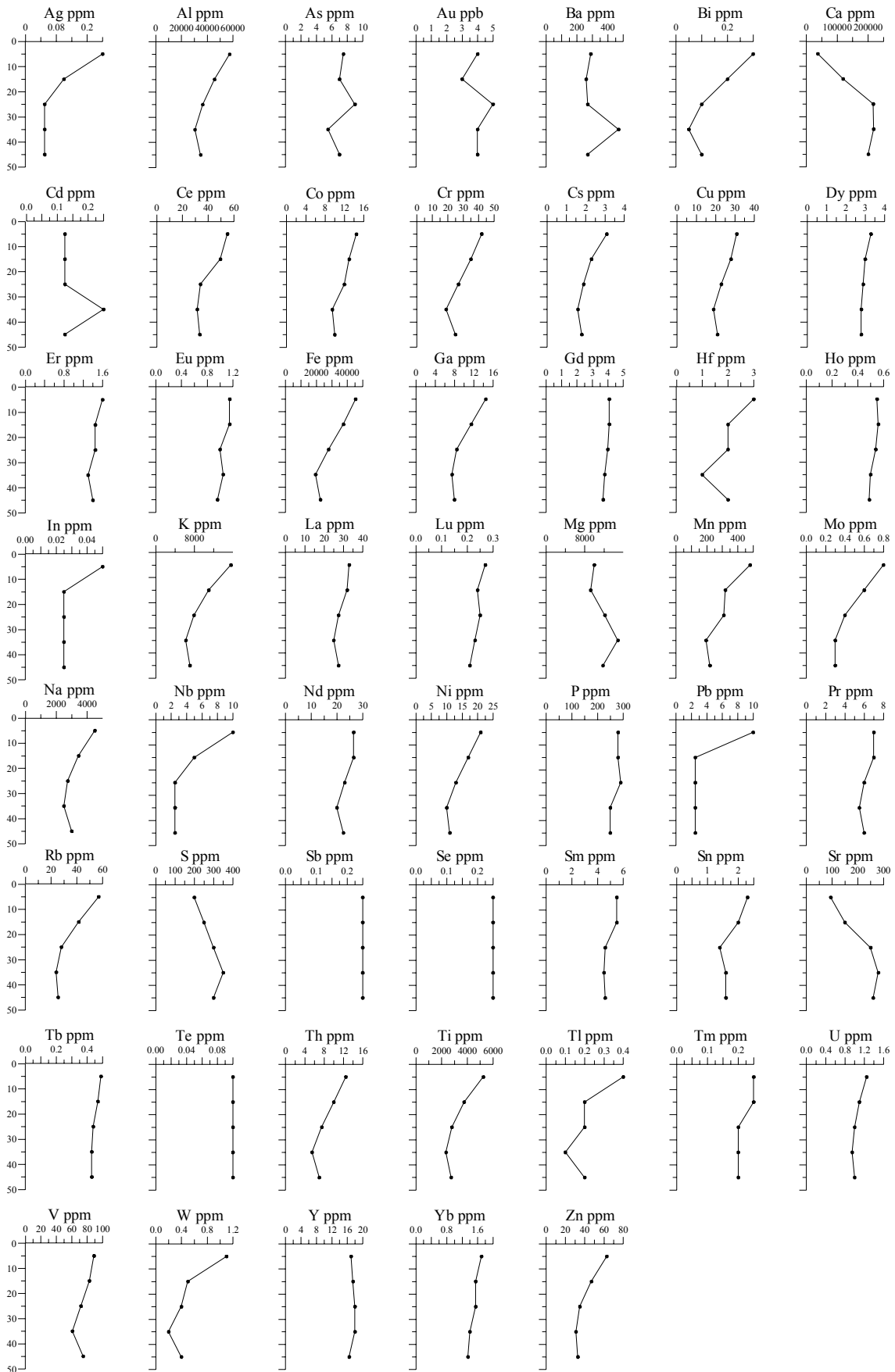


Figure 28: Element concentrations down the soil profile at Blue Rose (6388074N 428818E). The y axis is the depth (cm), whereas the x axis is concentration.

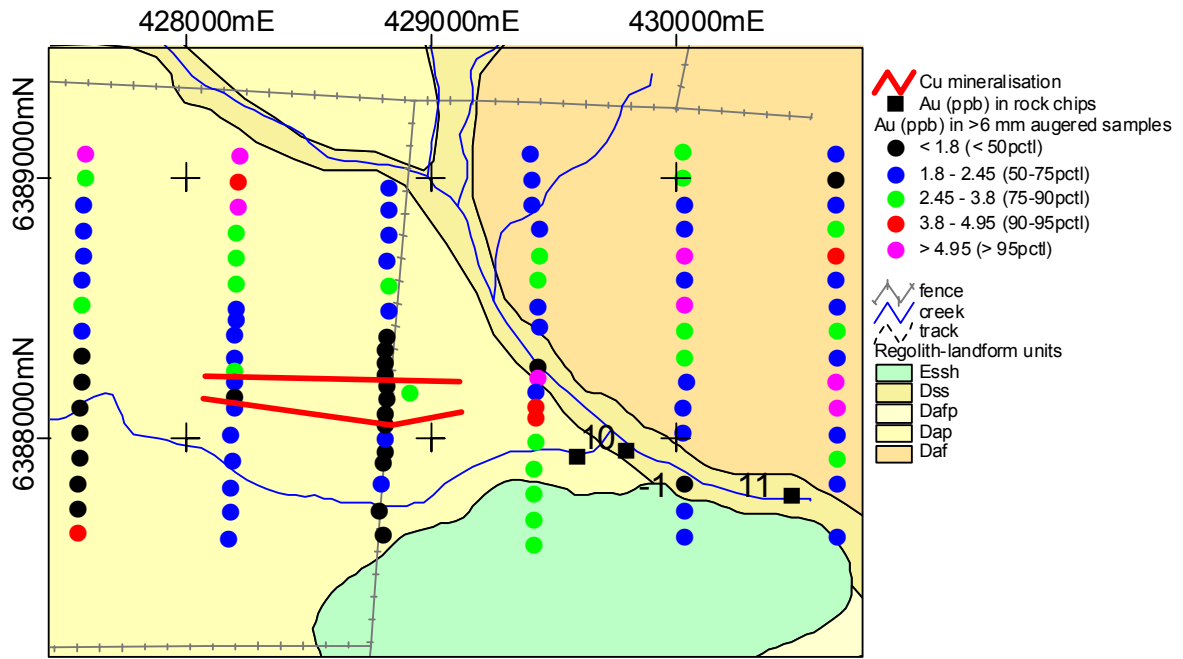


Figure 29: Distribution of Au (ppb) in >6 mm augered samples (soil and calcrete) and rock chip samples, Blue Rose. Full regolith landform unit descriptions are found in Appendix 6. A simplified regolith landform unit code is used here.

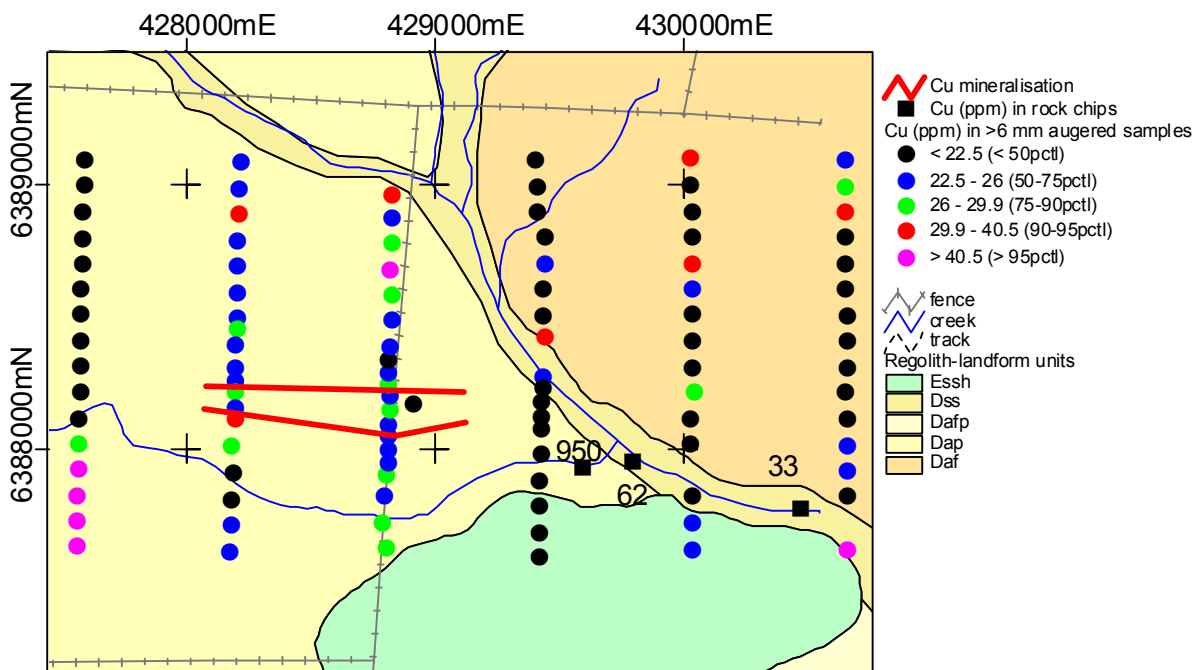


Figure 30: Distribution of Cu (ppm) in >6 mm augered samples (soil and calcrete) and rock chip samples, Blue Rose. Full regolith landform unit descriptions are found in Appendix 6. A simplified regolith landform unit code is used here.

7.8.5 Soil geochemistry

The results are plotted in Figure 32, Figure 33 and Appendix Figure A3.5.

7.8.5.1 Grid line 428820E

These samples were collected in two phases. Most elements show little variance along the traverse, and, except for Mo and W, give no indication of the mineralised zone. Molybdenum and W (Figures A3.5.30 and A3.5.53) show low-level anomalies over the mineralised zone (125 m wide at <0.9 ppm and 150 m wide at <2.3 ppm, respectively). It is uncertain whether these responses are truly indicative of the mineralised zone below, or whether they reflect slight increases in the abundance of magnetic granules in the samples. Copper concentrations are close to background (30 ppm) and give no indication of underlying mineralisation. Calcium and Sr are variable along the traverse, and reflect variations in the calcite content of the soils. Arsenic, Ba, Th and Ti are also irregular in distribution, which may inversely relate to calcrete content.

7.8.5.2 Grid line 427250E

In general, the distributions of elements in the soil are similar to those in the auger samples, except that absolute concentrations are greater in the soil. The exceptions to this are As, Ba, Ca, Cd, Mg, S and Sr, which are less abundant. These differences relate to the vertical distribution of elements in the uppermost 50 cm of the profile (see section 6.4.4) – those elements with greater concentrations in soil are most abundant in the upper 10 cm, those elements with greater concentrations in augered samples are more abundant at 20-40 cm depth.

Copper and Au anomalies are coincident (Figure 32) and are up to 125 m wide, with up to 280 ppm Cu and 21.5 ppb Au. Cobalt, Na and P anomalies are also coincident with Au and Cu, but there is no response in Mo. Fe or Mn oxides control none of the distribution patterns.

This indicates that there is no advantage in using auger drilling where the transported overburden is thin and where soil sampling (0-10 cm depth) is equally effective. Where transported overburden is thick (>6 m), neither soil sampling nor auger drilling are likely to yield useful samples.

7.8.6 Lag geochemistry

The magnetic lag is Fe-rich (~50% Fe); slight variations are probably due to composite grains containing non-magnetic material. This suggests that the lag may have been derived either from a common source or represents an average composition of materials derived from multiple sources.

Gold is generally below detection (Figure 33, 1 ppb) and Cu concentrations are minor (Figure 32, <50 ppm). There is no relationship between lag geochemistry and the mineralisation. The uniform composition of the lag and local concentration by sheetwash indicate that the lag has been transported and its composition is likely to be independent of the substrate.

7.8.7 Partial leach analyses

Soil samples (<2 mm fraction) were collected at 50 m intervals at 10-20 cm depths along grid line 428820E, over the mineralised zone. The results are plotted in Appendix 3.7, where the data for partial leaches is compared with that for <2 mm soil, >6 mm auger, <6 mm auger and 2-6 mm lag samples.

None of the partial leach analyses gives any indication at all over the mineralised zone (see, for example, Figure 31), where transported overburden varies between 8 and 19 m in thickness. The only possible response is a weak Mo anomaly in >6 mm auger and <2 mm soils.

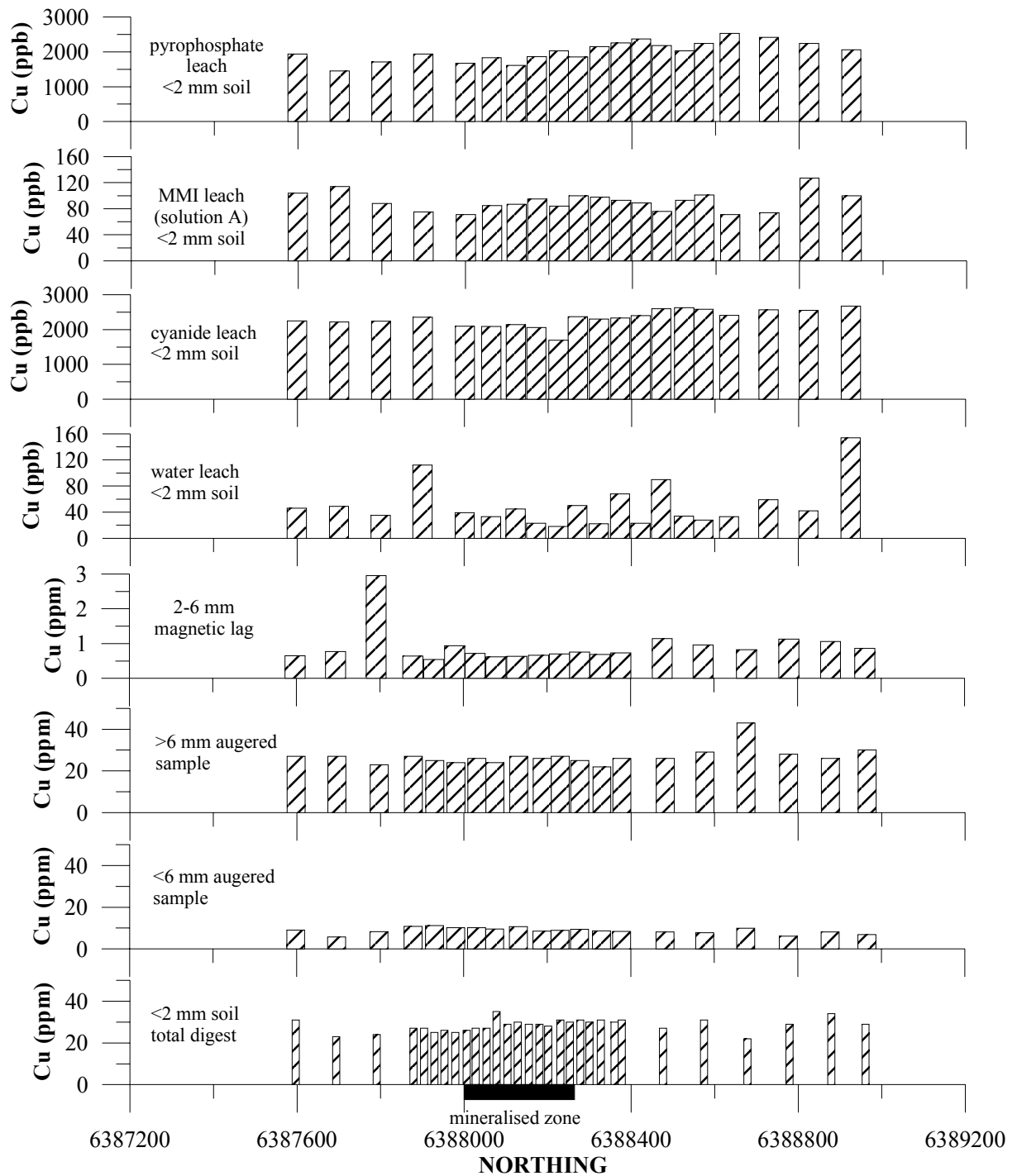


Figure 31: The concentration of Cu (ppm) in soil (<2 mm, 0.1-0.2 m depth) along grid line 428820E showing the responses from various sample media and partial leaches. Note that the presence of mineralisation has not been identified in the partial leach analyses. The lag, soil and calcretes sample analyses were determined by ICP-OES after dissolution by mixed acid digest.

7.9 A comparison of geochemical responses in augered, soil and lag samples along grid lines 427600E and 428820E

The results are listed in Appendix 3.5.

7.9.1 <6 mm versus >6 mm augered samples (428820E)

The following trends were noted (Figure 33, Figure A3.5d):

- (i) there is more Ca and less Fe in the >6 mm samples, reflecting the coarse grain size of the calcrete nodules;
- (ii) there is more Au, Cd, Mg, S, Sr and W tend in the >6 mm fraction, indicating some affinity with carbonate;
- (iii) most of the remaining elements (Al, Co, Cr, Cs, Ga, Hf, K, Mn, Na, Nb, Ni, Pb, Rb, most REE, Th, Ti, Tl, V and Zn) are more abundant in the <6 mm fraction, reflecting association with Fe oxides and clay minerals, and dilution by carbonate in the >6 mm fraction;
- (iv) Cu concentrations are similar in both fractions, and hence it is unnecessary to sieve augered samples when exploring for Cu;
- (v) there is no indication of mineralisation in either fraction, except possibly for spikes in Ag, As, Bi and Mo in the >6 mm fraction.

7.9.2 <2 mm soils versus >6 mm augered samples (427600E)

The following trends were noted (Figure 32, Figure A3.5a):

- (i) Ca concentrations are significantly greater (and Fe lower) in >6 mm augered samples, reflecting a greater proportion of carbonate below 10 cm depth in the profile;
- (ii) S, Sr and W concentrations are also greater in the augered samples;
- (iii) Ag, Al, Bi, Co, Cr, Cs, Ga, Hf, K, Mn, Na, Ni, Pb, Ti and Zn concentrations are greater in the soil; concentrations of the remaining elements are generally similar in both media;
- (iv) anomalous Au and Cu occur at the southern end of the traverse, suggesting the presence of mineralisation;
- (v) Cu (and possibly Au) concentrations are similar in both <2 mm soils and >6 mm augered samples.

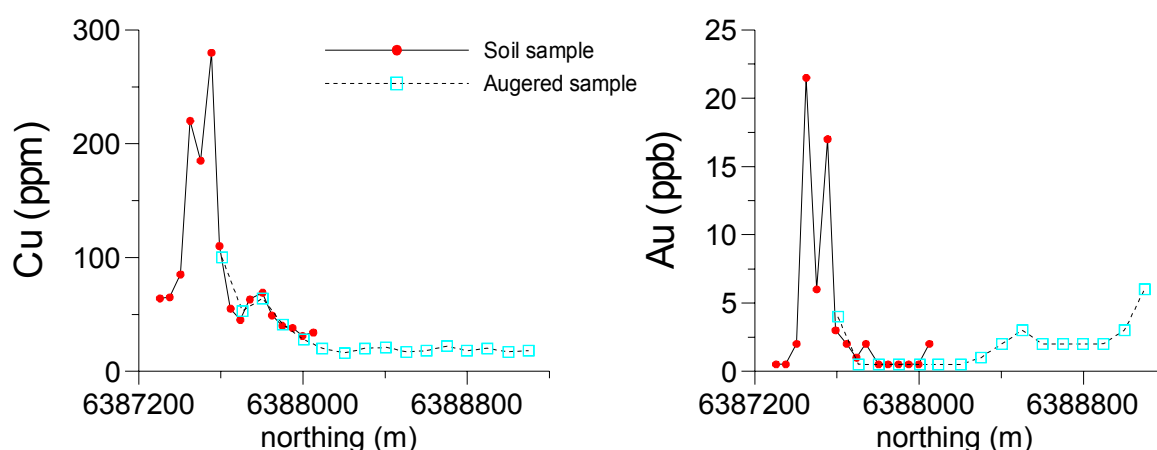


Figure 32: Comparison of Au and Cu geochemistry for different sample media on 427600E at Blue Rose:

7.9.3 <2 mm soils versus >6 mm augered samples (428820E)

The following trends were noted (Figure 33, Figure A3.5b):

- (i) as noted above, Ca concentrations are greater and Fe concentrations lower in >6 mm augered samples;
- (ii) S and Sr concentrations are generally greater in >6 mm augered samples;
- (iii) Al, Co, Cr, Cs, Ga, Hf, K, Mn, Na, Ni, Rb, most REE, Sn, Th, Ti, Tl, V and Zn concentrations are generally greater in <2 mm soils;

- (iv) Au concentrations are marginally greater in soils, whereas Cu concentrations are similar in both media; however, average concentrations are low;
- (v) single-point spikes in As, W and possibly Au occur above mineralisation, but these may also be related to analytical and/or sampling noise.

7.9.4 <2 mm soils versus 2-6 mm lags (428820E)

The following trends were noted (Figure 33, Figure A3.5c):

- (i) lag samples are rich in Fe (and As, Ba, Bi, Cd, Co, Cr, Cu, Ga, Hf, In, Mn, Mo, Ni, P, Pb, Sb, Se, Sn, Te, Th, U, V, W and Y);
- (ii) Al, Ca, Cs, K, Mg, Na, Rb and Ti are richer in soil;
- (iii) erratic data for some elements in soil (e.g., Ce, Er, Rb and Y) may indicate an analytical noise;
- (iv) there is a weak signal in Au, Ce, La, U and possibly Sn over mineralisation, but this may be related to analytical noise;
- (v) Au is generally more abundant in soil than lag; whereas the converse is true for Cu, perhaps reflecting an association with Fe oxides.

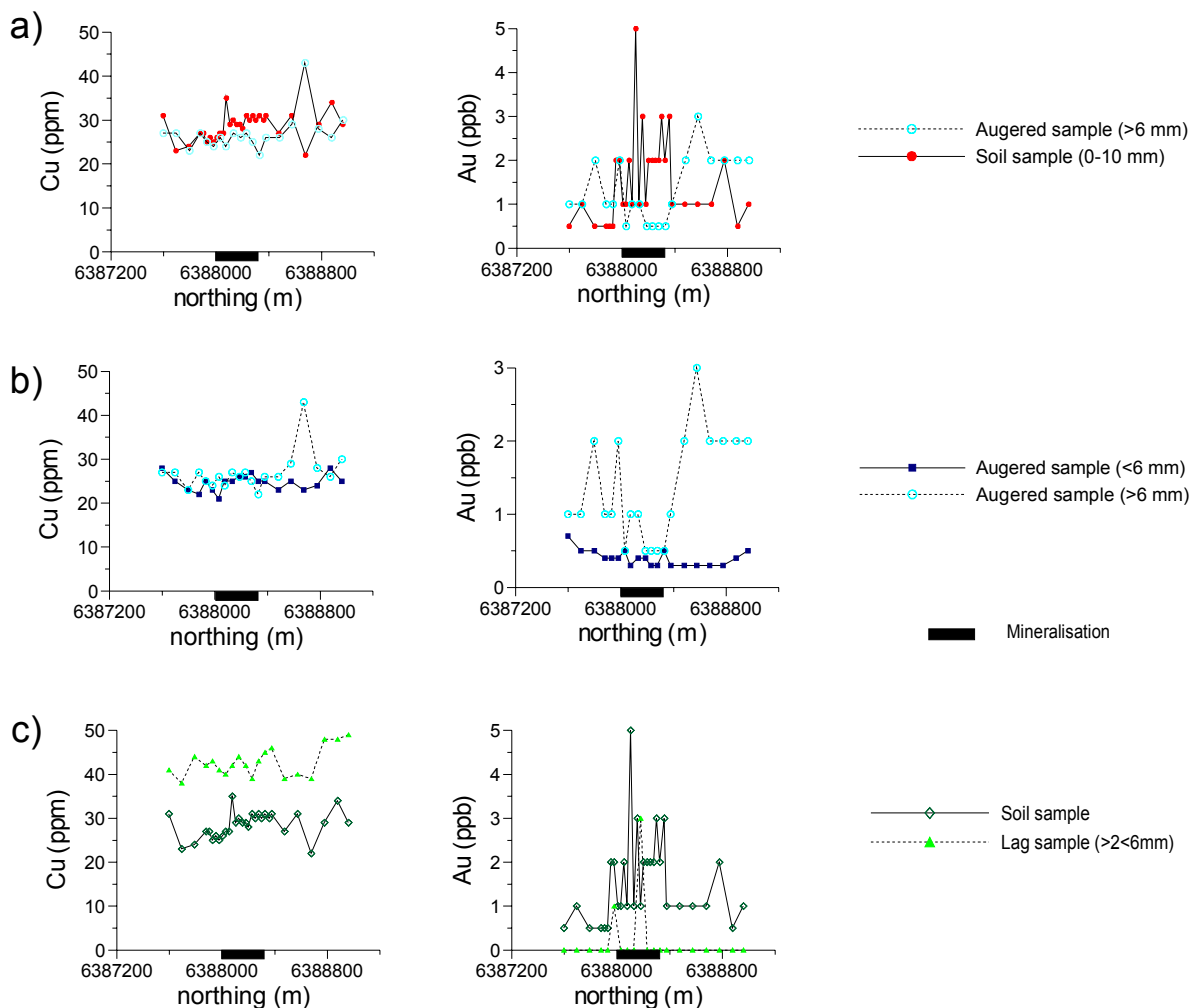


Figure 33: Comparison of Au and Cu geochemistry for different sample media on 428820E at Blue Rose: a) Augered sample (>6 mm) vs soil sample. b) Fine augered sample (<6 mm) vs coarse augered sample (>6 mm). c) Soil sample vs lag sample (>2<6 mm).

7.10 Summary

- 1) Most of the Blue Rose area is in a depositional regime. The thickness of transported overburden varies between 2 and 42 m.
- 2) The general stratigraphic sequence of the transported overburden, from the top downwards is:
 - (i) calcareous soil
 - (ii) calcrete and silcrete
 - (iii) colluvial gravel and clay, cemented by calcrete, silcrete and chalcedony
 - (iv) clay with chalcedony veining
 - (v) plastic, mottled clay, locally with white or grey plastic clay at the base
 - (vi) white clay and quartz gravel
- 3) Copper mineralisation occurs in dolomitic rocks with disseminated sulphides, serpentine, tremolite and talc. There is no evidence for skarn-type mineralisation. The mineral assemblages are typical of low-grade regional metamorphism of impure dolomites.
- 4) The geochemical signature of the mineralisation (based on high-grade intervals from the RC drill holes) is Bi, Cu, Cs, In, K, Mo, Rb, S, Se and Tl.
- 5) Copper dispersion haloes in saprock and saprolite are broader than in bedrock, and extend into the basal 2 m of the transported overburden.
- 6) There is a vertical zonation in element distribution in the upper 50 cm of the soil-calcrete profile. Arsenic, Au, Ba, Ca, Mg, S, Se, Sr and Y are most abundant at 20-40 cm depth, whereas the remaining elements are most abundant at 0-10 cm depth. Care should be taken in soil sampling to collect the appropriate horizon; samples should be analysed for Ca.
- 7) Auger drilling failed to provide unequivocal indications of mineralisation at depth, except at the southern end of the traverse on grid line 427250E, where transported overburden is relatively thin (<6 m). In general, samples with the greatest element abundances occur where transported overburden is relatively thin (<6 m thick).
- 8) Soil sampling (<2 mm fraction) over the mineralised zone on grid line 428820E failed to detect any unequivocal evidence of mineralisation. Infill sampling over the Cu anomaly at the southern end of grid line 427250E corroborated the earlier auger drilling results and has yielded a zone up to 125 m wide, with coincident Au-Cu anomalies. Where transported overburden is known to be thin, collection of <2 mm soils (0-10 cm depth) appear to be a more reliable and cheaper option than auger drilling. Where transported overburden is relatively thick, drilling to residual Regolith is required.
- 9) Analysis of the magnetic fraction of the 2-6 mm lag failed to detect underlying mineralisation.
- 10) Partial leach analyses were unable to detect mineralisation at depth through 8-9 m of transported overburden.

8 MISCELLANEOUS REGIONAL ROCK-CHIP SAMPLES

Twelve miscellaneous rock-chip samples were collected and analysed. Nine of these were from old workings at Taylors and Victoria Tower, at the western end of the Wadnaminga Goldfield. One sample was of crystalline Fe oxides in quartz veining from the Anabama Granite, and two regional samples of ferruginous material were collected by one of the authors in the course of the 1:100 000 regolith-landform mapping. The results are listed in Appendix 5.

Taylor's and Victoria Tower

These samples vary from calcareous soils, ferruginised/gossanous bedrock, and quartz veining with sulphides from old workings. The quartz veins from Victoria Tower contain anomalous Au (865 ppb), Cu (340 ppm), Pb (4.23%), S (3150 ppm), Zn (460 ppm), Ag (25 ppm), Bi (2.1 ppm), Sb (13 ppm), Se (2 ppm) and Hg (1.8 ppm). These elements are potentially useful as pathfinders for Au mineralisation. The remaining samples contain only low levels of Au (<25 ppb).

Anabama Granite

This sample contains 170 ppb Au, 1600 ppm Cu, 4.8 ppm Ag, 4.4 ppm Bi, 33 ppm Mo, 4 ppm Se, 10.5 ppm Th, 61 ppm U and 0.25 ppm Hg and occurred in an alteration zone in the granite.

Regional samples

Sample REGR1 is the more interesting. It contains anomalous Ba (1.74%), Cu (400 ppm), Mn (0.67%), Pb (135 ppm), Zn (490 ppm), Ag (5 ppm), Cd (3.9 ppm), Co (500 ppm), Mo (155 ppm), Tl (135 ppm), U (24 ppm) and W (17.5 ppm). Some of these elements may have been scavenged by Mn oxides, but this site is worthy of further investigation.

9 CONCLUSIONS AND NEW TARGETS

9.1 Wadnaminga

9.1.1 Summary

Gold mineralisation occurs in metasedimentary rocks of the Adelaidean Burra Group, along the northern limb of the Wadnaminga Anticlinorium. Sulphidic quartz veins are anomalous in Ag, As, Au, Bi, Cd, Cu, Hg, Pb, S, Sb, Se and Zn. Calcrete sampling over the lodes indicates that only As, Au, Pb and, to a lesser extent, Cu and Zn are useful in targeting the mineralisation. Additional assistance may be gained by also utilising those elements derived from narrow alteration haloes around the veins, namely Ba, K, Mg, Na, Rb, Sr, Tl, U and W. However, these geochemical haloes appear to be relatively narrow compared to those generated from auger drilling, where the ore-associated elements (As, Au, Bi, Cd, Cu, Pb and Zn) form haloes 25-50 m wide and elements (Ba, K, Mg, Na, Sr, Tl, U and W) form haloes up to 150 m wide.

9.1.2 Implications for exploration

Both auger drilling and the specific collection of calcrete are effective sampling techniques in this environment, although a sufficient density of sample sites (25 m spacings) would be required for calcrete sampling at the prospect scale. By analogy with Blue Rose, soils would probably be a valid sampling medium and may be more cost-effective than auger or calcrete sampling.

The geochemical suite should include: As, Au, Ba, Ca, Cu, Fe, K, Mg, Mn, Pb, U, W and Zn. If soil sampling is chosen, the optimum size fraction would need to be determined by an orientation study.

9.1.3 Further work

The sampling has not located any new zones of mineralisation. There appear to be numerous untested quartz veins which might be high-grade, but are likely to be thin.

9.2 Faugh-a-Ballagh

9.2.1 Summary

The Faugh-a-Ballagh prospect occurs within metasedimentary units, quartzofeldspathic rocks, gneisses and migmatites of the Olary Domain. Stratabound Cu mineralisation occurs in magnetite-bearing rocks.

The mineralised ironstones are anomalous in Ag, Al, Au, Cs, Cu, Ga, In, K, Mg, REE, Rb, Sr, Th, U, Y and Zn compared to barren ironstones. Despite this, Cu and Au are the only reliable indicators of

mineralisation in the <6 mm soil. The Cu dispersion halo in the soil around mineralisation on Faugh-a-Ballagh Hill is irregular but extends over an area of about 750 m by 250 m and is in part related to an east-west shear. The Au dispersion is much narrower, but appears to be restricted to a linear zone about 1500 m in length. Arsenic, Bi, U and W are also locally anomalous. Other, less well-defined zones with anomalous Cu occur to the west and southwest of Faugh-a-Ballagh Hill.

9.2.2 Implications for exploration

Soil appears to be the most effective medium. The <6 mm fraction appears to be adequate, but the finer fractions (<180 µm) may be more effective. Stream-sediment sampling (<2 mm fraction) indicates that Cu dispersion is very limited, although the results obtained for the <75 µm fraction indicate wider dispersion and greater abundance. There is no useful improvement using magnetic fractions of soil, lag or stream sediments. The geochemical suite for any further exploration should include As, Au, Bi, Cu, Fe, Mn, U and W. Lithological indicators, such as Na and Ca, could also be considered (for calc-silicate or albitic rocks).

9.2.3 Further work

The principal target is the southern side of Faugh-a-Ballagh Hill and the east-west shear (Figure 34). This zone has not been tested by drilling. Infill soil sampling is likely to better define the Cu-Au anomalies. The Cu anomalies to the west and southwest require infill soil sampling to better define them. It is likely that the anomalies may be obscured by alluvium further to the west.

9.3 Blue Rose

9.3.1 Summary

Copper mineralisation occurs in dolomitic rocks of the Adelaidean Burra Group, beneath transported overburden up to 42 m thick. The geochemical signature of the mineralised zones is: Bi, Cu, Cs, In, K, Mo, Rb, S, Se and Tl. Auger drilling and follow-up <2 mm soil sampling have identified an anomalous zone (up to 125 m wide) to the west of the presently known zone of mineralisation, in an area where transported overburden is thought to be relatively thin. Partial leaches of surficial samples have failed to detect mineralisation at depth.

9.3.2 Implications for exploration

The failure of partial leach analyses, even though transported cover is only 8-9 m thick, indicates that the use of partial leach technology is unlikely to be an effective exploration tool. Drilling is the only reliable technique where transported cover is >6 m thick. Broad zones of Cu dispersion in saprolite and in basal parts of the transported overburden provide a larger target than the primary zones themselves. Soil sampling is effective where transported overburden is thin (<6 m). Geochemical dispersion in the <75 µm fraction of the soil should be investigated. The geochemical suite for further exploration should include: Au, Bi, Cu, Fe, K, Mg, Mn, Mo, Se and Tl.

9.3.3 Further work

The known mineralised zone is open both along strike and at depth. Two other zones of potential mineralisation occur to the southwest and southeast, related to Au-Cu soil anomalies and to rock-chip samples (Figure 35). If mineralisation is related to the Anabama Granite, dolomitic units along strike are also potential hosts. Greisen at Blue Rose suggests association of mineralisation with a high-level pluton (cf. Giles Knob).

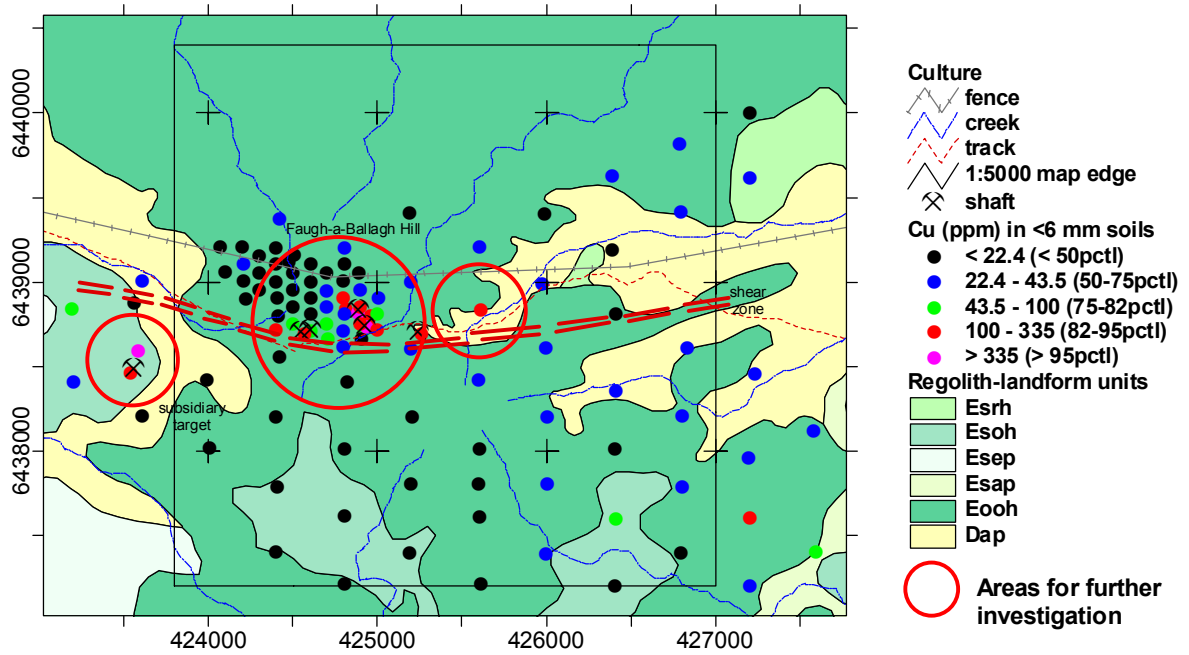


Figure 34: Areas for further investigation, Faugh-a-Ballagh prospect. Full regolith landform unit descriptions are found in Appendix 6

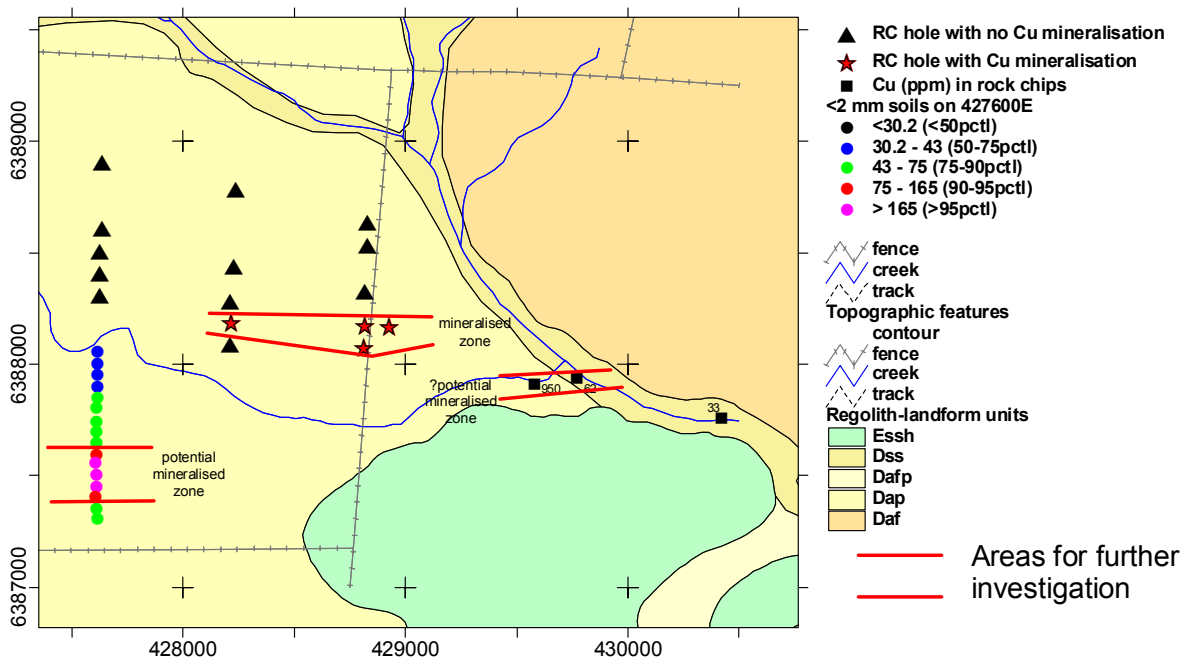


Figure 35: Areas for further investigation, Blue Rose prospect. Full regolith landform unit descriptions are found in Appendix 6

10 ACKNOWLEDGEMENTS

This project was jointly funded by CRC LEME, TEISA (through PIRSA), and Lynas Corporation Ltd.

Assistance during fieldwork was provided by G. Gouthas (PIRSA) and S. Lintern (stream sediments and vegetation). S. Lintern described the vegetation. G. Gouthas also assisted greatly in sample processing and sieving.

At CSIRO Exploration and Mining in Perth, XRF geochemical analyses were provided by M.K.W. Hart. Sample sieving was carried out by P. Thornley and R.J. Bilz. X-ray diffraction analysis was by M.K.W Hart; sample preparation was carried out by P. Thornley. D. Winchester prepared the thin sections. J. Hall and A.Vartesi provided some of the colour artwork. A. Cornelius assisted with the production of several figures and compiled the CD. G.D. Longman compiled tables in the Appendix. The draft report was reviewed by D.J. Gray, I.D.M. Robertson and C.R.M. Butt.

At CSIRO Land and Water in Adelaide, M. Raven and W. Gates assisted in the interpretation of the XRD patterns. G. Rinder scanned various diagrams. P. Davies plotted the regolith maps.

All this assistance is acknowledged with appreciation.

11 REFERENCES

- Anand, R.R., Smith, R.E., Innes, J. and Churchward, H.M. (1989) Exploration geochemistry about the Mt Gibson Gold Deposits, WA, CSIRO Division of Exploration Geoscience Restricted Report 20R, 93pp.
- Anand, R.R., Churchward, H.M., Smith, R.E., Smith, K., Gozzard, J.R., Craig, M.A. and Munday, T.J. (1993) Classification and atlas of regolith-landform mapping units: Exploration perspectives for the Yilgarn Craton. CSIRO Exploration and Mining Restricted Report 440R.
- Anand, R.R., Phang, C., Wildman, J.E. and Lintern, M.J. (1997) Genesis of some calcretes in the southern Yilgarn Craton, Western Australia: implications for mineral exploration. *Australian Journal of Earth Sciences*, 44: 87-103.
- Beckton, J.M.X. (1993) Geology of the Faugh-a-Ballagh area with special reference to ironstone and copper mineralisation, Olary Block, South Australia. *B.Sc. (Hons) thesis (unpubl.), University of Melbourne.*
- Brown, H.Y.L. (1908) Record of the mines of South Australia. 4th edition. *Government Printer, Adelaide*, 382pp.
- Chapman, D.M. (1988) Quarterly report of exploration on EL1430, Olary Province, to 31/2/88. Indian Ocean Resources Ltd. *South Australian, Department of Mines and Energy, Open File Envelope 6932.*
- Cross, K.C., Daly, S. and Flint, R.B. (1993) Mineralisation associated with the GRV and Hiltaba Suite granitoids – Olympic Dam deposit. In: J.F. Drexel, W.V. Preiss and A.J. Parker (eds) – The geology of South Australia, vol. 1, The Precambrian. *South Australia, Geological Survey Bulletin 54*, p.132-138.
- Flint, D.J. (1977) Evaluation of the Olary silver mine and the Mount Perseverance mine. *South Australia, Department of Mines, Report Book 77/145.*
- Flint, R.B. (1993) Mesoproterozoic. In: J.F. Drexel, W.V. Preiss and A.J. Parker (eds) – The geology of South Australia, vol. 1, The Precambrian. *South Australia, Geological Survey Bulletin 54*, p.107-169.
- Forbes, B.G. (1991) Olary, South Australia. 1:250,000 Geological Series Sheet SI54-2 – explanatory notes. *Geological Survey South Australia*, 47pp.
- Gartrell, H.W. (1934) Report on the advisability of using table concentration in the treatment of the Wadnaminga gold ore. *Mining Review, Adelaide 61*, p.49-52.
- Henley, K.J. and Moeskops, P.G. (1976) Gold mineralisation in the Adelaide Geosyncline. Progress Report No. 1: the Wadnaminga Goldfield. *South Australian, Department of Mines and Energy, Open File Envelope 2792.*
- Keighery, B. (1994) Bushland plant survey – a guide to plant community survey for the community. Wildflower Society of WA (Inc.), Western Australia, 69pp.
- Morris, B.J. (1975) EL16. Progress report for the six monthly period ending 25 October, 1974. Final report. *South Australia, Department of Mines, Report Book 75/39.*
- Morris, B.J. (1981) Porphyry style copper/molybdenum mineralization at Anabama Hill. *Mines and Energy Review, South Australia*, No. 150, p.5-24.
- Morris, B.J. and Horn, C.M. (1990) Review of gold mineralisation in the Nackara Arc. *Mines and Energy Review, South Australia*, No. 157, p.51-58.
- Olliver, J.G. and Preiss, W.V. (1990) Adelaide Geosyncline – regional geology and mineralisation. In: F.E. Hughes (ed.), *Geology of the mineral deposits of Australia and Papua New Guinea*, Australasian Institute of Mining and Metallurgy, Melbourne, p.1145-1149.

- Page, R.W. and Laing, W.P. (1992) Felsic metavolcanic rocks related to the Broken Hill Pb-Zn-Ag orebody, Australia: geology, depositional age and timing of high-grade metamorphism. *Economic Geology* 87, p.2138-2168.
- Preiss, W.V. (compiler) (1987) The Adelaide Geosyncline – late Proterozoic stratigraphy, sedimentation, palaeontology and tectonics. *South Australia, Geological Survey Bulletin* 53.
- Preiss, W.V. (1995) Delamerian Orogeny. In: J.F. Drexel and W.V. Preiss (eds) – The geology of South Australia, vol. 2, The Phanerozoic. *South Australia, Geological Survey Bulletin* 54, p. 45-54.
- Robertson, R.S., Preiss, W.V., Crooks, A.F. Hill, P.W. and Sheard, M.J. (1998) Review of the Proterozoic geology and mineral potential of the Curnamona Province in South Australia. *AGSO Journal of Australian Geology and Geophysics* 17(3), p.169-182.
- Shelton, S.J. (1999) Olary Joint Venture Project, South Australia. Exploration Licenses 2295, 2297 and 2299. *Second annual technical report for the period ending 2 April 1999*. Lynas Gold NL, 2 vols.
- Westhoff, J. (1970) Report on exploration 20-5-70 to 20-8-70, SML419 for Australian Gold and Uranium. *South Australia, Department of Mines, Open File Envelope* 1436.